CHARACTERIZATION OF THE NEUROGENIC MICROENVIRONMENT IN THE MOUSE HIPPOCAMPUS FOLLOWING CHEMICAL-INDUCED NEURONAL INJURY.

Christopher A. McPherson

A dissertation submitted to the faculty of the University of North Carolina at Chapel Hill in partial fulfillment of the requirements for the degree of Doctor of Philosophy in the Curriculum of Toxicology

Chapel Hill
2011

Approved by:

Advisor: G. Jean Harry, Ph.D.

Thomas W. Bouldin, M.D.

Fulton T. Crews, Ph.D.

Steven R. Kleeberger, Ph.D.

Glenn K. Matsushima, Ph.D.

Dedicated to:

Hazel J. Tripp

Abstract

CHRISTOPHER A. MCPHERSON: Characterization of the neurogenic microenvironment in the mouse hippocampus following chemical induced neuronal injury.
(Under the direction of Dr. G. Jean Harry.)

Adult neurogenesis occurs in the subgranular zone (SGZ) of the hippocampal dentate dyrus generating new dentate granule neurons and can be induced with brain injury. Resident microglia cells and infiltrating macrophages produce inflammatory molecules in response to brain injury. While inflammation has been reported to be detrimental to hippocampal neurogenesis, other studies have suggested that the localized inflammatory response and stimulation of microglial cells can promote neurogensis. The working hypothesis of this work was that activated resident mircroglia serve a supportive role during injury-induced neurogenesis in the hippocampus. To examine this hypothesis the hippocampal toxicant, trimethyltin was used (TMT; 2.3 mg/kg, i.p.) to selectively target dentate granule cell death in adolescent and 1 year-old CD-1 male mice. mRNA of pro-inflammatory M1 markers and anti-inflammatory M2 genes were measured during the temporal injury response were measured in subdissected DG. Within 2 d post-TMT, neuronal death was accompanied by resident microglia activation in the abscence of infiltrating peripheral macrophages, and elevations in mRNA expression of M1 markers interleukin (IL)-1α, IL-1β, IL-6, and tumor necrosiss factor alpha (TNFα). Bromodeoxyuridine (BrdU) incorporation identified the peak time of neurogenesis as coinciding with this upregulation of M1 markers. At 14 d post-TMT new cells migrated to the GCL, expressed the mature neuronal marker NeuN. At this time of differentiation increased expression of the M2 markers IL-1 receptor antagonist (IL-1Ra), arginase 1 (AG-I), chitinase 3-like-3 (YM-1), brain derived neurotrophic factor (BDNF), glial cell line derived growth factor (GDNF), and nerve growth factor (NGF). The proliferative response was sufficient to fully repopulate

neurons in the GCL and provide functional recovery. The neurogenic response to injury differs with age. In this model, fewer $BrdU^+$ NPCs were observed in naive and injured adult hippocampus as compared to the corresponding number seen in adolescent mice. At 2 d post-TMT, a similar level of neuronal death was observed across ages, yet activated microglia were observed in the adolescent and hypertrophic process-bearing microglia in the adult. IL-1α mRNA levels were elevated in the adolescent hippocampus; IL-6 mRNA levels were elevated in the adult. In the SGZ isolated by laser capture microdissection, IL-1β was detected but not elevated bby TMT, IL-1α was elevated at both ages, while IL-6 was elevated only in the adult. Naive NPCs isolated from the hippocampus expressed transcripts for IL-1R1, IL-6Rα, and gp-130 with significantly higher levels of IL-6Rα mRNA in the adult. *In vitro*, IL-1α (150 pg/ml) stimulated proliferation of adolescent and adult NPCs. Microarray analysis of the SGZ post-TMT indicated a prominence of IL-1α/IL-1R1 signaling in the adolescent and IL-6/gp130 signaling in the adult.

Acknowledgements

I would like to thank my advisor G. Jean Harry for giving me on opportunity to begin working in her lab as a summer intern many years ago, and providing me with outstanding mentorship over the subsequent years. A special thanks goes to former lab members Dr. Christian Lefebvre d'Hellencourt, Dr. Mineyoshi Aoyama, Rob Wine, and Dr. Andrew Kraft, each of which provided me scientific and personal support throughout this project. I must also thank Drs. Fulton Crews, Thomas Bouldin, Steven Kleeberger, and Glenn Matsushima for serving on my committee providing me with invaluable mentorship throughout my project.

Table of Contents

List of Tables

List of Figures

List of Abbreviations

AC3	active caspase 3
AG-I	arginase-1
BDNF	brain derived neurotrophic factor
BrdU	5'-bromo-3'-deoxyuridine
CA1	cornus ammonis 1
CA2	cornus ammonis 2
CA3	conrus ammonis 3
CA4	cornus ammonis 4
DCX	doublecortin
DG	dentate gyrus
GABA	gamma-aminobutyric-acid
GCL	granule cell layer
GDNF	glial cell line derived neurotrophic factor
GFAP	glial fibrillary acidic protein
H&E	hematoxylin and eosin
Iba1	ionized calcium-binding adaptor molecule
IL-1α	interleukin 1 alpha
IL-1β	interleukin 1 beta
IL-1R1	interleukin 1 receptor 1
IL-1Ra	interleukin 1 receptor antagonist
IL-4	interleukin 4

IL-6	interleukin 6
IL-6Rα	interleukin 6 receptor alpha
IL-1RAcP	interleukin 1 receptor accessory protein
MAM	methylazoxymethanol acetate
MWM	Morrris water maze
NeuN	mouse neuronal nuclei
NGF	nerve growth factor
NPC	neural progenitor cell(s)
NSA	neurosphere assay
Prox-	prospero-related homeobox-1
PSA-NCAM	polysialated form of neural cell adhesion molecule
PVC	polyvinyl chloride
qRT-PCR	quantitative real time polymerase chain reaction
ROI	region of interest
SAL	saline
SE	status epilepticus
SGZ	subgranular zone
SVZ	subventricular zone
TBI	traumatic brain injury
TGFβ1	transforming growth factor beta 1
TMT	trimethyltin
TNFα	tumor necrosis factor alpha
TNFp55R	55kDa type-1 TNF receptor

TNTp75R	75kDa type 2 TNT receptor
YM-1	chintinase 3-like

Chapter 1

Introduction

1.1 Historical overview of adult neurogenesis

In the early 20th century, the preeminent neuroanatomist, Ramon y Cajal, concluded, “Once development has ended the fonts of growth and regeneration of axons and dendrites dried up irrevevocably. In adult centers, the nerve paths are something fixed and immutable: everything may die, nothing may be regenerated. It is for the science of the future to change, if possible, this harsh decree” (Ramon y Cajal, 1928). This quotation represents a presumption held for over a century in the field of neuroscience that has influenced our approach to evaluating the repair capability of the brain. The predominant idea that neurons are generated only during fetal development of the brain, with no capability for generation after birth, established the dogma that no new neurons are generated in the adult mammalian brain and that all the future holds is a loss of these critical cells. It was not until the early 1960’s that pioneers within the field were bold enough to suggest that the neurogenic capability of the brain and the generation of new neurons could extend well after birth and into the young adult age. These data set the framework for subsequent investigations to change the “harsh decree” of Cajal and, as such, represent a major paradigm shift in the field of neuroscience.

In the early 1960's, Altman and co-investigators used the newly available tool [^{3}H]-thymidine, a thymidine homologue, to birthdate mitotic cells within distinct brain structures. Pulse-labeling newly proliferating cells in the rat brain with [^{3}H]-thymidine at distinct developmental periods demonstrated that neuronal proliferation continues into the postnatal developmental period. Two specific and distinct locations were identified to contain postnatally generated neurons, the hippocampus and the olfactory bulb (Altman, 1963, 1969; Altman and Das, 1965). Building upon these reports, Kaplan coupled ultrastructural analysis with [^{3}H]-thymidine uptake and reported that newly generated cells within the adult rat brain displayed characteristics of neurons. Newly generated neurons were identified in the olfactory bulb, hippocampus, and throughout the cortex (Kaplan, 1981; Kaplan and Bell, 1984; Kaplan and Hinds, 1977). These findings initiated a series of studies to determine whether the generation of new neurons was species specific. Using a similar approach, Pasko Rakic and co-workers evaluated the potential for this process in the non-human primate brain (Rakic, 1974, 1985). The generation of neurons was identified as a process in the fetal and in early postnatal brain but was not observed in the adult brain. Rakic and colleagues attributed this difference to evolutionary behavior complexity between the rodent and primate brain (Eckenhoff and Rakic, 1988; Rakic, 1985).

Newly generated neurons were identified in the adult rodent brain; however, functional integration was not identified until the process was examined in the songbird brain (Alvarez-Buylla et al., 1988; Burd and Nottebohm, 1985; Goldman and Nottebohm, 1983). This work by Nottebohm and colleagues reinvigorated the

examination of neurogenesis in the rodent brain, and during the early 1990's, significant research was generated laying the framework of our current understanding of the process of adult neurogenesis. The co-localization of neural cell specific markers with the thymidine homologue, 5'-bromo-2'-deoxyuridine (BrdU), for incorporation into the s-phase of the cell cycle confirmed the generation of neurons within the hippocampus of the adult rodent brain (Kempermann et al., 1997; Kuhn et al., 1996). This process was confirmed within the non-human primate brain (Gould et al., 1999; Gould et al., 1998; Kornack and Rakic, 1999) and finally, newly generated neurons were identified in human post-mortem tissue (Eriksson et al., 1998). After decades of debate, beginning with the seminal work of Altman and Kaplan in the 1960's and 1970's, it is now accepted that mitotically active precursor cells are present in specialized neurogenic regions of the adult brain. This population of cells is comprised of stem cells with the capacity to self-renew, and undergo multi-lineage differentiation, as well as, lineage-restricted progenitor cells with limited self-renewal capacity (Seaberg and van der Kooy, 2002, 2003).

Under normal conditions, neurogenic regions of the mammalian brain produce or recruit new neurons throughout adulthood. Two established neurogenic regions include the subventricular zone (SVZ) of the lateral ventricle and the subgranular zone (SGZ) of the hippocampus (Bayer, 1983; Cameron et al., 1993; Kuhn et al., 1996). Other regions of the brain are usually considered non-neurogenic because new neurons are not generated or recruited to these regions under normal conditions (Fricker et al., 1999). While the SVZ and SGZ are considered the only established neurogenic regions in the adult brain, neurogenesis

in other brain regions such as the neocortex, striatum, and substantia nigra remains in question (Gould, 2007). There is strong evidence that the SVZ and SGZ receive and integrate newly generated neurons, olfactory bulb interneurons and dentate granule neurons, respectively throughout adulthood. These new neurons are capable of functionally integrating into the neural circuitry of the terminal structure. Thus, adult neurogenesis may represent an inherent capacity of the olfactory bulb and the hippocampus to respond to environmental stimuli or the organism's internal state (Lledo et al., 2006).

1.2 Characterization of newly generated cells in the SGZ

Adult neurogenesis in the hippocampus is initiated by a relatively small population of neural progenitor cells (NPCs) located within the SGZ between the glia-rich hilus and the tightly packed neurons of the granule cell layer (GCL) of the dentate gyrus (DG). This zone includes the basal cell band of the granule cell layer and a two-cell-wide layer into the hilus. The SGZ is a multi-cellular microenvironment comprised of NPCs, astrocytes, microglia, and a limited population of oligodendroglia (Seri et al., 2004; Sierra et al., 2010). While a resident stem cell population has been demonstrated within the SVZ, a prominent stem cell population has not been clearly demonstrated in the SGZ. The initial cell isolations of cells from the SGZ, demonstrated stem cell features of self-renewal capacity and multipotent characteristics of differentiating into astrocytes, oligodendrocytes, and neurons (Palmer et al., 1999; Palmer et al., 1995; Palmer et al., 1997). In these studies, cell self-renewal and multipotency were based predominantly on the characterization of neural precursor cells *in vitro* using the neurosphere assay (NSA)

and the monolayer culture assay. These assays assume clonality of all of the spheres formed in the assay, in that each neurosphere is derived from a single neural stem cell. The neural precursor cell's ability to proliferate over an extended period of time, and to generate large numbers of progeny that differentiated into primary neuronal cell types has been examined (Reynolds and Rietze, 2005; Seaberg and van der Kooy, 2003). With further characterization, a large proportion of the proliferative cell population was identified as lineage-specific NPCs with limited self-renewal capacity (Bull and Bartlett, 2005; Seaberg and van der Kooy, 2002). While it is generally accepted that the proliferating cell in the SGZ is a lineage specific NPC, there is also limited supporting evidence for a neural stem cell in the adult mammalian SGZ (Suh et al., 2007).

1.3 Stages of adult hippocampal neurogenesis

NPCs in the hippocampus undergo distinct developmental stages as they are generated in the SGZ and migrate into the granule cell layer. They are classified by these developmental stages as type-1, type-2, or type-3 cells (Fig. 1). The type-1 cell is the early NPC of the hippocampus located in the SGZ and demonstrates morphological characteristics of radial glia with large triangular-shaped soma and long apical processes reaching into the granule cell layer. Type-1 cells express the intermediate filament protein nestin, the astrocytic marker, glial fibrillary acidic protein (GFAP), and do not express S110β, a calcium binding protein and marker of post-mitotic astrocytes (Filippov et al., 2003; Seri et al., 2001). They comprise 66% of the nestin positive cells; however, their basal rate of cell division is rare with only

5% of the cells undergoing cell division (Filippov et al., 2003; Kronenberg et al., 2003) giving rise to type-2 daughter cells (Filippov et al., 2003; Fukuda et al., 2003).

The expansion of newly born cells in the SGZ occurs primarily during the type-2 stage, as they are fast proliferating lineage specific progenitor cells. Located in the SGZ, type-2 cells express nestin but do not express GFAP. Morphologically these cells display an irregular shaped cell body with short, plump, non-apical processes oriented parallel to the SGZ. Type-2 cells are further classified into two subtypes based on the expression of nestin and the immature neuronal marker doublecortin (DCX). Type-2a cells express both nestin and DCX, while type-2b cells express DCX in the absence of nestin (Brandt et al., 2003; Brown et al., 2003). The type-2b cells can express the mature neuronal marker, mouse neuronal nuclei (NeuN), and a specific marker for dentate granule cell neurons, prospero-related homeobox-1 (Prox-1) (Brandt et al., 2003; Steiner et al., 2004). As the cells transition from proliferating neuroblast to postmitotic immature neuron, they are considered a type-3 stage cell. While these cells maintain the capacity to undergo mitotic cell division, they undergo a morphological shift to cells with a rounded soma and processes of various lengths and complexities. At this stage, the cells no longer express nestin but prominently express DCX and the neuronal lineage markers polysialated form of neural cell adhesion molecule (PSA-NCAM), NeuroD, and Prox-1. Within 2-3 weeks post-generation, the type-3 cells migrate into the granule cell layer. With this migration, the type-3 cell downregulates calretinin expression, upregulates expression of calbindin as an effect on calcium binding proteins (Brandt et al., 2003), and loses mitotic capability (Encinas et al., 2006).

Only a small fraction of immature neurons in the adult hippocampus are destined for long-term incorporation into the hippocampal structure (Biebl et al., 2000; Kempermann et al., 2003). In the early stages of progenitor cell proliferation, the majority of type-1 cells undergo apoptosis during their transition to later staged type-2 or-3 neuroblasts. These apoptotic newborn cells are then rapidly cleared by unchallenged phagocytotic microglia within the SGZ (Sierra et al., 2010). Under normal conditions, adult-generated hippocampal cells migrate primarily to the inner third of the granule cell layer, extending many fine dendritic processes from a globular cell body into the molecular layer (Toni et al., 2007; Zhao et al., 2006) and axons into the cornus ammonis 3 (CA3) pyramidal cell layer (Hastings and Gould, 1999; Toni et al., 2008). The regulation for further maturation of these cells has been attributed to contact interactions with both microglia and astrocytes during migration (Aarum et al., 2003; Song et al., 2002).

Within approximately 2 months of cell division, cells assume the nuclear and cytoplasmic morphology of the surrounding neurons, express biochemical markers of immature and mature neurons and receive functional gamma-aminobutyric-acid (GABA)ergic contacts. Thus, at this stage interactions between the new neurons and existing dentate granule neurons and inhibitory inter-neurons contribute to the fate of the cells within the hippocampus. When the neurons are established in their final position within the GCL, they develop spiny dendrites reaching the outer molecular layer and an increase is observed in functional glutamatergic afferents. With the final stages of maturation, the cells obtain perisomatic GABAergic contacts (Schmidt-Hieber et al., 2004; van Praag et al., 2002).

In summary, adult hippocampal NPCs undergo stages of development, which include a slow proliferation of NPCs within the SGZ. This slow proliferation gives rise to daughter cells that further proliferate and become lineage restricted. Following specific developmental stages, these lineage-restricted daughter cells migrate into the hippocampal granule cell layer where they enter a second post-mitotic phase subsequently differentiating into immature neurons. Upon maturation into dentate granule neurons these cells extend both axonal and dendritic projections to integrate into the functioning hippocampal circuitry. Each of these discrete events occurs within microenvironment uniquely permissive to the stage of neurogenesis allowing for successful proliferation, differentiation, and maturation of cells.

1.4 Functional role of newly generated hippocampal neurons

The acceptance of neurogenesis as an ongoing process in the adult brain raised questions regarding the functional role of this process and the new neurons. A large body of literature has clearly demonstrated the role of the hippocampus and the dentate granule neurons in learning and memory and poses the possibility that newly generated neurons are associated with short-term and working memory. Whether or not maintenance of the hippocampal NPC population is required for hippocampal dependent tasks is a question that is just recently being addressed.

The hippocampal formation is a central component of the limbic system critically involved in learning, memory, and emotional responses. Structurally, the hippocampus is comprised of the Ammon's horn, DG, and the subiculum. The Ammon's horn is subdivided into the CA1, CA2, and CA3-4 pyramidal cell layers and

the DG is composed of two blades (suprapyramidal and infrapyramidal) of granule neurons and the mossy fibers of the hilus. The hippocampus receives sensory input from functionally distinct brain regions and is required for the formation and storage of declarative memories (Eichenbaum et al., 1992). The main relay point for this hippocampal circuitry is the entorhinal cortex. This cortical structure provides a predominantly unidirectional input to the DG via the perforant pathway. The dentate granule neurons are responsible for holding this short-term memory and then relaying this input information primarily to the CA3 pyramidal neurons via the mossy fibers. Signals from the CA3 pyramidal neurons are relayed along the Schaffer collaterals forming contacts with the CA1 pyramidal neurons. The intra-hippocampal tri-synaptic loop is completed with the projections of the CA1 pyramidal neurons to the subiculum. At this point, the subiculum projects back to the entorhinal cortex (Martin and Clark, 2007). From the entorhinal cortex the information can then be sent to widespread neocortical areas for long-term memory storage and retrieval (Eichenbaum et al., 1992).

Some of the first work to understand the overall functional contribution of newborn neurons was the demonstration of preferential incorporation into hippocampal-dependent declarative memory networks (Kee et al., 2007; van Praag et al., 2002). Initial work by Shors et al. (2001; 2002) demonstrated that a transient inhibition of neuroprogenitor cell proliferation using the anti-mitotic agent, methylazoxymethanol acetate (MAM), resulted in a deficit in hippocampal dependent trace conditioning (Shors et al., 2001) with no alteration observed in spatial learning in a Morris water maze or in contextual fear conditioning (Shors et al., 2002). The

selectivity of the contribution may have been related to the transient nature of the inhibition. Depletion of the proliferating cell population by irradiation caused impaired long-term spatial memory in the Morris water maze (Madsen et al., 2003; Meshi et al., 2006; Saxe et al., 2006) with no effects on short-term memory. With this level of depletion, deficits were also reported for contextual fear conditioning (Saxe et al., 2006; Snyder et al., 2009). Similar patterns of effects have been observed with chemical exposure models that decreased NPC proliferation. Following toluene exposure, deficits in fear conditioning and novel object recognition were reported(Seo et al., 2010). With ongoing lead acetate exposure, the downregulation of hippocampal NPC proliferation showed no effects on water maze performance in rats (Gilbert et al., 2005). Overall, these data suggest that inhibition of NPC proliferation can alter normal hippocampal dependent tasks and that the nature of the task altered may depend on the severity of the inhibition.

1.5 Neurogenic niches of the hippocampus

Proliferation and differentiation of NPCs does not exist independently but rather reflects a dynamic interaction between NPCs and their surrounding multicellular microenvironment to regulate the process. Within the milieu of cells (NPCs, astrocytes, neurons, microglia, oligodendrocytes) and secreted factors, a SGZ neurogenic niche exists to support NPC self-renewal (Fig. 2). The concept of a stem cell “niche” was first introduced in 1978 through studies of hematopoietic stem cells (Schofield, 1978). Since then stem cell niches have been identified in multiple organ systems and their study assumes a major role in understanding the regulation of stem cell proliferation and survival (Morrison and Spradling, 2008). Stem cell

niches are defined by a number of characteristics. For example, they provide an environment to prevent excessive stem cell production and to sequester cells from signals that would deplete stem cell reserves (i.e. differentiation signals, death). The niche maintains the critical balance of stem cell quiescence and, upon activation, is able to orchestrate the proliferation of progenitor cells that become mature cell lineages (Moore and Lemischka, 2006). In the hippocampus, by strict definition, the SGZ should be considered the NPC niche, as this is the site for maintenance of proliferative type-1 NPCs. As the cells differentiate into type-2 and type-3 cells they begin migrating into the multi-cellular microenvironment of the granule cell layer that is permissive to neuronal differentiation and thus, represents a secondary niche. Therefore, one can consider the process of adult hippocampal neurogenesis as a "two-niche" event. Within the SGZ or primary niche, cells and secreted factors serve as the primary unit of interaction between NPCs and their environment to promote an appropriate level of proliferation and survival of healthy NPCs. In the GCL or secondary niche, the microenvironment of the mature granule cell layer serves as a regulatory site for the migration and differentiation of NPCs into mature neurons or glia (Fig. 3). Distinct differences between these two niches provide key signaling events for the multi-stage differentation of NPCs into mature neurons or glia. In addition, they may represent two distinct critical target sites for endogenous and exogenous factors, including genetic and environmental factors, to interfere with a compensatory process within the adult brain.

1.6 Regulation of hippocampal neurogenesis

It has been proposed that adult neurogenesis may represent an inherent capacity of the olfactory bulb and the hippocampus to respond to the host environment (Lledo et al., 2006). It is also possible that the inherent characteristics of mature neurons within these regions differ from the majority of terminally differentiated long-lived neurons in the brain and may be more susceptible to changes in their environment. Current understanding of the neurogenic capability of the adult brain has been derived from studies examining the response following stimulation by extrinsic and intrinsic factors. Extrinsic factors including physical exercise (van Praag et al., 1999) and enriched environment (Kempermann et al., 1997) can stimulate the proliferation and survival of newly generated cells from the SGZ, respectively, supporting the idea of multiple environments influencing the outcome of neurogenesis. Alternatively, stress can serve to down regulate NPC proliferation (Tanapat et al., 2001; Vollmayr et al., 2003) with the demonstration that corticocosteroid hormone inhibits SGZ neurogenesis (Cameron and Gould, 1994). Hormones such as estrogen have been reported to enhance NPC proliferation in females during times of pro-estrous (Tanapat et al., 1999). Additionally, neurotransmitters, including GABA (Bernabeu and Sharp, 2000; Cameron et al., 1995), serotonin (Brezun and Daszuta, 1999), norepinephrine (Kulkarni et al., 2002), and acetylcholine (Cooper-Kuhn et al., 2004) are capable of modulating adult neurogenesis. As are trophic factors, including brain derived neurotrophic factor (BDNF), glia cell line-derived neurotrophic factor (GDNF), and nerve growth factor (NGF) (Aberg et al., 2000; Chen et al., 2005; Frielingsdorf et al., 2007; Larsson et al., 2002). A contributory

role for glia and glial-derived cytokines to modulate adult neurogenesis in the hippocampus has also been reported (Battista et al., 2006; Ekdahl et al., 2003; Jin et al., 2002; Kaneko et al., 2006; Lu et al., 2002; Monje et al., 2003).

Age is a very potent regulator of hippocampal neurogenesis. Compared to the young adult, by middle age the rate of proliferation and the number of NPCs in the hippocampus are reduced (Kuhn et al., 1996). This coincides with a decreased ability of these cells to differentiate into a neuronal phenotype (McDonald and Wojtowicz, 2005; Rao et al., 2005). Associations between age-related reduction in hippocampal neurogenesis and decreased cognitive function have been demonstrated (Klempin and Kempermann, 2007) and suggested to be linked with a diminished capability for repair (Hattiangady et al., 2008; Shetty et al., 2010). Thus the higher level of neurogenesis in the young brain, compared to an aging brain, may reflect a greater level of plasticity in the young (Altman et al., 1973; Changeux and Danchin, 1976) and a loss of plasticity in the aged. A number of factors have been proposed to account for this decline with age such as a depletion of the progenitor cell pool, diminished neurotrophic factors, senescence of microglia and their decreased ability to remove toxic debris from the environment or provide a level of neuroprotection. While proposed, strong supporting data for each of these factors is not currently available.

1.7 Neurogenesis following hippocampal insult

Sensitivity and vulnerability of dentate granule neurons has been demonstrated across a number of hippocampal insults (Harry and Lefebvre d'Hellencourt, 2003). Damage to dentate granule neurons is often accompanied by

a proliferative response of NPCs in the SGZ. In many cases, the severity of the injury will correlate with the robustness of proliferation. While it was previously thought that ischemic insults damaged only CA1 pyramidal neurons, it has been shown that dentate granule cell apoptosis occurs shortly after ischemic injury (Siren et al., 2002; Wang et al., 1999). One may consider that the death of dentate granule neurons remained unidentified in earlier ischemia studies due to the later time frame for histological examination that would allow for the clearance of dead cells by microglia and potential replacement by newly generated neurons hippocampal neurogenesis (Liu et al., 1998). Seizure activity can also induce apoptotic cell death of dentate granule neurons (Bengzon et al., 1997; Sloviter et al., 1996) followed by an induction of NPC proliferation. Epileptic seizures in the adolescent demonstrate susceptibility of dentate granule neurons in the human (Dam, 1980; Tang et al., 2001). Even with a relatively remote damage such as traumatic brain injury (TBI), proliferation of NPCs in the SGZ is induced (Jin et al., 2001; Keiner et al., 2010; Kim et al., 2009). This often follows an early stage of apoptosis of dentate granule neurons (Clark et al., 1997; McCullers et al., 2002) linked with associated memory loss (Smith et al., 1994). With ischemic damage, the proliferation of NPCs within the SGZ is followed by migration into the GCL and differentiation into mature neurons within 14-28 d in adult mice (Keiner et al., 2010). Other studies demonstrated that many of the neurons generated in response to ischemic insult die in the adult mouse (Liu et al., 1998; Tureyen et al., 2004; Yagita et al., 2001) while the surviving replacement neurons established synapses within the existing hippocampal circuitry (Jakubs et al., 2006; Wang et al., 2005).

Dentate granule neurons are susceptible to environmental and occupational toxicants such as ozone, soman, benzyl acetate, ethanol, and organometals (Abdo et al., 1998; Bhagat et al., 2005; Obernier et al., 2002; Reuhl and Cranmer, 1984; Rivas-Arancibia et al., 2010). One model for which a selective vulnerability of dentate granule neurons across multiple species is the organometal, trimethyltin (Chang et al., 1982; Fortemps et al., 1978; Reuhl and Cranmer, 1984). Using this model system to examine the association between localized neuronal death and the induction of hippocampal NPCs, different laboratories have demonstrated a rapid stimulation of NPC proliferation (Harry et al., 2004; Ogita et al., 2005) sufficient to ameliorate the associated short-term learning and memory impairment (Ogita et al., 2005). Using a more extended exposure model, 4 h of daily inhalation exposure of 0.25 parts per millions (ppm) ozone for 90 days, a decrease in $NeuN^+$ cells within the GCL in rats is seen with a concurrent increase in proliferative $p53^+$ cells (Rivas-Arancibia et al., 2010). DCX expressing cells were increased at 30 days suggesting an induction of NPCs; however, this increase was not evident at longer time points. The transient nature of the effect could be due to an adaptation of the SGZ niche or a depletion of the NPC pool. In any case, the lack of a sustained proliferation of NPCs in the hippocampus with continued ozone exposure likely contributed to the observed deficits in short and long-term memory as assessed using a passive avoidance paradigm (Rivas-Arancibia et al., 2010). A 7-day exposure to the neurotoxicant Soman (pinacolyl methylphono-fluoridate) resulted in damage of CA1 pyramidal cell and dentate granule neurons of the hippocampus in rats and mice (Bhagat et al., 2005; Collombet et al., 2005). Examination of the temporal

progression of the injury identified an early NPC proliferative response in the SGZ within 3 days (Collombet et al., 2005); however, no studies have been conducted to determine if the NPCs serve to provide a functional repair of the hippocampus. Overall, the body of literature on adult hippocampal neurogenesis, whether under normal conditions or following injury or insult, demonstrate a capability of the brain to maintain a level of plasticity and self-repair throughout life.

1.8 Microglia and pro-inflammatory cytokines in the neurogenic niche

Recent research has started to address questions regarding how the neurogenic microenvironment 1) serves to foster the proliferation of NPCs, 2) contributes to the survival of NPCs and neuroblasts, 3) allows for the migration of neuroblasts to the appropriate location, 4) supports differentiation of neuroblasts to mature neurons, and 5) allows for differentiated neurons to develop functional circuitry within the hippocampus (Ekdahl et al., 2009). Within the neurogenic niche, astrocytes and microglia have been identified as putative regulators of neurogenesis (Barkho et al., 2006; Ekdahl et al., 2003; Monje et al., 2003). In the normal brain, the processes of ramified microglia serve a specialized phagocytic function to remove any unhealthy proliferative cells (Sierra et al., 2010). While different than the amoeboid microglia response for phagocytosis of mature neurons, the ability of the microglia projections to engulf localized unhealthy cells demonstrates the adaptation of a regulatory role of microglia. This action maintains a homeostatic balance within the local region, potentially enhancing the survival of healthy NPCs (Mattocks and Tropepe, 2010). With injury to the hippocampus, microglia within the GCL, including the SGZ, undergo a morphological shift and display both stellate and

amoeboid morphologies accompanying neuronal death (Davalos et al., 2005; Nimmerjahn et al., 2005). The morphology ranges from hyper-ramified cells, enlarged cell bodies with thickened and retracted processes, to a full amoeboid phagocytic phenotype (Kreutzberg, 1996). It is usually considered that upon such activation, microglia are the predominant source of pro-inflammatory cytokines in the brain including interleukin-1α (IL-1α), IL-1β, IL-6, and tumor necrosis factorα (TNFα).

Regulatory effects of multiple inflammatory cytokines including IL-1, IL-6 and TNFα on NPC proliferation, differentiation, and survival have been reported (Ekdahl et al., 2003; Iosif et al., 2006; Monje et al., 2003; Spulber et al., 2008). TNFα is expressed at low levels in the normal brain (Pitossi et al., 1997) as either a soluble or transmembrane molecule. TNFα initiates signaling by binding to two distinct cell surface receptors, a 55 kDa type-1 receptor (TNFp55R) and a 75 kDa type-2 receptor (TNFp75R). TNFp55R contains a cytoplasmic sequence identifying an intracellular death domain essential for the transduction of an apoptotic signal (Micheau and Tschopp, 2003; Thorburn, 2004) whileTNFp75R activation primarily initiates trophic/protective actions (Shen et al., 1997; Yang et al., 2002). It has been suggested that the effect of TNFα on NPCs depends upon localized receptor expression (Ben-Hur et al., 2003; Iosif et al., 2006; Klassen et al., 2003). Cultured NPCs from human fetal brain express TNFα, as well as, TNFp55R and TNFp75R (Klassen et al., 2003; Sheng et al., 2005). Mouse embryonic hippocampal NSCs express both TNFp55R and TNFp75R and in culture and cell survival was significantly diminished with the addition of recombinant TNFα protein (Cacci et al., 2005). *In vivo,* NPCs within the hippocampal SGZ selectively express TNFp75R

potentially as a mechanism to utilize TNFα as a neurotrophic factor, allowing for survival in a highly pro-inflammatory environment following localized injury (Harry et al., 2008). Support for TNFα signaling as a regulatory component of NPC proliferation has been provided from the work of Iosif et al., (2006) in which mice lacking TNFp55R showed an increase in newly generated $BrdU^+/NeuN^+$ cells, while mice lacking TNFp75R showed a minor decrease in these hippocampal cells.

Interleukin-1α and IL-1β are proteins synthesized from two different genes. They have <30% structural homology and bind to the same surface receptor, IL-1 receptor (IL-1R1), which requires binding to IL-1R accessory protein (IL-1RAcP) for signal transduction (Dinarello, 1996; Greenfeder et al., 1995). Regulation of IL-1 occurs primarily via binding of the IL-1R1 by the competitive IL-1 receptor 1 antagonist (IL-1ra) for downregulation (Greenfeder et al., 1995). IL-1 can induce the production of inflammatory cytokines, chemokines, and prostaglandins by activated microglia and astrocytes (Aloisi et al., 1992; Basu et al., 2002). In the normal hippocampus, IL-1 and IL-1R1 are constitutively expressed in the hippocampus at low levels (Ban, 1994); however, with injury expression can be significantly elevated. Within the hippocampus, IL-1 receptors are present in the molecular and granular layers of the dentate gyrus (Cunningham et al., 1992) and IL-1 receptor mRNA is seen in dentate granule cells, pyramidal cells of the hilus, and CA3 pyramidal cell region (Cunningham et al., 1992). Isolated hippocampal NPCs express IL-1R1 and treatment with recombinant IL-1β inhibited cell proliferation, which could be blocked by IL-1ra treatment (Koo and Duman, 2008). Similar effects were demonstrated *in vivo*, where extended intracerebroventricular administration of recombinant IL-1β

inhibited hippocampal NPC proliferation (Koo and Duman, 2008). Concurrent administration of IL-1ra blocked the anti-proliferative effects of IL-1 (Koo and Duman, 2008). Further examination of the impact of IL-1R1 activation on hippocampal NPC proliferation demonstrated a deficit in constitutive proliferation in transgenic mice with GFAP-directed over-expression of human soluble IL-1ra (Tg hsIL-1ra) (Spulber et al., 2008). A similar downregulation of hippocampal NPC proliferation in the transgenic *hsIL-1ra* mice was observed following kainic acid-induced hippocampal seizures (Spulber et al., 2008).

Along with IL-1 and TNFα, IL-6 is a pleiotropic cytokine involved in the regulation of inflammatory and immunologic responses (Kishimoto et al., 1992). However, many of the TNFα and IL-1 actions are modulated by the anti-inflammatory properties of IL-6 that activate both local and systemic host defense mechanisms in response to injury and secretion of TNFα and IL-1 (Aderka et al., 1989; Schindler et al., 1990; Ulich et al., 1991). It can induce the expression of soluble TNFα receptors and IL-1ra (Tilg et al., 1994) and downregulate TNFα expression (Aderka et al., 1989). Its expression in cultured astrocytes is regulated by cytokines such as IL-1b and TNFα (Norris et al., 1994). In the brain, IL-6 and its receptors are expressed on neurons and glial cells under normal physiological conditions (Gadient and Otten, 1997). One of the first studies to examine the effects of IL-6 on adult hippocampal NPCs was conducted by Monje et al., (2003). In this study, conditioned media from lipopolysaccharide (LPS) stimulated microglia decreased neuronal differentiation of NPCs. Normal rates of neuronal differentiation were restored with administration of a blocking antibody to IL-6 concurrent with LPS.

A similar decline in NPC proliferation has been demonstrated in the hippocampus *in vivo* in transgenic mice over-expressing IL-6 in astrocytes (Vallieres et al., 2002). Overall these studies suggested that IL-6 adversely affects the proliferation and differentiation of NPCs in the hippocampus. While still in question, the current data is clear in that the inflammatory environment and activation of the pro-inflammatory cascade contributes significantly to the regulation of the hippocampal NPC proliferation and differentiation. The differential regulation properties as a function of cellular source, astrocytes, resident microglia, or infiltrating blood-borne monocytes remains a critical question in addressing the impact of various injuries and neurodegenerative diseases on the neurogenic niche and the NPC population.

1.9 Assessing functional states of microglia

Concepts in assessing the inflammatory response within the injured brain have focused on the functional activation stages of microglia and are derived from biological studies of other mononuclear phagocytes, monocytes and macrophages. Macrophages and monocytes activated by pathogens or cytokines initiate a pro-inflammatory response, which is a tissue defense mechanism specializing in pathogen elimination. This initial activation state has been designated as classical activation, or the M1 activation state, which is characterized by the production of IL-1, IL-6, and TNFα (Gordon, 2003; Mantovani et al., 2005). While the initiation of this response is beneficial for survival of the organism, the immune response is also capable of inducing a toxic environment for the surrounding tissue (Colton and Wilcock, 2009). In order to return damaged tissue to homeostasis, the M1 activation phase is followed by an anti-inflammatory and repair phase. This phase, designated

M2, leads to immunoresolution and wound healing (Mantovani et al., 2005). The M2 activation phase has been further broken down into two subgroups designated alternatively activated and acquired deactivation (Gordon, 2003). These phenotypes have been characterized based on the expression of specific genes, proteins or enzymes associated with the pro- and anti-inflammatory response. In macrophages, the phenotypic change from M1 to M2 has been suggested to be a linear shift with M1 representing one extreme and M2 representing another. However, macrophages as a population appear to exist in a wide range of activation states that depend on the sequence of exposure to various cellular cues (Mosser and Edwards, 2008).

Recently, attempts have been made to translate these markers of activation state from peripheral macrophages to brain microglia/macrophages. Anti-inflammatory molecules expressed in the M2 activation phase include IL-4, IL-10, arginase 1 (AG-I), and transforming growth factor beta 1 (TGFβ1). Molecules associated with the repair phase of M2 activation include BDNF, chitinase 3-like 3 (YM-1), GDNF, and NGF (Colton and Wilcock, 2010; Michelucci et al., 2009). While assessing microglia activation using the M1/M2 phenotypic approach exists as a framework to attempt to classify microglia, it is highly likely that a continuum of intermediate microglia activation states exists (Colton and Wilcock, 2010) as well as cell-cell interactions with other neural cells, including astrocytes. With injury, it is highly likely that the various stages of microglia represent a well-regulated inflammatory response and subsequent down-regulation may provide an environment for NPC proliferation, differentiation and repopulation. Understanding how inflammatory signaling within the injured hippocampus changes during this time

may lead to a better understanding of how the hippocampus is capable of self-repair following injury. Further, the ability to identify a "trigger" that serves to shift microglia from one functional phenotype to another is a critical step in identifying the key regulatory events of neuroinflammation.

1.10 Model of chemical injury-induced neurogenesis

For many injury models associated with increased neurogenesis in the SGZ, there is an associated early death of the dentate granule neurons. While the severity of neuronal loss may be marginal, the early events of cell death and the associated microglia response likely serve as a stimulus for the generation of replacement neurons. Given that SGZ NPC proliferate and mature into dentate granule neurons, an injury model focused selectively on apoptotic damage to this specific neuronal population would allow for the examination of regulatory changes that occurred within the SGZ as well as the dentate granule cell layer.

There are a number of chemicals or surgical manipulations that cause localized damage to the dentate granule neurons such as the microtubule disruptor, colchicine (Goldschmidt and Steward, 1980), viral infection (Gerber et al., 2003; Tauber et al., 2005), and adrenalectomy (Nichols et al., 2005; Spanswick et al., 2011). However, each of these is limited in either a direct effect on the NPC population, the route of administration, the surgery requirement, and the timeframe of the insult. One well established model of chemical induced hippocampal damage is the organometal, trimethyltin (TMT). This compound is used commercially as polyvinyl chloride (PVC) heat stabilizer, catalyst, and in biocides (ATSDR, 2005). More recently, the drinking water contaminant, dimethyltin, has been demonstrated

to undergo endogenous methylation to trimethyltin in rodents and humans, raising a new level of concern for TMT-induced neurotoxicity (Furuhashi et al., 2008). A consistent pattern of susceptibility of the dentate granule neurons has been demonstrated in multiple species, including humans (Fortemps et al., 1978; Kreyberg et al., 1992; Rey et al., 1984). In mice, a single intraperitoneal injection of TMT selectively damages the DG within 24 h, sparing the CA pyramidal cell layer of the hippocampus, with continued cell death lasting until 72 h post-TMT (Cockerill et al., 1987). Microglia and astrocyte activation accompany the DG damage induced by TMT (Fiedorowicz et al., 2001; O'Callaghan, 1991). Further work demonstrated that the response was limited to resident microglia with a lack of infiltrating blood-borne macrophages (Funk et al., 2011). A temporal induction of inflammatory cytokines (IL-1 and TNFα) mRNA is seen during the 72 h of DG granule cell apoptosis and gliosis (Bruccoleri et al., 1998) with evidence that the neuronal death is related to TNF-α signaling (Harry et al., 2008). Previous work demonstrated that within this defined period of neuronal death, a burst of NPC proliferation occurs (Corvino et al., 2005; Ogita et al., 2005) and that these cells mature into dentate granule neurons (Harry et al., 2004). Given the temporal and spatial dynamics of neuronal death, microglia activation, and NPC proliferation, this model system was selected to examine the impact of the microglia response and production of pro-inflammatory cytokines on the NPC proliferation and differentiation occurring as representative of injury-induced hippocampal neurogenesis.

1.11 Scope of this dissertation

The recent paradigm shift with regards to ongoing neurogenesis in the adult brain offers a new model to study the impact of disease, genetics, or environmental exposures on the ability of the brain to restore and maintain normal level of function. While the NPC has received the greatest level of attention over the last few years, research on regulatory and supportive nature of the neurogenic niches for promoting proliferation, cell migration, differentiation, and survival of NPC has gained momentum. This is based on a number of factors, not the least of which is that the neurogenic niche and the cells comprising the niche represent a critical potential target for changes, whether due to genetic background, early life exposure, or direct effect of disease or environmental exposures. It also represents a potential target for pharmacological intervention. Further interest has developed given the influence of inflammatory factors on NPCs with regards to proliferation and differentiation.

Most neurological diseases in humans display a progressive nature with regards to clinical signs; however, recent data suggests that cellular and morphological events in the brain may actually occur in a series of acute events (Combrinck et al., 2002; Cunningham et al., 2008; Cunningham et al., 2005; Meyer-Luehmann et al., 2008). It is possible that one could view such events like acute injury and the associated stimulation of NPCs as representative of the series of events that may occur during aging and age related diseases. The following series of studies was designed to address specific and focused questions with regards to the role and contribution of microglia to the functioning of the neurogenic niche.

In the initial study presented in chapter 2, the interaction of NPCs with microglia and astrocytes was examined in the TMT-induced focal injury to the DG. In the early stages of hippocampal injury and repair following a systemic injection of trimethyltin (TMT), microglia were found in a contact relationship with the newly generated cells. This relationship was predominant in the SGZ and, with migration of the new neurons into the GCL, the primary glial contact shifted to the astrocyte. Given that this region reflected a high inflammatory environment, it was considered that the microglia served in a protective role for the new neurons. In addition, the differential protein expression of TNFp75R in NPCs in the absence of TNFp55R possibly allowed for the new cells to utilize TNFa as a growth factor rather than an inducer of apoptosis.

The next series of studies, detailed in chapter 3, examined the temporal changes in the neurogenic environment and the differentiation of NPCs into functioning dentate granule cells following TMT-induced injury. The neurogenic response was characterized with regard to peak time of NPC proliferation, differentiation and migration of DCX^+ cells, and the subsequent expression of the mature neuronal marker, NeuN, by newly generated cells. Within this time frame of events, microglia cells shifted their morphological phenotype suggesting a possible shift in functional phenotype. This possible shift from injurious to reparative microglia phenotype was evaluated by determining the M1 and M2 immune profile based upon the work from Colton and Wilcock (2010). At defined periods representing different stages of the injury response and repair, the molecular profile of the DG was examined using quantitative real-time polymerase chain reaction

(qRT-PCR) for molecules previously reported to be associated with inflammation, anti-inflammatory, and repair. The functional incorporation of cells generated during the high injury/inflammatory period was confirmed by a recovery of performance on a hippocampal dependent spatial learning and memory task, the Morris Water Maze (MWM), and the performance-dependent activation of the transcription factor Fos in $BrdU^+$ dentate granule neurons. In addition, the structural recovery of the dentate granule cell layer was confirmed by a return to normal dentate neuron number as determined by unbiased stereology.

The final study, detailed in chapter 4, expanded upon the observations in the previous study of an involvement of interluekin-1 and interleukin-6 in defining the various stages of the GCL environment. To further examine the impact of age on the neurogenic capacity and the involvement of the pro-inflammatory cytokines, multiple responses in adolescent mice were compared with responses in the adult 1-year-old mouse. An age-related shift in IL-1α and IL-6 within the SGZ was identified. Upon further examination of primary NPCs cultured from the hippocampus at each age, age-related effects of IL-1α and IL-6 were identified, with IL-1α showing a prominent regulatory role in the young tissue and IL-6 showing a regulatory role in the adult. This data supported a differential effect of pro-inflammatory cytokines on hippocampal NPC self-renewal following injury. In the final chapter, chapter 5, the major findings of the studies are summarized and discussed within the framework of the current level of understanding of injury-induced neurogenesis . Future research directions are identified and discussed within the framework of specific questions and contribution to the field as it currently stands.

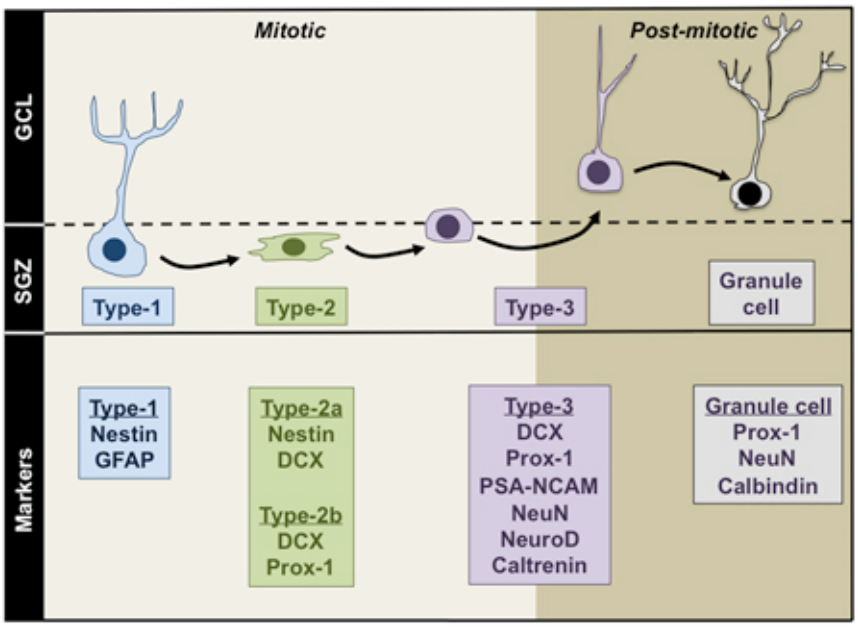

Figure 1.1. Stages of adult hippocampal neurogenesis.
Neural progenitor cells (NPCs) in the hippocampus undergo distinct developmental stages as they are generated in the subgranular zone (SGZ) and migrate into the granule cell layer (GCL). Cells can be identified based on their morphology, proliferative capability, and their expression of lineage specific proteins markers. The type-1 cell is a slow proliferating cell with long apical processes that extend into the GCL and expresses both Nestin and GFAP. Type-2a and type-2b cells are transit amplifying NPCs that express the neural specific markers Nestin, doublecortin (DCX), and prospero homeobox-1 (Prox-1). Type-3 NPCs maintain a limited proliferative capacity and in their later stages of development express mature neuronal markers.

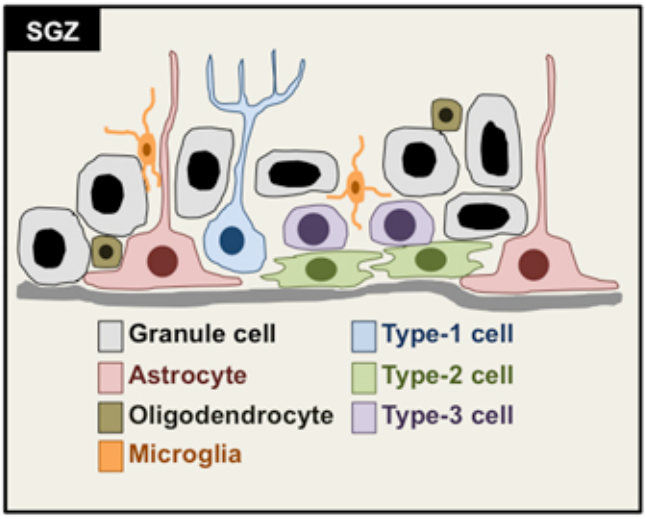

Figure 1.2. Multiple cell types compose the SGZ.
Multiple cell types compose the neurogenic SGZ including: mature granule cells, astrocytes, oligodendrocytes, microglia and the neural progenitor cells (NPCs). These cells as well as the cell-cell contacts and their secreted factors maintain a neurogenic niche, which serves as the primary unit of interaction between the NPCs and their environment.

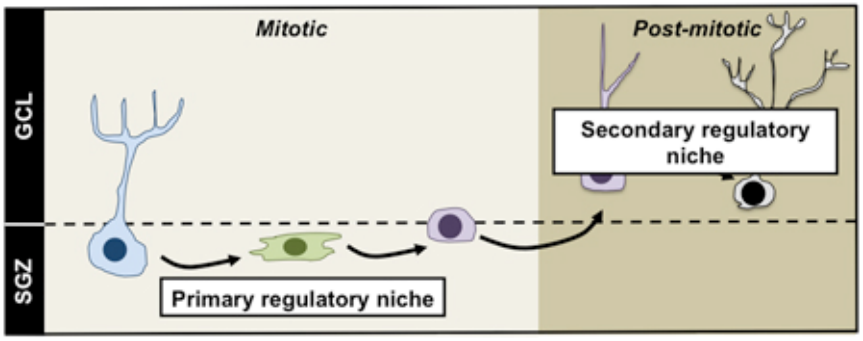

Figure 1.3. NPC regulatory niches in the dentate gyrus.
Adult hippocampal NPCs encounter two neurogenic niches during their development. Within the SGZ or primary niche, cells and secreted factors serve as the primary unit of interaction between NPCs and their environment. In the GCL or secondary niche, the microenvironment of the mature granule cell layer serves as a regulatory site for the migration and maturation of NPCs into neurons or glia.

References

Aarum, J., Sandberg, K., Haeberlein, S.L., Persson, M.A., 2003. Migration and differentiation of neural precursor cells can be directed by microglia. Proc Natl Acad Sci U S A 100, 15983-15988.

Abdo, K.M., Wenk, M.L., Harry, G.J., Mahler, J., Goehl, T.J., Irwin, R.D., 1998. Glycine modulates the toxicity of benzyl acetate in F344 rats. Toxicol Pathol 26, 395-402.

Aberg, M.A., Aberg, N.D., Hedbacker, H., Oscarsson, J., Eriksson, P.S., 2000. Peripheral infusion of IGF-I selectively induces neurogenesis in the adult rat hippocampus. J Neurosci 20, 2896-2903.

Aderka, D., Le, J.M., Vilcek, J., 1989. IL-6 inhibits lipopolysaccharide-induced tumor necrosis factor production in cultured human monocytes, U937 cells, and in mice. J Immunol 143, 3517-3523.

Aloisi, F., Care, A., Borsellino, G., Gallo, P., Rosa, S., Bassani, A., Cabibbo, A., Testa, U., Levi, G., Peschle, C., 1992. Production of hemolymphopoietic cytokines (IL-6, IL-8, colony-stimulating factors) by normal human astrocytes in response to IL-1 beta and tumor necrosis factor-alpha. J Immunol 149, 2358-2366.

Altman, J., 1963. Autoradiographic investigation of cell proliferation in the brains of rats and cats. Anat Rec 145, 573-591.

Altman, J., 1969. Autoradiographic and histological studies of postnatal neurogenesis. IV. Cell proliferation and migration in the anterior forebrain, with special reference to persisting neurogenesis in the olfactory bulb. J Comp Neurol 137, 433-457.

Altman, J., Brunner, R.L., Bayer, S.A., 1973. The hippocampus and behavioral maturation. Behav Biol 8, 557-596.

Altman, J., Das, G.D., 1965. Autoradiographic and histological evidence of postnatal hippocampal neurogenesis in rats. J Comp Neurol 124, 319-335.

Alvarez-Buylla, A., Theelen, M., Nottebohm, F., 1988. Birth of projection neurons in the higher vocal center of the canary forebrain before, during, and after song learning. Proc Natl Acad Sci U S A 85, 8722-8726.

ATSDR, 2005. Toxicological Profiles of tin and tin compounds.

Ban, E.M., 1994. Interleukin-1 receptors in the brain: characterization by quantitative in situ autoradiography. Immunomethods 5, 31-40.

Barkho, B.Z., Song, H., Aimone, J.B., Smrt, R.D., Kuwabara, T., Nakashima, K., Gage, F.H., Zhao, X., 2006. Identification of astrocyte-expressed factors that modulate neural stem/progenitor cell differentiation. Stem Cells Dev 15, 407-421.

Basu, A., Krady, J.K., O'Malley, M., Styren, S.D., DeKosky, S.T., Levison, S.W., 2002. The type 1 interleukin-1 receptor is essential for the efficient activation of microglia and the induction of multiple proinflammatory mediators in response to brain injury. J Neurosci 22, 6071-6082.

Battista, D., Ferrari, C.C., Gage, F.H., Pitossi, F.J., 2006. Neurogenic niche modulation by activated microglia: transforming growth factor beta increases neurogenesis in the adult dentate gyrus. Eur J Neurosci 23, 83-93.

Bayer, S.A., 1983. 3H-thymidine-radiographic studies of neurogenesis in the rat olfactory bulb. Exp Brain Res 50, 329-340.

Ben-Hur, T., Ben-Menachem, O., Furer, V., Einstein, O., Mizrachi-Kol, R., Grigoriadis, N., 2003. Effects of proinflammatory cytokines on the growth, fate, and motility of multipotential neural precursor cells. Mol Cell Neurosci 24, 623-631.

Bengzon, J., Kokaia, Z., Elmer, E., Nanobashvili, A., Kokaia, M., Lindvall, O., 1997. Apoptosis and proliferation of dentate gyrus neurons after single and intermittent limbic seizures. Proc Natl Acad Sci U S A 94, 10432-10437.

Bernabeu, R., Sharp, F.R., 2000. NMDA and AMPA/kainate glutamate receptors modulate dentate neurogenesis and CA3 synapsin-I in normal and ischemic hippocampus. J Cereb Blood Flow Metab 20, 1669-1680.

Bhagat, Y.A., Obenaus, A., Hamilton, M.G., Mikler, J., Kendall, E.J., 2005. Neuroprotection from soman-induced seizures in the rodent: evaluation with

diffusion- and T2-weighted magnetic resonance imaging. Neurotoxicology 26, 1001-1013.

Biebl, M., Cooper, C.M., Winkler, J., Kuhn, H.G., 2000. Analysis of neurogenesis and programmed cell death reveals a self-renewing capacity in the adult rat brain. Neurosci Lett 291, 17-20.

Brandt, M.D., Jessberger, S., Steiner, B., Kronenberg, G., Reuter, K., Bick-Sander, A., von der Behrens, W., Kempermann, G., 2003. Transient calretinin expression defines early postmitotic step of neuronal differentiation in adult hippocampal neurogenesis of mice. Mol Cell Neurosci 24, 603-613.

Brezun, J.M., Daszuta, A., 1999. Depletion in serotonin decreases neurogenesis in the dentate gyrus and the subventricular zone of adult rats. Neuroscience 89, 999-1002.

Brown, J.P., Couillard-Despres, S., Cooper-Kuhn, C.M., Winkler, J., Aigner, L., Kuhn, H.G., 2003. Transient expression of doublecortin during adult neurogenesis. J Comp Neurol 467, 1-10.

Bruccoleri, A., Brown, H., Harry, G.J., 1998. Cellular localization and temporal elevation of tumor necrosis factor-alpha, interleukin-1 alpha, and transforming growth factor-beta 1 mRNA in hippocampal injury response induced by trimethyltin. J Neurochem 71, 1577-1587.

Bull, N.D., Bartlett, P.F., 2005. The adult mouse hippocampal progenitor is neurogenic but not a stem cell. J Neurosci 25, 10815-10821.

Burd, G.D., Nottebohm, F., 1985. Ultrastructural characterization of synaptic terminals formed on newly generated neurons in a song control nucleus of the adult canary forebrain. J Comp Neurol 240, 143-152.

Cacci, E., Claasen, J.H., Kokaia, Z., 2005. Microglia-derived tumor necrosis factor-alpha exaggerates death of newborn hippocampal progenitor cells in vitro. J Neurosci Res 80, 789-797.

Cameron, H.A., Gould, E., 1994. Adult neurogenesis is regulated by adrenal steroids in the dentate gyrus. Neuroscience 61, 203-209.

Cameron, H.A., McEwen, B.S., Gould, E., 1995. Regulation of adult neurogenesis by excitatory input and NMDA receptor activation in the dentate gyrus. J Neurosci 15, 4687-4692.

Cameron, H.A., Woolley, C.S., McEwen, B.S., Gould, E., 1993. Differentiation of newly born neurons and glia in the dentate gyrus of the adult rat. Neuroscience 56, 337-344.

Chang, L.W., Tiemeyer, T.M., Wenger, G.R., McMillan, D.E., 1982. Neuropathology of mouse hippocampus in acute trimethyltin intoxication. Neurobehav Toxicol Teratol 4, 149-156.

Changeux, J.P., Danchin, A., 1976. Selective stabilisation of developing synapses as a mechanism for the specification of neuronal networks. Nature 264, 705-712.

Chen, Y., Ai, Y., Slevin, J.R., Maley, B.E., Gash, D.M., 2005. Progenitor proliferation in the adult hippocampus and substantia nigra induced by glial cell line-derived neurotrophic factor. Exp Neurol 196, 87-95.

Clark, R.S., Kochanek, P.M., Dixon, C.E., Chen, M., Marion, D.W., Heineman, S., DeKosky, S.T., Graham, S.H., 1997. Early neuropathologic effects of mild or moderate hypoxemia after controlled cortical impact injury in rats. J Neurotrauma 14, 179-189.

Cockerill, D., Chang, L.W., Hough, A., Bivins, F., 1987. Effects of trimethyltin on the mouse hippocampus and adrenal cortex. J Toxicol Environ Health 22, 149-161.

Collombet, J.M., Four, E., Bernabe, D., Masqueliez, C., Burckhart, M.F., Baille, V., Baubichon, D., Lallement, G., 2005. Soman poisoning increases neural progenitor proliferation and induces long-term glial activation in mouse brain. Toxicology 208, 319-334.

Colton, C.A., Wilcock, D.M., 2009. Assessing Activation States in Microglia. CNS Neurol Disord Drug Targets.

Colton, C.A., Wilcock, D.M., 2010. Assessing activation states in microglia. CNS Neurol Disord Drug Targets 9, 174-191.

Combrinck, M.I., Perry, V.H., Cunningham, C., 2002. Peripheral infection evokes exaggerated sickness behaviour in pre-clinical murine prion disease. Neuroscience 112, 7-11.

Cooper-Kuhn, C.M., Winkler, J., Kuhn, H.G., 2004. Decreased neurogenesis after cholinergic forebrain lesion in the adult rat. J Neurosci Res 77, 155-165.

Corvino, V., Geloso, M.C., Cavallo, V., Guadagni, E., Passalacqua, R., Florenzano, F., Giannetti, S., Molinari, M., Michetti, F., 2005. Enhanced neurogenesis during trimethyltin-induced neurodegeneration in the hippocampus of the adult rat. Brain Res Bull 65, 471-477.

Cunningham, C., Campion, S., Lunnon, K., Murray, C.L., Woods, J.F., Deacon, R.M., Rawlins, J.N., Perry, V.H., 2008. Systemic Inflammation Induces Acute Behavioral and Cognitive Changes and Accelerates Neurodegenerative Disease. Biol Psychiatry.

Cunningham, C., Wilcockson, D.C., Campion, S., Lunnon, K., Perry, V.H., 2005. Central and systemic endotoxin challenges exacerbate the local inflammatory response and increase neuronal death during chronic neurodegeneration. J Neurosci 25, 9275-9284.

Cunningham, E.T., Jr., Wada, E., Carter, D.B., Tracey, D.E., Battey, J.F., De Souza, E.B., 1992. In situ histochemical localization of type I interleukin-1 receptor messenger RNA in the central nervous system, pituitary, and adrenal gland of the mouse. J Neurosci 12, 1101-1114.

Dam, A.M., 1980. Epilepsy and neuron loss in the hippocampus. Epilepsia 21, 617-629.

Davalos, D., Grutzendler, J., Yang, G., Kim, J.V., Zuo, Y., Jung, S., Littman, D.R., Dustin, M.L., Gan, W.B., 2005. ATP mediates rapid microglial response to local brain injury in vivo. Nat Neurosci 8, 752-758.

Dinarello, C.A., 1996. Biologic basis for interleukin-1 in disease. Blood 87, 2095-2147.

Eckenhoff, M.F., Rakic, P., 1988. Nature and fate of proliferative cells in the hippocampal dentate gyrus during the life span of the rhesus monkey. J Neurosci 8, 2729-2747.

Eichenbaum, H., Otto, T., Cohen, N.J., 1992. The hippocampus--what does it do? Behav Neural Biol 57, 2-36.

Ekdahl, C.T., Claasen, J.H., Bonde, S., Kokaia, Z., Lindvall, O., 2003. Inflammation is detrimental for neurogenesis in adult brain. Proc Natl Acad Sci U S A 100, 13632-13637.

Ekdahl, C.T., Kokaia, Z., Lindvall, O., 2009. Brain inflammation and adult neurogenesis: the dual role of microglia. Neuroscience 158, 1021-1029.

Encinas, J.M., Vaahtokari, A., Enikolopov, G., 2006. Fluoxetine targets early progenitor cells in the adult brain. Proc Natl Acad Sci U S A 103, 8233-8238.

Eriksson, P.S., Perfilieva, E., Bjork-Eriksson, T., Alborn, A.M., Nordborg, C., Peterson, D.A., Gage, F.H., 1998. Neurogenesis in the adult human hippocampus. Nat Med 4, 1313-1317.

Fiedorowicz, A., Figiel, I., Kaminska, B., Zaremba, M., Wilk, S., Oderfeld-Nowak, B., 2001. Dentate granule neuron apoptosis and glia activation in murine hippocampus induced by trimethyltin exposure. Brain Res 912, 116-127.

Filippov, V., Kronenberg, G., Pivneva, T., Reuter, K., Steiner, B., Wang, L.P., Yamaguchi, M., Kettenmann, H., Kempermann, G., 2003. Subpopulation of nestin-expressing progenitor cells in the adult murine hippocampus shows electrophysiological and morphological characteristics of astrocytes. Mol Cell Neurosci 23, 373-382.

Fortemps, E., Amand, G., Bomboir, A., Lauwerys, R., Laterre, E.C., 1978. Trimethyltin poisoning. Report of two cases. Int Arch Occup Environ Health 41, 1-6.

Fricker, R.A., Carpenter, M.K., Winkler, C., Greco, C., Gates, M.A., Bjorklund, A., 1999. Site-specific migration and neuronal differentiation of human neural progenitor cells after transplantation in the adult rat brain. J Neurosci 19, 5990-6005.

Frielingsdorf, H., Simpson, D.R., Thal, L.J., Pizzo, D.P., 2007. Nerve growth factor promotes survival of new neurons in the adult hippocampus. Neurobiol Dis 26, 47-55.

Fukuda, S., Kato, F., Tozuka, Y., Yamaguchi, M., Miyamoto, Y., Hisatsune, T., 2003. Two distinct subpopulations of nestin-positive cells in adult mouse dentate gyrus. J Neurosci 23, 9357-9366.

Funk, J.A., Gohlke, J., Kraft, A.D., McPherson, C.A., Collins, J.B., Jean Harry, G., 2011. Voluntary exercise protects hippocampal neurons from trimethyltin injury: Possible role of interleukin-6 to modulate tumor necrosis factor receptor-mediated neurotoxicity. Brain Behav Immun.

Furuhashi, K., Ogawa, M., Suzuki, Y., Endo, Y., Kim, Y., Ichihara, G., 2008. Methylation of dimethyltin in mice and rats. Chem Res Toxicol 21, 467-471.

Gadient, R.A., Otten, U.H., 1997. Interleukin-6 (IL-6)--a molecule with both beneficial and destructive potentials. Prog Neurobiol 52, 379-390.

Gerber, J., Bottcher, T., Bering, J., Bunkowski, S., Bruck, W., Kuhnt, U., Nau, R., 2003. Increased neurogenesis after experimental Streptococcus pneumoniae meningitis. J Neurosci Res 73, 441-446.

Gilbert, M.E., Kelly, M.E., Samsam, T.E., Goodman, J.H., 2005. Chronic developmental lead exposure reduces neurogenesis in adult rat hippocampus but does not impair spatial learning. Toxicol Sci 86, 365-374.

Goldman, S.A., Nottebohm, F., 1983. Neuronal production, migration, and differentiation in a vocal control nucleus of the adult female canary brain. Proc Natl Acad Sci U S A 80, 2390-2394.

Goldschmidt, R.B., Steward, O., 1980. Preferential neurotoxicity of colchicine for granule cells of the dentate gyrus of the adult rat. Proc Natl Acad Sci U S A 77, 3047-3051.

Gordon, S., 2003. Alternative activation of macrophages. Nat Rev Immunol 3, 23-35.

Gould, E., 2007. How widespread is adult neurogenesis in mammals? Nat Rev Neurosci 8, 481-488.

Gould, E., Reeves, A.J., Fallah, M., Tanapat, P., Gross, C.G., Fuchs, E., 1999. Hippocampal neurogenesis in adult Old World primates. Proc Natl Acad Sci U S A 96, 5263-5267.

Gould, E., Tanapat, P., McEwen, B.S., Flugge, G., Fuchs, E., 1998. Proliferation of granule cell precursors in the dentate gyrus of adult monkeys is diminished by stress. Proc Natl Acad Sci U S A 95, 3168-3171.

Greenfeder, S.A., Nunes, P., Kwee, L., Labow, M., Chizzonite, R.A., Ju, G., 1995. Molecular cloning and characterization of a second subunit of the interleukin 1 receptor complex. J Biol Chem 270, 13757-13765.

Harry, G.J., Lefebvre d'Hellencourt, C., 2003. Dentate gyrus: alterations that occur with hippocampal injury. Neurotoxicology 24, 343-356.

Harry, G.J., Lefebvre d'Hellencourt, C., McPherson, C.A., Funk, J.A., Aoyama, M., Wine, R.N., 2008. Tumor necrosis factor p55 and p75 receptors are involved in chemical-induced apoptosis of dentate granule neurons. J Neurochem 106, 281-298.

Harry, G.J., McPherson, C.A., Wine, R.N., Atkinson, K., Lefebvre d'Hellencourt, C., 2004. Trimethyltin-induced neurogenesis in the murine hippocampus. Neurotox Res 5, 623-627.

Hastings, N.B., Gould, E., 1999. Rapid extension of axons into the CA3 region by adult-generated granule cells. J Comp Neurol 413, 146-154.

Hattiangady, B., Rao, M.S., Shetty, A.K., 2008. Plasticity of hippocampal stem/progenitor cells to enhance neurogenesis in response to kainate-induced injury is lost by middle age. Aging Cell 7, 207-224.

Iosif, R.E., Ekdahl, C.T., Ahlenius, H., Pronk, C.J., Bonde, S., Kokaia, Z., Jacobsen, S.E., Lindvall, O., 2006. Tumor necrosis factor receptor 1 is a negative regulator of progenitor proliferation in adult hippocampal neurogenesis. J Neurosci 26, 9703-9712.

Jakubs, K., Nanobashvili, A., Bonde, S., Ekdahl, C.T., Kokaia, Z., Kokaia, M., Lindvall, O., 2006. Environment matters: synaptic properties of neurons born in the epileptic adult brain develop to reduce excitability. Neuron 52, 1047-1059.

Jin, K., Minami, M., Lan, J.Q., Mao, X.O., Batteur, S., Simon, R.P., Greenberg, D.A., 2001. Neurogenesis in dentate subgranular zone and rostral subventricular zone after focal cerebral ischemia in the rat. Proc Natl Acad Sci U S A 98, 4710-4715.

Jin, K., Zhu, Y., Sun, Y., Mao, X.O., Xie, L., Greenberg, D.A., 2002. Vascular endothelial growth factor (VEGF) stimulates neurogenesis in vitro and in vivo. Proc Natl Acad Sci U S A 99, 11946-11950.

Kaneko, N., Kudo, K., Mabuchi, T., Takemoto, K., Fujimaki, K., Wati, H., Iguchi, H., Tezuka, H., Kanba, S., 2006. Suppression of cell proliferation by interferon-alpha through interleukin-1 production in adult rat dentate gyrus. Neuropsychopharmacology 31, 2619-2626.

Kaplan, M.S., 1981. Neurogenesis in the 3-month-old rat visual cortex. J Comp Neurol 195, 323-338.

Kaplan, M.S., Bell, D.H., 1984. Mitotic neuroblasts in the 9-day-old and 11-month-old rodent hippocampus. J Neurosci 4, 1429-1441.

Kaplan, M.S., Hinds, J.W., 1977. Neurogenesis in the adult rat: electron microscopic analysis of light radioautographs. Science 197, 1092-1094.

Kee, N., Teixeira, C.M., Wang, A.H., Frankland, P.W., 2007. Preferential incorporation of adult-generated granule cells into spatial memory networks in the dentate gyrus. Nat Neurosci 10, 355-362.

Keiner, S., Walter, J., Oberland, J., Redecker, C., 2010. Contribution of constitutively proliferating precursor cell subtypes to dentate neurogenesis after cortical infarcts. BMC Neurosci 11, 146.

Kempermann, G., Gast, D., Kronenberg, G., Yamaguchi, M., Gage, F.H., 2003. Early determination and long-term persistence of adult-generated new neurons in the hippocampus of mice. Development 130, 391-399.

Kempermann, G., Kuhn, H.G., Gage, F.H., 1997. More hippocampal neurons in adult mice living in an enriched environment. Nature 386, 493-495.

Kim, M.S., Park, H.R., Park, M., Kim, S.J., Kwon, M., Yu, B.P., Chung, H.Y., Kim, H.S., Kwack, S.J., Kang, T.S., Kim, S.H., Lee, J., 2009. Neurotoxic effect of 2,5-hexanedione on neural progenitor cells and hippocampal neurogenesis. Toxicology 260, 97-103.

Kishimoto, T., Akira, S., Taga, T., 1992. Interleukin-6 and its receptor: a paradigm for cytokines. Science 258, 593-597.

Klassen, H.J., Imfeld, K.L., Kirov, II, Tai, L., Gage, F.H., Young, M.J., Berman, M.A., 2003. Expression of cytokines by multipotent neural progenitor cells. Cytokine 22, 101-106.

Klempin, F., Kempermann, G., 2007. Adult hippocampal neurogenesis and aging. Eur Arch Psychiatry Clin Neurosci 257, 271-280.

Koo, J.W., Duman, R.S., 2008. IL-1beta is an essential mediator of the antineurogenic and anhedonic effects of stress. Proc Natl Acad Sci U S A 105, 751-756.

Kornack, D.R., Rakic, P., 1999. Continuation of neurogenesis in the hippocampus of the adult macaque monkey. Proc Natl Acad Sci U S A 96, 5768-5773.

Kreutzberg, G.W., 1996. Microglia: a sensor for pathological events in the CNS. Trends Neurosci 19, 312-318.

Kreyberg, S., Torvik, A., Bjorneboe, A., Wiik-Larsen, W., Jacobsen, D., 1992. Trimethyltin poisoning: report of a case with postmortem examination. Clin Neuropathol 11, 256-259.

Kronenberg, G., Reuter, K., Steiner, B., Brandt, M.D., Jessberger, S., Yamaguchi, M., Kempermann, G., 2003. Subpopulations of proliferating cells of the adult hippocampus respond differently to physiologic neurogenic stimuli. J Comp Neurol 467, 455-463.

Kuhn, H.G., Dickinson-Anson, H., Gage, F.H., 1996. Neurogenesis in the dentate gyrus of the adult rat: age-related decrease of neuronal progenitor proliferation. J Neurosci 16, 2027-2033.

Kulkarni, V.A., Jha, S., Vaidya, V.A., 2002. Depletion of norepinephrine decreases the proliferation, but does not influence the survival and differentiation, of granule cell progenitors in the adult rat hippocampus. Eur J Neurosci 16, 2008-2012.

Larsson, E., Mandel, R.J., Klein, R.L., Muzyczka, N., Lindvall, O., Kokaia, Z., 2002. Suppression of insult-induced neurogenesis in adult rat brain by brain-derived neurotrophic factor. Exp Neurol 177, 1-8.

Liu, J., Solway, K., Messing, R.O., Sharp, F.R., 1998. Increased neurogenesis in the dentate gyrus after transient global ischemia in gerbils. J Neurosci 18, 7768-7778.

Lledo, P.M., Alonso, M., Grubb, M.S., 2006. Adult neurogenesis and functional plasticity in neuronal circuits. Nat Rev Neurosci 7, 179-193.

Lu, M., Grove, E.A., Miller, R.J., 2002. Abnormal development of the hippocampal dentate gyrus in mice lacking the CXCR4 chemokine receptor. Proc Natl Acad Sci U S A 99, 7090-7095.

Madsen, T.M., Kristjansen, P.E., Bolwig, T.G., Wortwein, G., 2003. Arrested neuronal proliferation and impaired hippocampal function following fractionated brain irradiation in the adult rat. Neuroscience 119, 635-642.

Mantovani, A., Sica, A., Locati, M., 2005. Macrophage polarization comes of age. Immunity 23, 344-346.

Martin, S.J., Clark, R.E., 2007. The rodent hippocampus and spatial memory: from synapses to systems. Cell Mol Life Sci 64, 401-431.

Mattocks, M., Tropepe, V., 2010. Waste management and adult neurogenesis. Cell Stem Cell 7, 421-422.

McCullers, D.L., Sullivan, P.G., Scheff, S.W., Herman, J.P., 2002. Traumatic brain injury regulates adrenocorticosteroid receptor mRNA levels in rat hippocampus. Brain Res 947, 41-49.

McDonald, H.Y., Wojtowicz, J.M., 2005. Dynamics of neurogenesis in the dentate gyrus of adult rats. Neurosci Lett 385, 70-75.

Meshi, D., Drew, M.R., Saxe, M., Ansorge, M.S., David, D., Santarelli, L., Malapani, C., Moore, H., Hen, R., 2006. Hippocampal neurogenesis is not required for behavioral effects of environmental enrichment. Nat Neurosci 9, 729-731.

Meyer-Luehmann, M., Spires-Jones, T.L., Prada, C., Garcia-Alloza, M., de Calignon, A., Rozkalne, A., Koenigsknecht-Talboo, J., Holtzman, D.M., Bacskai, B.J., Hyman, B.T., 2008. Rapid appearance and local toxicity of amyloid-beta plaques in a mouse model of Alzheimer's disease. Nature 451, 720-724.

Micheau, O., Tschopp, J., 2003. Induction of TNF receptor I-mediated apoptosis via two sequential signaling complexes. Cell 114, 181-190.

Michelucci, A., Heurtaux, T., Grandbarbe, L., Morga, E., Heuschling, P., 2009. Characterization of the microglial phenotype under specific pro-inflammatory and anti-inflammatory conditions: Effects of oligomeric and fibrillar amyloid-beta. J Neuroimmunol 210, 3-12.

Monje, M.L., Toda, H., Palmer, T.D., 2003. Inflammatory blockade restores adult hippocampal neurogenesis. Science 302, 1760-1765.

Moore, K.A., Lemischka, I.R., 2006. Stem cells and their niches. Science 311, 1880-1885.

Morrison, S.J., Spradling, A.C., 2008. Stem cells and niches: mechanisms that promote stem cell maintenance throughout life. Cell 132, 598-611.

Mosser, D.M., Edwards, J.P., 2008. Exploring the full spectrum of macrophage activation. Nat Rev Immunol 8, 958-969.

Nichols, N.R., Agolley, D., Zieba, M., Bye, N., 2005. Glucocorticoid regulation of glial responses during hippocampal neurodegeneration and regeneration. Brain Res Brain Res Rev 48, 287-301.

Nimmerjahn, A., Kirchhoff, F., Helmchen, F., 2005. Resting microglial cells are highly dynamic surveillants of brain parenchyma in vivo. Science 308, 1314-1318.

Norris, J.G., Tang, L.P., Sparacio, S.M., Benveniste, E.N., 1994. Signal transduction pathways mediating astrocyte IL-6 induction by IL-1 beta and tumor necrosis factor-alpha. J Immunol 152, 841-850.

O'Callaghan, J.P., 1991. Quantification of glial fibrillary acidic protein: comparison of slot-immunobinding assays with a novel sandwich ELISA. Neurotoxicol Teratol 13, 275-281.

Obernier, J.A., Bouldin, T.W., Crews, F.T., 2002. Binge ethanol exposure in adult rats causes necrotic cell death. Alcohol Clin Exp Res 26, 547-557.

Ogita, K., Nishiyama, N., Sugiyama, C., Higuchi, K., Yoneyama, M., Yoneda, Y., 2005. Regeneration of granule neurons after lesioning of hippocampal dentate gyrus: evaluation using adult mice treated with trimethyltin chloride as a model. J Neurosci Res 82, 609-621.

Palmer, T.D., Markakis, E.A., Willhoite, A.R., Safar, F., Gage, F.H., 1999. Fibroblast growth factor-2 activates a latent neurogenic program in neural stem cells from diverse regions of the adult CNS. J Neurosci 19, 8487-8497.

Palmer, T.D., Ray, J., Gage, F.H., 1995. FGF-2-responsive neuronal progenitors reside in proliferative and quiescent regions of the adult rodent brain. Mol Cell Neurosci 6, 474-486.

Palmer, T.D., Takahashi, J., Gage, F.H., 1997. The adult rat hippocampus contains primordial neural stem cells. Mol Cell Neurosci 8, 389-404.

Pitossi, F., del Rey, A., Kabiersch, A., Besedovsky, H., 1997. Induction of cytokine transcripts in the central nervous system and pituitary following peripheral administration of endotoxin to mice. J Neurosci Res 48, 287-298.

Rakic, P., 1974. Neurons in rhesus monkey visual cortex: systematic relation between time of origin and eventual disposition. Science 183, 425-427.

Rakic, P., 1985. Limits of neurogenesis in primates. Science 227, 1054-1056.

Ramon y Cajal, S., 1928. Degeneration and regeneration of the nervous system. Oxford University Press, London.

Rao, M.S., Hattiangady, B., Abdel-Rahman, A., Stanley, D.P., Shetty, A.K., 2005. Newly born cells in the ageing dentate gyrus display normal migration, survival and neuronal fate choice but endure retarded early maturation. Eur J Neurosci 21, 464-476.

Reuhl, K.R., Cranmer, J.M., 1984. Developmental neuropathology of organotin compounds. Neurotoxicology 5, 187-204.

Rey, C., Reinecke, H.J., Besser, R., 1984. Methyltin intoxication in six men; toxicologic and clinical aspects. Vet Hum Toxicol 26, 121-122.

Reynolds, B.A., Rietze, R.L., 2005. Neural stem cells and neurospheres--re-evaluating the relationship. Nat Methods 2, 333-336.

Rivas-Arancibia, S., Guevara-Guzman, R., Lopez-Vidal, Y., Rodriguez-Martinez, E., Zanardo-Gomes, M., Angoa-Perez, M., Raisman-Vozari, R., 2010. Oxidative stress caused by ozone exposure induces loss of brain repair in the hippocampus of adult rats. Toxicol Sci 113, 187-197.

Saxe, M.D., Battaglia, F., Wang, J.W., Malleret, G., David, D.J., Monckton, J.E., Garcia, A.D., Sofroniew, M.V., Kandel, E.R., Santarelli, L., Hen, R., Drew, M.R., 2006. Ablation of hippocampal neurogenesis impairs contextual fear conditioning and synaptic plasticity in the dentate gyrus. Proc Natl Acad Sci U S A 103, 17501-17506.

Schindler, R., Mancilla, J., Endres, S., Ghorbani, R., Clark, S.C., Dinarello, C.A., 1990. Correlations and interactions in the production of interleukin-6 (IL-6), IL-1, and tumor necrosis factor (TNF) in human blood mononuclear cells: IL-6 suppresses IL-1 and TNF. Blood 75, 40-47.

Schmidt-Hieber, C., Jonas, P., Bischofberger, J., 2004. Enhanced synaptic plasticity in newly generated granule cells of the adult hippocampus. Nature 429, 184-187.

Schofield, R., 1978. The relationship between the spleen colony-forming cell and the haemopoietic stem cell. Blood Cells 4, 7-25.

Seaberg, R.M., van der Kooy, D., 2002. Adult rodent neurogenic regions: the ventricular subependyma contains neural stem cells, but the dentate gyrus contains restricted progenitors. J Neurosci 22, 1784-1793.

Seaberg, R.M., van der Kooy, D., 2003. Stem and progenitor cells: the premature desertion of rigorous definitions. Trends Neurosci 26, 125-131.

Seo, H.S., Yang, M., Song, M.S., Kim, J.S., Kim, S.H., Kim, J.C., Kim, H., Shin, T., Wang, H., Moon, C., 2010. Toluene inhibits hippocampal neurogenesis in adult mice. Pharmacol Biochem Behav 94, 588-594.

Seri, B., Garcia-Verdugo, J.M., Collado-Morente, L., McEwen, B.S., Alvarez-Buylla, A., 2004. Cell types, lineage, and architecture of the germinal zone in the adult dentate gyrus. J Comp Neurol 478, 359-378.

Seri, B., Garcia-Verdugo, J.M., McEwen, B.S., Alvarez-Buylla, A., 2001. Astrocytes give rise to new neurons in the adult mammalian hippocampus. J Neurosci 21, 7153-7160.

Shen, Y., Li, R., Shiosaki, K., 1997. Inhibition of p75 tumor necrosis factor receptor by antisense oligonucleotides increases hypoxic injury and beta-amyloid toxicity in human neuronal cell line. J Biol Chem 272, 3550-3553.

Sheng, W.S., Hu, S., Ni, H.T., Rowen, T.N., Lokensgard, J.R., Peterson, P.K., 2005. TNF-alpha-induced chemokine production and apoptosis in human neural precursor cells. J Leukoc Biol 78, 1233-1241.

Shetty, A.K., Hattiangady, B., Rao, M.S., Shuai, B., 2010. Deafferentation enhances neurogenesis in the young and middle aged hippocampus but not in the aged hippocampus. Hippocampus.

Shors, T.J., Miesegaes, G., Beylin, A., Zhao, M., Rydel, T., Gould, E., 2001. Neurogenesis in the adult is involved in the formation of trace memories. Nature 410, 372-376.

Shors, T.J., Townsend, D.A., Zhao, M., Kozorovitskiy, Y., Gould, E., 2002. Neurogenesis may relate to some but not all types of hippocampal-dependent learning. Hippocampus 12, 578-584.

Sierra, A., Encinas, J.M., Deudero, J.J., Chancey, J.H., Enikolopov, G., Overstreet-Wadiche, L.S., Tsirka, S.E., Maletic-Savatic, M., 2010. Microglia shape adult hippocampal neurogenesis through apoptosis-coupled phagocytosis. Cell Stem Cell 7, 483-495.

Siren, A.L., Lewczuk, P., Hasselblatt, M., Dembowski, C., Schilling, L., Ehrenreich, H., 2002. Endothelin B receptor deficiency augments neuronal damage upon exposure to hypoxia-ischemia in vivo. Brain Res 945, 144-149.

Sloviter, R.S., Dean, E., Sollas, A.L., Goodman, J.H., 1996. Apoptosis and necrosis induced in different hippocampal neuron populations by repetitive perforant path stimulation in the rat. J Comp Neurol 366, 516-533.

Smith, D.H., Lowenstein, D.H., Gennarelli, T.A., McIntosh, T.K., 1994. Persistent memory dysfunction is associated with bilateral hippocampal damage following experimental brain injury. Neurosci Lett 168, 151-154.

Snyder, J.S., Choe, J.S., Clifford, M.A., Jeurling, S.I., Hurley, P., Brown, A., Kamhi, J.F., Cameron, H.A., 2009. Adult-born hippocampal neurons are more numerous, faster maturing, and more involved in behavior in rats than in mice. J Neurosci 29, 14484-14495.

Song, H., Stevens, C.F., Gage, F.H., 2002. Astroglia induce neurogenesis from adult neural stem cells. Nature 417, 39-44.

Spanswick, S.C., Epp, J.R., Sutherland, R.J., 2011. Time-course of hippocampal granule cell degeneration and changes in adult neurogenesis after adrenalectomy in rats. Neuroscience 190, 166-176.

Spulber, S., Oprica, M., Bartfai, T., Winblad, B., Schultzberg, M., 2008. Blunted neurogenesis and gliosis due to transgenic overexpression of human soluble IL-1ra in the mouse. Eur J Neurosci 27, 549-558.

Steiner, B., Kronenberg, G., Jessberger, S., Brandt, M.D., Reuter, K., Kempermann, G., 2004. Differential regulation of gliogenesis in the context of adult hippocampal neurogenesis in mice. Glia 46, 41-52.

Suh, H., Consiglio, A., Ray, J., Sawai, T., D'Amour, K.A., Gage, F.H., 2007. In vivo fate analysis reveals the multipotent and self-renewal capacities of Sox2+ neural stem cells in the adult hippocampus. Cell Stem Cell 1, 515-528.

Tanapat, P., Hastings, N.B., Reeves, A.J., Gould, E., 1999. Estrogen stimulates a transient increase in the number of new neurons in the dentate gyrus of the adult female rat. J Neurosci 19, 5792-5801.

Tanapat, P., Hastings, N.B., Rydel, T.A., Galea, L.A., Gould, E., 2001. Exposure to fox odor inhibits cell proliferation in the hippocampus of adult rats via an adrenal hormone-dependent mechanism. J Comp Neurol 437, 496-504.

Tang, F.R., Lee, W.L., Yeo, T.T., 2001. Expression of the group I metabotropic glutamate receptor in the hippocampus of patients with mesial temporal lobe epilepsy. J Neurocytol 30, 403-411.

Tauber, S.C., Stadelmann, C., Spreer, A., Bruck, W., Nau, R., Gerber, J., 2005. Increased expression of BDNF and proliferation of dentate granule cells after bacterial meningitis. J Neuropathol Exp Neurol 64, 806-815.

Thorburn, A., 2004. Death receptor-induced cell killing. Cell Signal 16, 139-144.

Tilg, H., Trehu, E., Atkins, M.B., Dinarello, C.A., Mier, J.W., 1994. Interleukin-6 (IL-6) as an anti-inflammatory cytokine: induction of circulating IL-1 receptor antagonist and soluble tumor necrosis factor receptor p55. Blood 83, 113-118.

Toni, N., Laplagne, D.A., Zhao, C., Lombardi, G., Ribak, C.E., Gage, F.H., Schinder, A.F., 2008. Neurons born in the adult dentate gyrus form functional synapses with target cells. Nat Neurosci 11, 901-907.

Toni, N., Teng, E.M., Bushong, E.A., Aimone, J.B., Zhao, C., Consiglio, A., van Praag, H., Martone, M.E., Ellisman, M.H., Gage, F.H., 2007. Synapse formation on neurons born in the adult hippocampus. Nat Neurosci 10, 727-734.

Tureyen, K., Vemuganti, R., Sailor, K.A., Bowen, K.K., Dempsey, R.J., 2004. Transient focal cerebral ischemia-induced neurogenesis in the dentate gyrus of the adult mouse. J Neurosurg 101, 799-805.

Ulich, T.R., Yin, S., Guo, K., Yi, E.S., Remick, D., del Castillo, J., 1991. Intratracheal injection of endotoxin and cytokines. II. Interleukin-6 and transforming growth factor beta inhibit acute inflammation. Am J Pathol 138, 1097-1101.

Vallieres, L., Campbell, I.L., Gage, F.H., Sawchenko, P.E., 2002. Reduced hippocampal neurogenesis in adult transgenic mice with chronic astrocytic production of interleukin-6. J Neurosci 22, 486-492.

van Praag, H., Kempermann, G., Gage, F.H., 1999. Running increases cell proliferation and neurogenesis in the adult mouse dentate gyrus. Nat Neurosci 2, 266-270.

van Praag, H., Schinder, A.F., Christie, B.R., Toni, N., Palmer, T.D., Gage, F.H., 2002. Functional neurogenesis in the adult hippocampus. Nature 415, 1030-1034.

Vollmayr, B., Simonis, C., Weber, S., Gass, P., Henn, F., 2003. Reduced cell proliferation in the dentate gyrus is not correlated with the development of learned helplessness. Biol Psychiatry 54, 1035-1040.

Wang, H.D., Fukuda, T., Suzuki, T., Hashimoto, K., Liou, S.Y., Momoi, T., Kosaka, T., Yamamoto, K., Nakanishi, H., 1999. Differential effects of Bcl-2 overexpression on hippocampal CA1 neurons and dentate granule cells following hypoxic ischemia in adult mice. J Neurosci Res 57, 1-12.

Wang, S., Kee, N., Preston, E., Wojtowicz, J.M., 2005. Electrophysiological correlates of neural plasticity compensating for ischemia-induced damage in the hippocampus. Exp Brain Res 165, 250-260.

Yagita, Y., Kitagawa, K., Ohtsuki, T., Takasawa, K., Miyata, T., Okano, H., Hori, M., Matsumoto, M., 2001. Neurogenesis by progenitor cells in the ischemic adult rat hippocampus. Stroke 32, 1890-1896.

Yang, L., Lindholm, K., Konishi, Y., Li, R., Shen, Y., 2002. Target depletion of distinct tumor necrosis factor receptor subtypes reveals hippocampal neuron death and survival through different signal transduction pathways. J Neurosci 22, 3025-3032.

Zhao, C., Teng, E.M., Summers, R.G., Jr., Ming, G.L., Gage, F.H., 2006. Distinct morphological stages of dentate granule neuron maturation in the adult mouse hippocampus. J Neurosci 26, 3-11.

Chapter 2

Injury-induced neurogenesis: consideration of resident microglia as supportive of neural progenitor cells.[1]

2.1 Introduction

It is now accepted that the adult brain maintains neurogenic capability in discrete germinal regions, the subgranular zone (SGZ) of the dentate gyrus (DG) within the hippocampus and in the subventricular zone (SVZ) of the lateral ventricle. The SGZ, located between the glia-rich hilus and the tightly-packed neurons of the granule cell layer (GCL), is the result of a continued presence of a relatively small number of proliferating cells derived from the cells of the hippocampal pseudostratified ventricular epithelium during embryogenesis. Neurons generated from hippocampal neural progenitor cells (NPCs) migrate primarily to the inner third of the GCL. Once there, they assume the nuclear and cytoplasmic morphology of surrounding dentate granule neurons, express biochemical markers of immature and mature neurons (Kempermann et al., 2004), and become incorporated into hippocampal-dependent declarative memory networks (Kee et al., 2007; van Praag et al., 2002).

The specialized SGZ microenvironment or "niche" for NPCs is comprised of astrocytes, microglia, and a limited population of oligodendroglia. In particular,

---

[1] McPherson, C.A., Kraft, A.D., and Harry, G.J. 2011. *Neurotox. Res.* 19(2):341-352.

microglia within the neurogenic “niche” have been identified as putative regulators of adult neurogenesis (Barkho et al., 2006; Butovsky et al., 2006; Ekdahl et al., 2003; Monje et al., 2002; Monje et al., 2003). For example, down-regulation of NPC proliferation and neuronal differentiation has been attributed to injury-induced microglia release of pro-inflammatory cytokines, interleukin-1β (IL-1β), interleukin-6 (IL-6) and tumor necrosis factor α (TNFα) (Monje et al., 2002; Monje et al., 2003) Acute brain insults, e.g., stroke and status epilepticus (SE), can induce a neuroinflammatory and microglia response but they also trigger increased neurogenesis. In addition, the survival, migration, and differentiation of NPCs into neurons can be directed by microglia (Aarum et al., 2003)

One of the primary microglia-secreted pro-inflammatory cytokines is TNFα. *In vitro* studies demonstrate a detrimental effect of TNFα on NPC survival and differentiation (Cacci et al., 2005; Liu et al., 2005). TNFα initiates its multiple effects on cell function by binding to two distinct cell surface receptors, a 55kDa type-1 receptor (TNFp55R) and a 75kDa type-2 receptor (TNFp75R)**.** TNFp55R contains a cytoplasmic sequence identifying an intracellular death domain required for transduction of apoptotic signals (Micheau and Tschopp, 2003; Thorburn, 2004). In contrast, TNFp75R activation primarily initiates trophic / protective actions (Shen et al., 1997; Yang et al., 2002). Cultured NPCs from human fetal brain express low levels of TNFα as well as TNFp55R and TNFp75R (Klassen et al., 2003; Sheng et al., 2005). NPCs isolated from the mouse striatum express TNFp55R (Ben-Hur et al., 2003). Iosif et al. (2006) demonstrated an increase in NPC proliferation in mice lacking TNFp55R, while mice lacking TNFp75R showed a minor decrease,

suggesting a regulatory component of the TNFα signaling pathway. Given that microglia are the primary source of TNFα within the brain, the expression of TNFRs on NPCs provides a possible mechanism by which, upon stimulation, microglia influence injury-induced neurogenesis.

An apparent sensitivity and vulnerability of dentate granule neurons is demonstrated across a wide spectrum of hippocampal injuries thus, various models have been developed to examine injury-induced stimulation of hippocampal neurogenesis. For example, following acute ischemic insult, a significant amount of dentate granule cell apoptosis occurs that is accompanied by an increase in proliferation of new cells in the SGZ and migration to the GCL within 7-10 d (Jin et al., 2001). In rodent models of temporal lobe epilepsy, an increased rate of neurogenesis occurs in the hippocampus within a week of seizure activity (Bengzon et al., 1997; Gray and Sundstrom, 1998; Parent et al., 1997). Traumatic brain injury results in apoptosis of DG neurons within 6 h of injury (Clark et al., 1997; McCullers et al., 2002) and neurogenesis at 7 d (Lu et al., 2007; Yu et al., 2008). Systemic exposure to the organometal, trimethyltin (TMT) induces active apoptosis of dentate granule neurons between 6 and 72 h; however, contrary to the other injury models, this results in a concurrent rapid and robust proliferation of NPCs in the SGZ between 2-5 d of insult (Corvino et al., 2005; Harry and Lefebvre d'Hellencourt, 2003; Harry et al., 2004; Ogita et al., 2005). This activity occurs during the peak level of microgliosis and elevations in IL-1α and TNFα (Bruccoleri et al., 1998; Bruccoleri and Harry, 2000; Harry et al., 2008a; Harry and Lefebvre d'Hellencourt, 2003). Ogita et al. (2005) and Harry et al. (2004) reported that the newly generated cells matured

into dentate neurons within 10 d suggesting proliferation and survival within a high inflammatory environment. As this would be inconsistent with the proposed detrimental effect of microglia activation on NPC proliferation, we examined the morphological phenotype and location of glia and NPCs to characterize changes in cell-cell contact with migration into the GCL. We proposed that glia serve a supportive role during injury-induced neurogenesis. We now provide data suggesting that an interaction between glia and proliferating cells within the hippocampus contributes to NPC proliferation and migration of generated cells following injury.

2.2 Materials and Methods

2.2.1 Animals.

Twenty-one day old CD-1 male mice (Charles River Labs, Raleigh, NC) and an additional cohort of mice, *tnfp75r*$^{-/-}$(C57BL/6-*Tnfrsf1btm1Mwm*) and C57BL/6J (WT) (Jackson Labs; Bar Harbor, ME) were examined. Mice were administered a single intraperitoneal (i.p.) injection of 2 mg/kg trimethyltin hydroxide (TMT; 2ml/kg) or saline (n=10). Previous work demonstrated that the peak time of NPC proliferation occurs within the first 24-96 h post-injection (McPherson et al., 2003). Thus, based upon this temporal pattern, mice were injected with bromodeoxyuridine (BrdU; 50 mg/kg i.p.) at the time of TMT dosing and at 12 h intervals for a total of 6 injections. The multiple injections of BrdU at 12 h intervals allowed for incorporation during discrete intervals within the peak time of proliferation and would generate a gradient of BrdU^{+} cells and their migration into the blades of the dentate. A relationship with glia could then be examined relative to distance from the SGZ within the same

animal.

Animals were individually housed in a dual corridor, semi-barrier animal facility (21°± 2℃; 50% ± 5% humidity; 12 h light/d ark cycle). Food (autoclaved NIH 31 rodent chow) and deionized, reverse osmotic-treated water were available *ad libitum*. At 72 h post-TMT, mice were deeply anesthetized with CO_2 and decapitated. Brains were dissected and bisected in the midsagittal plane. One hemisphere was immersion fixed in 4% paraformaldehyde (PFA)/0.1M phosphate buffer (PB; pH 7.2) overnight (ON), processed for paraffin embedding, and 10 μm serial sections cut through the hippocampus. Sentinel animals recorded negative for pathogenic bacteria, mycoplasma, viruses, ectoparasites, and endoparasites. All experiments were conducted according to an animal use protocol approved by NIEHS/NIH Animal Care and Use Committee.

2.2.2 Histology

To confirm the level of dentate granule cell death at 72 h post-TMT, one randomly selected paraffin-embedded section from each brain was subjected to terminal deoxynucleotidyl transferase-mediated dUTP-biotin *in situ* end labeling (TUNEL; ApopTag®, Intergen, Purchase, NY) and visualized by horseradish peroxidase-conjugated digoxigenin antibodies (diluted 1:1000 in PBS) and 3,3'-diaminobenzidine (DAB) substrate. A second randomly selected paraffin embedded section from the hippocampus of each mouse (n=10) was transferred to 0.01 M citrate buffer (pH 6.0), subjected to heat-induced epitope retrieval (HIER) using a decloaking chamber (Biocare Medical, Walnut Creak, CA), blocked with 10% normal goat serum/1%BSA in phosphate buffered saline for 30 min, then incubated with

rabbit polyclonal anti-active caspase 3 (AC3: 1:1000, 18 h, 4°C, Chemicon Intl., Temecula, CA) and visualized with goat anti-rabbit IgG AF 488 (1:1000; Molecular Probes, Inc., Eugene, OR). Neurons were labeled with Neurotrace® blue fluorescent Nissl stain (1:500, 1h, RT; Molecular Probes). To examine the localization of $BrdU^+$ cells or the proximity of microglia or astrocytes with such cells, one initial section of the hippocampus was randomly selected and then every 6^{th} section was collected for a total of 10 sections of the hippocampus per mouse (n=10). Based upon the work of Widera et al. (2006) showing that cyclin D1 plays a crucial role in the proliferation of NSCs induced by TNFα, we included cyclin D1 as an additional marker. This selection process was repeated for microglia and astrocyte staining, and for co-staining of BrdU or cyclin D1 and glia. Rehydrated sections were subjected HIER in 0.01 M citrate buffer (pH 6.0), and blocked with either a MOM™ immunodetection kit (Vector Labs, Burlingame, CA) or 10% normal goat serum/1% BSA/ PBS for 30 min. Sections were incubated 18 h at 4°C, with rat anti-BrdU (1:10,000, Chemicon, Temecula, CA) or with mouse anti-cyclin D1 (1:200; Zymed Labs, Inc., San Francisco, CA). Astrocytes were labeled by rabbit polyclonal anti-glial fibrillary acidic protein (GFAP; 1:200, 1 h, 24°C, Dako Corp, Carpinteria, CA). Microglia were identified by morphological criteria of size and ramification of cells stained with a rabbit polyclonal antibody to ionized calcium-binding adaptor molecule 1 (Iba-1; 1:500; 1 h, 24°C; Wako Chemicals, Richmond, VA). TNF receptor localization was detected with rabbit polyclonal anti-TNFR1 (p55; 1:500, #CSA-815, Stressgen, Ann Arbor, MI) or polyclonal goat anti-mouse TNFR2 (p75; 1:500, #AF426PB, R&D Systems, Minneapolis, MN). Antibody specificity was verified by

Western blots (Harry et al., 2008b). Staining was visualized with IgG Alexa Fluor® (1:1000, Molecular Probes). Coverslips were mounted with Prolong® Antifade Reagent with or without the nuclear stain, DAPI (Molecular Probes).

2.2.3 Microscopy

Digital images were acquired using a SpotRT™ cooled, charged-couple device camera (Diagnostic Instruments, Sterling Heights, MI) on a Leica DMRBE microscope (Wetzlar, Germany) equipped with epifluorescence and Z-control and Metamorph™ (Universal Imaging Co., Downingtown, PA). Contact between glia and $BrdU^+$ cells was further examined via deconvoluted z-stack images and nearest neighbor correction. Co-localization images and representative contact images were confirmed by confocal microscopy.

Three distinct sections (region of interest: ROI) of the hippocampal dentate granule layer (DGL) were identified at increasing distances from the SGZ with the assumption that this would represent cells at different stages of maturation and migration. ROI-1) a 2-cell width at the inner blade considered the SGZ; ROI-2) the next consecutive 5-6 neuron width, and ROI-3) the outer granular neuronal region of the dentate blade. The identification of $BrdU^+$ NPC derived cells adhered to exclusion criteria of a minimum of 8 μm diameter. These criteria were selected for two reasons. One was the fact that mature dentate granule neurons were undergoing apoptosis and we wanted to ensure that we did not include apoptotic neurons (< 6 μm) that may have incorporated BrdU. The second was based upon the fact that the early time interval of between 1 and 3 days allowed for the examination of proliferating cells but not for uniform co-labeling with markers of cell

fate determination. As we previously reported, the immature neuronal markers of doublecortin and Prox-1were not increased in this model until 4-7 d post-TMT (Harry et al., 2004; McPherson et al., 2003) and, at these earlier time points, we observed the NPC marker, nestin (data not shown) indicative of non-differentiated progenitor cells. According to design considerations for sampling of rare events, the total number of $BrdU^+$ cells, $BrdU^+$ cells in contact with microglia, and $BrdU^+$ cells in contact with astrocytes was determined for each region. Again a selection criterion was required as, by 72 h post-TMT, amoeboid microglia were actively phagocytizing dying neurons. Thus, contact between $BrdU^+$ cells and process bearing ramified microglia was recorded. If the microglia cell fully encircled the $BrdU^+$ cell or demonstrated an amoeboid like morphology it was excluded. If the $BrdU^+$ cell maintained a diameter >8 μm and a ramified microglia (nucleus size of maximum 2 μm) was in contact it was included. 2 independent trained investigators blind to the experimental conditions conducted evaluations.

2.2.4 Statistical analysis

Statistical significance was determined with Student's t-test. All data is presented as mean ± SD. All statistical significance levels were set at $p < 0.05$.

2.3 Results

2.3.1 TMT induced histopathology

The extent of NPC proliferation in the SGZ is dependent upon the severity of damage. In addition, the level and stage of microgliosis is also dependent upon the timing and severity of neuronal death. These two features can significantly confound the interpretation of any data with regards to neurogenesis or the impact of a

microglia response. The TMT mouse model is highly reproducibility in severity and timing of neuronal death across individual mice. Consistent with previous studies, acute exposure to TMT resulted in clinical signs of seizure activity between 18-30 h and apoptotic death of dentate granule cells as identified by TUNEL (Fig. 2.1A,B) and AC3 (Fig. 2.1E,F) characterized by nuclear pyknosis and karyolysis.

In the normal CD-1 mouse hippocampus, $GFAP^+$ astrocytes are observed primarily at the borders of the densely packed GCL. Consistent with radial astrocyte morphology, cell bodies were observed along the inner blade with fibrous astrocyte processes extending into the GCL (Fig. 2.1C). Similar to what has been previously reported (Harry et al., 2008a; Harry et al., 2008b) after an injection of TMT, GFAP immunoreactivity was elevated and astrocytes showed a slight thickening of the processes within the GCL (Fig. 2.1D).

In the normal hippocampus, microglia display very thin, ramified processes and normally, are not evident within the densely packed dentate GCL but rather seen within the hilus and molecular layer (Fig. 2.1G). Consistent with our previous work within the GCL, heterogeneity in microglia responses was observed at 72 h. Within proximity to dying neurons, microglia showed an amoeboid morphology characteristic of a phagocytic phenotype. In addition, increased staining was also observed for ramified process-bearing microglia also showing heterogeneity in morphology (Fig. 2.1H).

2.3.2 Induction of NPC proliferation in the SGZ

The BrdU dosing regimen allowed for a gradient of labeled cells within the GCL, representing different stages of generation and migration. Figure 2.2A

represents the mouse SGZ. In the normal adolescent hippocampus, while higher than what is observed in the adult mouse, $BrdU^+$ cells were sparse and restricted to the inner blade/SGZ layer of the dentate (Fig. 2.2B). Consistent with our previous work (Harry et al., 2004; McPherson et al., 2003), the increased number of $BrdU^+$ cells in the TMT dosed mice was distributed across the full width of the upper and lower blades of the dentate gyrus (Fig. 2.2B). The upper and lower blades of the GCL were demarcated into 3 distinct regions of interest (Fig. 2.2C). Region of interest (ROI) 1 was inclusive of the SGZ, ROI-2 represented the middle 3^{rd} of the GCL, and the outer 30% would represent the requirement for replacement of dentate granule neurons across the full width of the GCL. When we examined the distribution of $BrdU^+$ cells across the GCL as a function of identified ROIs (Fig. 2.2C), the $BrdU^+$ cells in the control hippocampus were located within the ROI-1 representing the SGZ. Following TMT, a significant increase in the number of $BrdU^+$ cells within ROI-1 was detected as well as the increased presence of $BrdU^+$ cells within both ROI-2 and -3 consistent with the visual images of a more uniform distribution across the GCL. In previous work, we confirmed this proliferation with multiple markers including PCNA and Ki-67 and demonstrated that the cells matured into dentate granule neurons by subsequent co-localization of staining with NeuN at 10-14 days (Harry et al., 2004). As an additional marker of cell proliferation, the cell cycle protein cyclin D1 is present in the adult SGZ (Heine et al., 2004) and plays a role in the proliferation of NPCs induced by TNFα and signaling via IKK/NF-kB (Widera et al., 2006). Cyclin D1 expression was increased, but to a significantly lesser extent than BrdU, after TMT (McPherson et al., 2003). Figure 3 illustrates the

co-localization of cyclin D1 and BrdU in the GCL. We estimated that 80% of the cyclin $D1^+$ cells co-stained with BrdU. Given the short half-life (approx. 1 h) at the end of mitosis of proteins like Ki-67 and the cyclins, versus the long-term expression of BrdU, would be consistent with the absence of a reverse association. However, staining for cyclin D1 provided us an additional marker for proliferating cells in the SGZ. Consistent with our previous work (McPherson et al., 2003), we found no co-localized staining between cyclin D1 or BrdU and GFAP or Iba-1 (data not shown).

2.3.3 Glia cells in contact with proliferating cells.

Given the neurogenesis previously reported for TMT-induced hippocampal damage occurring within a high pro-inflammatory cytokine environment, we examined the proximity and contact relationship between glia and proliferating cells within the peak interval of induction by the TMT insult. The BrdU dosing regimen allowed for a 3 d interval of labeling cells across a range of migration distances throughout the width of the GCL. Given that an active process of neuronal death and microglia activation was ongoing during the peak time of proliferation, it was necessary to set morphological criteria to distinguish between microglia of different morphological phenotypes. For inclusion in counting, $BrdU^+$ cells were required to be > 8 μm in diameter and the microglia cells to be of a ramified process bearing morphology. Figure 2.4 A (microglia) and 2.4B (astrocytes) provides representative images of cells in contact that meet the criteria for inclusion in the quantitation. Based upon our previous work with this model, any expression of active caspase 3 will be accompanied by a microglia cell that has shifted its morphological phenotype to amoeboid; while microglia with ramified processes, as represented in Figure 4B,

are associated with neuronal survival (Kraft et al., 2009). Once these morphological criteria were established for use at the light microscopic level, 2 investigators blind to the experimental conditions examined the sections for contact between $BrdU^+$ cells and microglia or astrocytes. Given the changes that occur in the shape of the hippocampus as the brain is sectioned, we ensured that equivalent sized regions across sections from all animals were used for quantitation. Contact between microglia and $BrdU^+$ cells was greatest within the inner third of the blade and less in the outer ROI-3 layer (Fig. 2.4C). Contact with $GFAP^+$ astrocytes was minimal within the inner ROI-1 section and became more pronounced in ROI-2 and 3. While we cannot rule out contact with fine non-$GFAP^+$ astrocytic processes, the $GFAP^+$ contacts detected were less in the inner region, ROI-1, as compared to the other two ROIs (Fig. 2.4C).

2.3.4 $BrdU^+$ cells in SGZ express TNFp75R.

Our previous work demonstrated by *in situ* hybridization, that both process-bearing and amoeboid microglia upregulated expression of TNFα in the hippocampus following TMT (Bruccoleri et al., 1998). In addition, the induction of NPC proliferation within the SGZ occurs during a period of peak elevation of mRNA levels for TNFα and receptors (Harry et al., 2008b; Lefebvre d'Hellencourt and Harry, 2005). Based upon earlier reports suggesting that the effect of TNFα on NPC could be dependent on receptor expression (Ben-Hur et al., 2003; Iosif et al., 2006; Klassen et al., 2003), we determined the expression of TNFRs by $BrdU^+$ cells in the SGZ following TMT. Within the SGZ and ROI-1 of the dentate gyrus, a limited number of $BrdU^+$ cells were found to express TNFp75R at 72 h (Fig. 2.5). We did not

detect such cells in the other two ROIs. We were unable to detect TNFp55R expression in $BrdU^+$ cells at this time; however, this does not rule out an earlier or transient expression. We then examined the injury and induced neurogenesis in mice deficient for TNFp75R. Consistent with our previous reports (Harry et al., 2008b) the absence of this receptor did not diminish the severity of the neuronal death following TMT nor modify the astrocyte or microglia response (data not shown). An increase was observed in the number of $BrdU^+$ cells along the SGZ in both WT and *tnfp75r*- deficient mice relative to saline controls. At the time point examined, $BrdU^+$ cells could be seen within the GCL in the WT mice (Fig. 6A) while, in the *tnfp75r*- deficient mice these cells remained within ROI-1 (Fig. 6B). We did not determine the number of $BrdU^+$ cells generated.

2.4 Discussion

Under normal conditions, adult-generated hippocampal cells migrate primarily to the inner third of the granular cell layer where they assume the nuclear and cytoplasmic morphology of surrounding neurons, express biochemical markers of immature and mature neurons (Kempermann et al., 2004), extend axonal projections to form synapses with CA3 pyramidal cell neurons (Markakis and Gage, 1999), and become incorporated into hippocampal-dependent declarative memory networks (Kee et al., 2007; van Praag et al., 2002). When significant damage occurs to the dentate granule cell population, NPCs are exposed to an environment of elevated pro-inflammatory cytokines including TNFα; yet, NPC proliferation is induced and migration of the generated cells is stimulated. We now provide data demonstrating a differential response and location of microglia within the GCL with injury that may

indicate the contribution of cell-cell interactions between the two cell populations during the proliferation and migration process.

While numerous studies have documented adverse effects of microglia and their secreted factors on NPC proliferation, others have suggested that these factors can be stimulatory to the repair and generation of NPCs within the brain (Aarum et al., 2003; Ekdahl et al., 2003). Thus, it is not unlikely that an injury in a young animal that initiates a microglia response would also initiate a neurogenic response. For example, previous work with adrenalectomy-induced apoptotic dentate granule cell death suggested that microglia activation contributed to an environment conducive to neurogenesis (Battista et al., 2006). In the case of TMT, the stimulation of NPCs occurs during the active period of neuronal death and elevated TNFα levels (Harry et al., 2008a). Additionally, a developmental ontogeny for responses to TNFα has been suggested due to the high expression of TNFα within the embryonic brain (Mehler and Kessler, 1997; Yamasu et al., 1989). It has been suggested that the effect of TNFα on NPCs depends upon localized receptor expression (Ben-Hur et al., 2003; Iosif et al., 2006; Klassen et al., 2003). There is a limited amount of information regarding the expression of TNFα or TNF receptors (TNFR) on NPCs. Klassen et al. (Klassen et al., 2003) demonstrated TNFα expression on NPC derived from neonatal rat hippocampus and in cultured NPCs from human fetal brain. The cultured human NPCs were found to express TNFp55R and TNFp75R (Klassen et al., 2003). Progenitor cells isolated from mouse striatum were found to express TNFp55R (Ben-Hur et al., 2003). In the current *in vivo* study, we demonstrate the expression of TNFp75R on $BrdU^+$ cells in the SGZ following TMT, suggestive of

localization on hippocampal NPCs. However, at the time point examined, we did not observe the expression of TNFp55R. It is possible that this is not necessarily reflective of a general lack of expression but rather that the expression of TNFp55R is transient and occurs at a different time. In our previous work, we demonstrated a transient expression of TNFp55R followed by the expression and internalization of TNFp75R in dentate granule neurons undergoing early stages of apoptosis that could be as short as 6 h (Harry et al., 2008b) . Thus, further examination along a temporal sequence would be required to determine receptor expression. To determine if the role for cyclin D1 in the TNFα signaling via IKK/NFkB identified by Widera et al. (2006) was also at play in the current model, additional studies are needed to examine the co-localization of cyclin D1, BrdU, and TNFp75R as the action may require concurrent expression or not utilize the TNFp75R. Although, given the relatively short half-life of cyclin D1 and the transient expression of TNFp75R this may be difficult to quantify. In fact, in the one time point examined in the *tnfp75r* knockout mice, we were unable to detect a sufficient number of cyclin D1 cells for analysis.

The work of Iosif et al. (2006) show increased cell proliferation with or without stimulation in mice lacking TNFp55R, while mice lacking TNFp75R showed no change in basal proliferation and a minor decrease in NPC proliferation following SE. Our findings are somewhat consistent with these results in that, at the early 72 h time point, $BrdU^+$ cells were localized at the SGZ layer in mice deficient for TNFp75R and there was no indication of migration into the dentate blades. However, with similar severity levels of dentate granule cell death, migration was observed in

the wildtype mouse within the first 72 h. We did not determine if the actual number of NPCs was increased. Further studies are required to determine if this represents a long-term deficit or only a delay in migration and the role that TNFR signaling may play in this process. Whether these differences are directly due to the absence of TNFp75R or the result of the production of other pro-inflammatory cytokines cannot be determined in the current study. In previous work (Harry et al., 2008b), we reported that at the dose level used in the current study, mRNA levels for various pro-inflammatory cytokines in the hippocampus was similar to the wildtype. However, at a lower dose level, when there was no elevation in the wildtype mouse, mRNA levels were elevated for MIP1α and IL-1α in the TNFp75ko mice. Thus, it is likely that other unique changes are occurring in the TNFp75ko mouse following TMT that may have a significant impact on the NPCs.

Our current data suggests that, as the $BrdU^+$ cells migrated through the GCL, contact with microglia cells is diminished and contact with $GFAP^+$ astrocytes becomes more prominent. This shift appeared to occur within ROI-2 and 3, which would be at a stage when the cells would be reaching their final migration site. While this may represent a normal shift that would occur under basal neurogenesis, it is difficult to determine given the minimal staining for either microglia or astrocytes within the densely packed GCL of the normal mouse. However, it is apparent that, with the loss of neurons within the GCL, there is a void for which both the astrocytes and microglia can fill as well as removal of the restrictive matrix allowing for cell migration. Thus, while the overall process may be similar the ability to distinguish the cell contacts may not be as robust in the control hippocampus. With the death of

dentate granule neurons one would expect a disruption in the integrity of the parenchyma. The associated loss of the cellular matrix may diminish the cellular barriers for soluble factors thus allowing for glial-glial interactions such as interactions with astrocytes by microglia release of IL-1 (Spranger et al., 1990). We have previously demonstrated elevations in IL-1 by microglia following TMT (Bruccoleri et al., 1998). Whether this represents a process unique to the injury or an enhancement of a normal migration of newly generated cells requires additional experimentation.

Microglia effects on granule neuron precursor cells have been previously reported by Morgan et al. (2004) as a mitogenic effect of microglia derived neurotrophic factors. Choi et al. (2008) demonstrated an upregulation of microglia insulin-like growth factor-1 (IGF-1) expression triggering p42/44 mitogen-activated protein kinase (MAPK) activation in NPC of the SGZ resulting in increased proliferation. With TMT injury to the hippocampus, the CA1 pyramidal neurons remain intact. In this case, IGF-1 immunostaining was observed in process-bearing microglia and along $GFAP^+$ processes of astrocytes (Wine et al., 2009). More recently, Thored et al. (2009) reported data suggesting that a long-term accumulation of microglia expressing IGF-1 served in a supportive role for neurogenesis in the SVZ following stroke. Thus, further examination of localized changes may help us understand dynamic interactions between microglia and astrocytes with regards to their effects on newly generated cells within the hippocampus. Gaining a better understanding of these events will significantly

enhance our ability to identify therapeutic intervention strategies to promote successful brain repair.

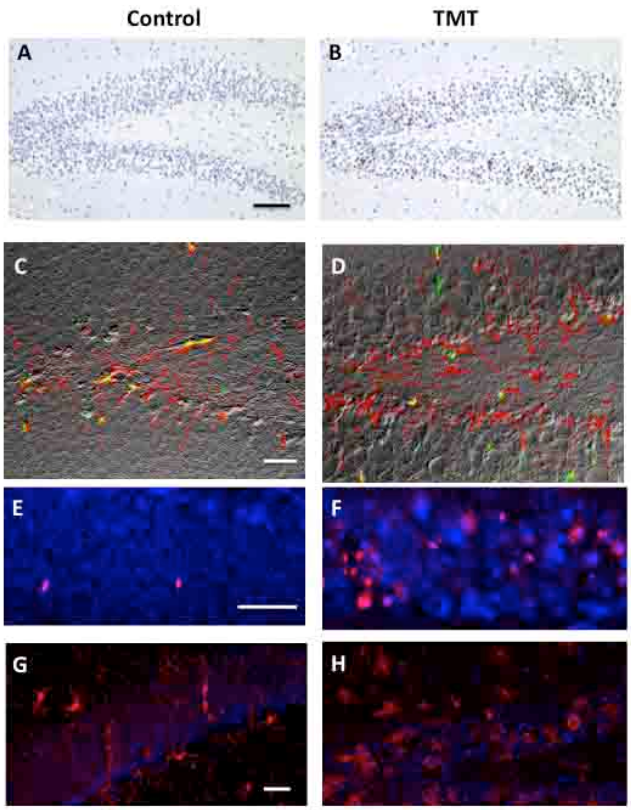

Figure 0.1. Histopathology of the hippocampus.
Representative images of the histopathology of the dentate granule cell layer (GCL) of the hippocampus in control CD-1 male mice (A,C,E,G) and in mice 72 h following trimethyltin (2.0 mg TMT/kg bwt, i.p.) (B,D,F,H). (A-B) Representative images of TUNEL$^+$ cells in (A) control and (B) TMT-dosed mice. A significant number of TUNEL$^+$ cells (brown) were evident within the GCL. Scale bar = 50 μm. (C-D) Representative DIC images of GFAP$^+$ astrocytes (red) showing thin processes through the GCL in (C) control mice (D) the increased GFAP staining in the GCL of mice dosed with TMT was characterized by thicker astrocyte processes throughout the GCL suggestive of hypertrophy. Scale bar = 25 μm. (E-F) Representative image of immunostaining for active caspase 3 (AC3; red) with a Nissl (blue) counterstain. (E) control mice displayed minimal staining for AC3 with punctate staining seen only in the blood vessel. In the mice dosed with TMT AC3 staining was evident in neurons showing evidence of collapsed nuclei. Nissl (blue) stained sections of the hippocampus from controls show normal cellular morphology and evidence of dense collapsed cells in the TMT dosed mice. Scale bar = 25 μm. (G-H) Representative images of process bearing Iba-1$^+$ microglia (red) in (G) control and (H) microglia displaying a thickening and retraction of processes and an amoeboid phenotype in TMT dosed mice. In control mice, microglia are present at both the inner and outer layer of the GCL with processes transverse across the layer. In the TMT dosed mice, round amoeboid microglia can be seen within the GCL. Blue – DAPI counterstain. Scale bar = 25 μm

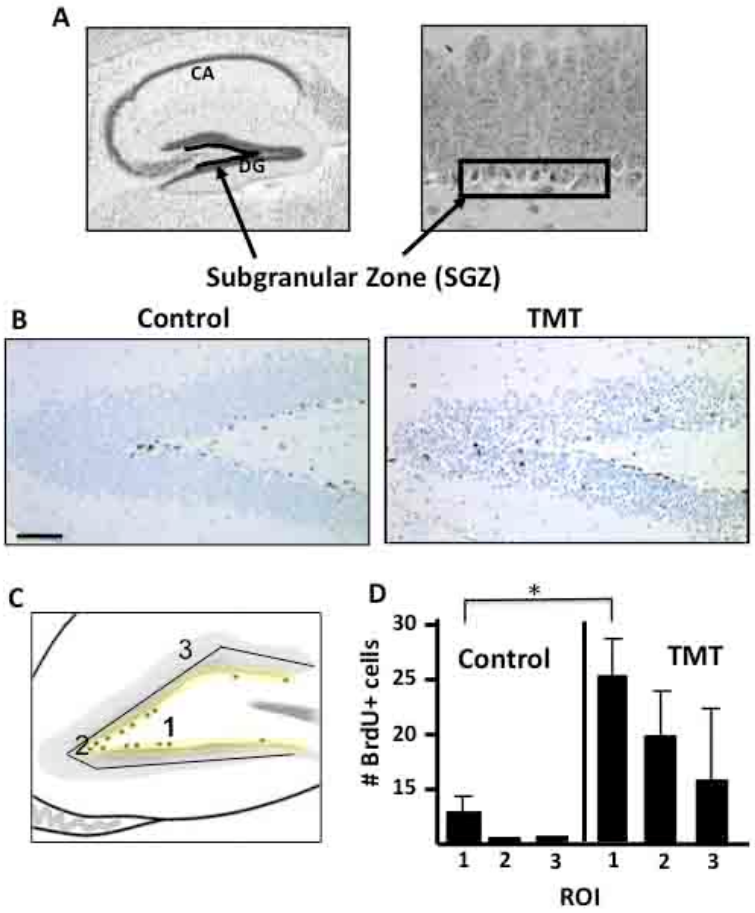

Figure 2.2. Localization of BrdU in the DG.
(A) Representative subgranular zone (SGZ) location and orientation along the two innermost cell layers (box) of the hippocampal dentate gyrus. (B) Representative image of $BrdU^+$ cells in the control hippocampus and in the hippocampus of mice 72 h following trimethyltin (2.0 mg TMT/kg bwt, i.p.). Mice received 2x day i.p. injection of BrdU (50 mg/kg body wt) at 12 h intervals, initiated with the saline or TMT injection, for a total of 6 injections. $BrdU^+$ cells (brown) were located at the SGZ layer in the control mice. In mice injected with TMT, there is significant amount of cell death as evidenced by hematoxylin counter stain indicating loss of cells and presence of dense cells with collapsed nuclei. $BrdU^+$ cells are detected along the SGZ and within the GCL. (C) Schematic of defined regions of interest (ROI) across the blades of the dentate. The upper and lower blades of the GCL were demarcated into 3 distinct regions of interest. ROI-1) a 2-cell width at the inner blade considered the SGZ; ROI-2) the next consecutive 5-6 neuron width, and ROI-3) the outer granular neuronal region of the dentate blade. (D) The mean (+/- SD) number of $BrdU^+$ cells in the SGZ and GCL in control CD-1 male mice and in mice dosed with TMT (10 sections, 10 mice per group). Total number of positive cells determined within each of the regions of interest (ROI) as a distance from the SGZ as described in the Methods section. Sections were counter stained with hematoxylin. Scale bar = 50 μm. *indicates statistical significance at $p<0.05$.

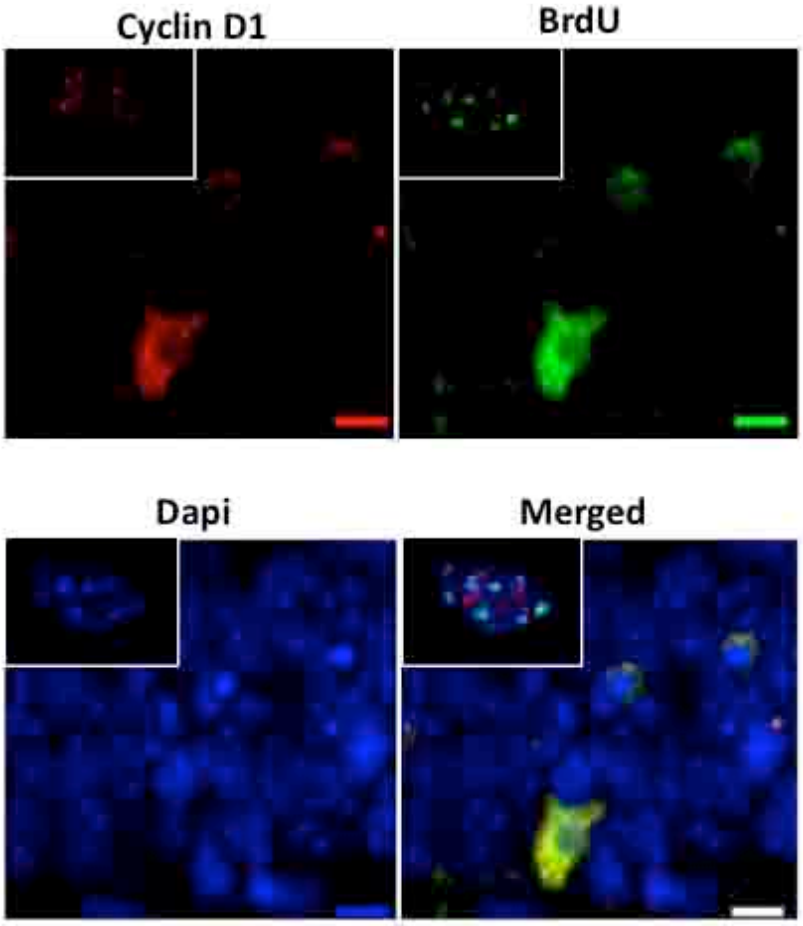

Figure 2.3. Cyclin D1 / BrdU immunofluorescence.
Representative image obtained from the hippocampus of CD-1 male mice dosed with 2mg/kg TMT, i.p. at PND 21 of the co-localization of BrdU (green) in cells immunopositive for cyclin D1 (red). Merged images demonstrate a co-expression of proteins in cells along the inner border of the GCL. Insets represent the z-stack images of the co-localization. DAPI (blue). Mice received 2x day i.p. injection of BrdU (50 mg/kg body wt) at 12 h intervals, initiating with the TMT injection, for a total of 6 injections. Scale bar = 10 μm.

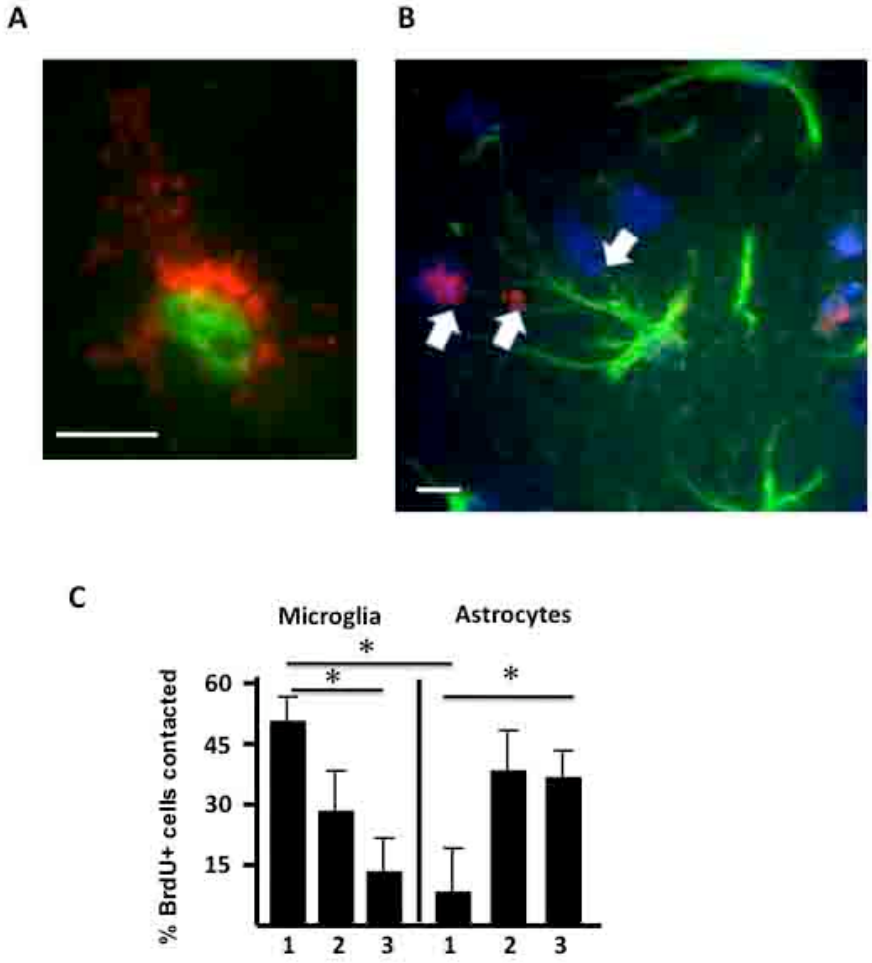

Figure 2.4. BrdU glial contact.
Representative images and quantitation of contact between BrdU$^+$ cells and Iba-1$^+$ microglia and GFAP$^+$ astrocytes in the GCL of male CD-1 mice at 72 h post-TMT. (A) As apoptosis was an active process at the 72 h time point following a systemic injection of TMT (2 mg/kg, i.p. at PND 21), criteria were required to distinguish non-amoeboid, process bearing microglia for contact with Brdu$^+$ cells. Using the "roundedness" as criteria for exclusion we identified Iba-1$^+$ (red) that presented with a process bearing phenotype in contact with BrdU$^+$ cells >8 μm (green). Scale bar = 10 μm. (B) Similar criteria was set for the inclusion of counting GFAP$^+$ astrocytes (green) in contact with BrdU$^+$ cells (red) within the different ROIs in the GCL. Contact could be with either the GFAP$^+$ processes or with the main GFAP$^+$ body of the astrocyte. Scale bar = 10 μm. (C) Quantitation of the percentage of BrdU$^+$ cells (>8 μm diameter) in contact with Iba1$^+$ microglia or GFAP$^+$ astrocytes within each of the ROIs (as described in Methods and in Figure 2) at 72 h post-dosing with either saline or TMT (2.0 mg/kg, i.p.; PND21). Data represents the mean +/- SD. * indicates statistically significance $p<0.05$.

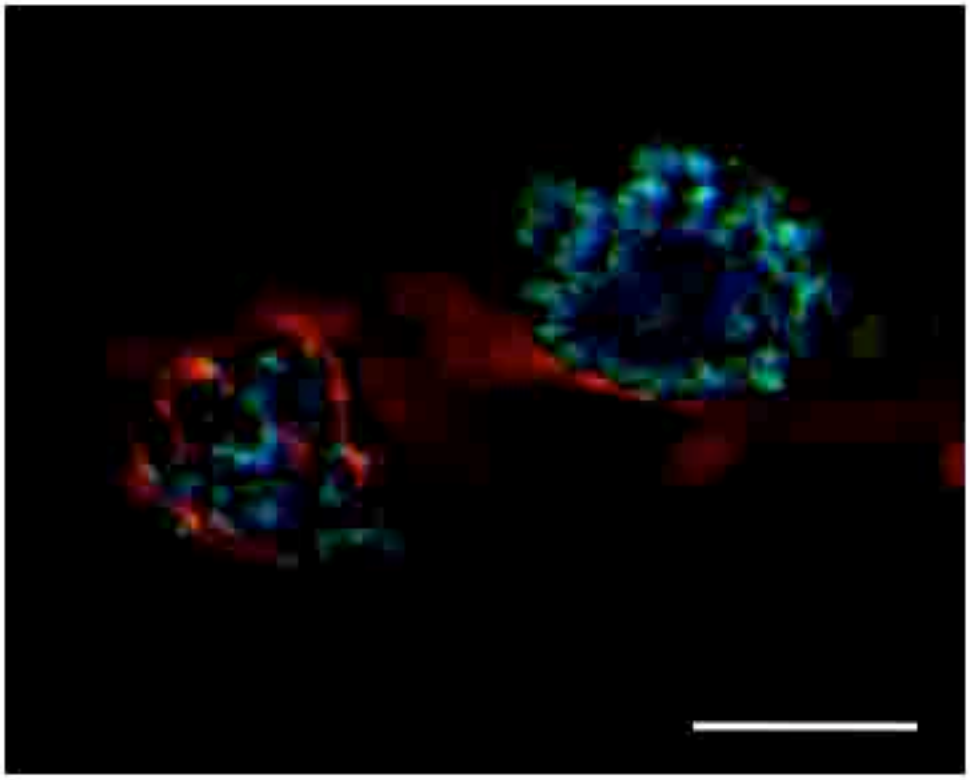

Figure 2.5. BrdU / TNFp75R immunofluorescence.
Representative con-focal image of the co-localization of TNFp75R (green) and BrdU (blue) within two cells identified along the inner blade of the GCL (ROI-1). Microglia processes are identified with Iba-1 immunostaining (red). Approximately 15% +/-4% of the $BrdU^+$ cells at the SGZ co-localized with TNFP75R. Scare bar = 10 μm.

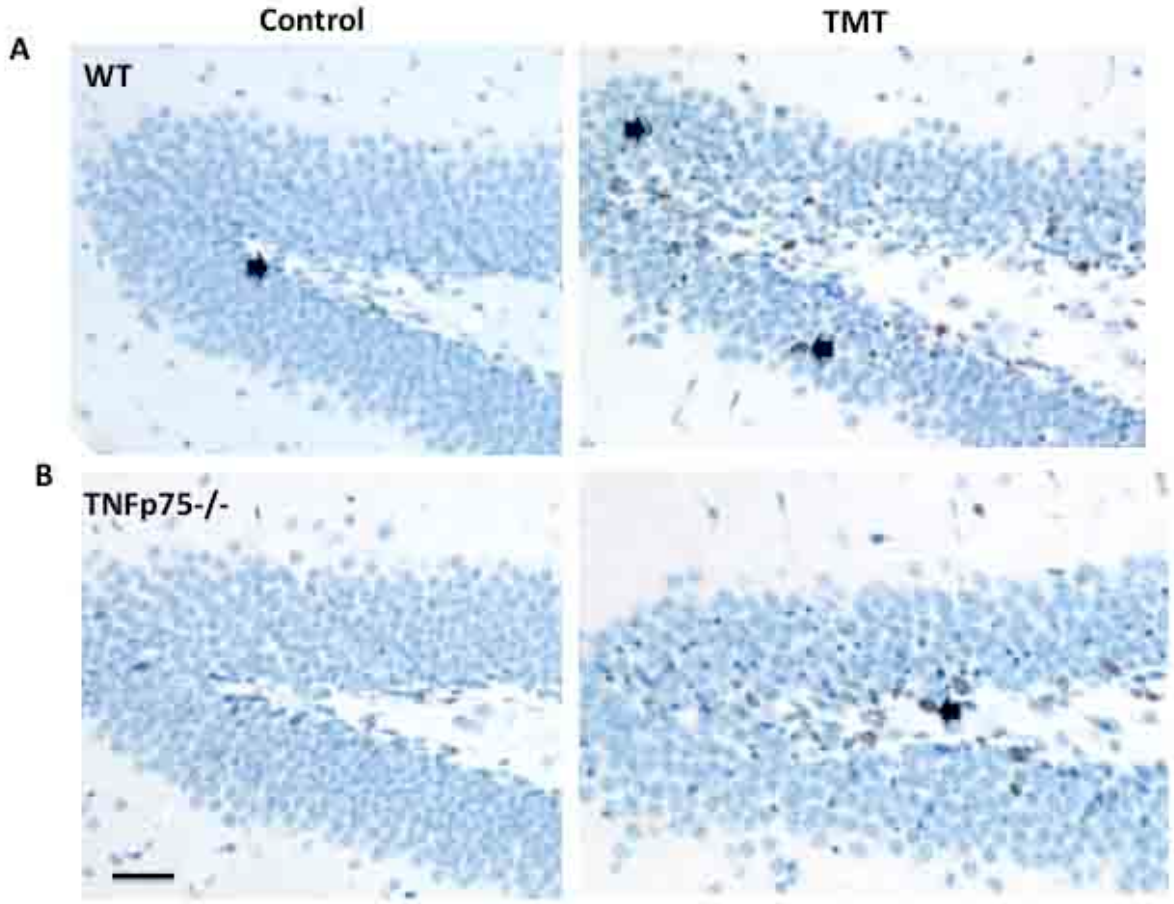

Figure 2.6. BrdU immunohistochemistry in TNFp75 -/- mice.
Representative image of $BrdU^+$ cells within the SGZ and GCL of (A) WT mice and (B) mice deficient for TNFp75R at 72 h post-TMT (2 mg/kg, i.p.; PND21). $BrdU^+$ cells stained black and were evident within the GCL in WT mice. In the TNFp75R mice $BrdU^+$ cells were localized along the SGZ and not seen within the GCL. Sections were counterstained with Nissl. Scare bar = 50 μm.

References

Aarum, J., Sandberg, K., Haeberlein, S.L., Persson, M.A., 2003. Migration and differentiation of neural precursor cells can be directed by microglia. Proc Natl Acad Sci U S A 100, 15983-15988.

Barkho, B.Z., Song, H., Aimone, J.B., Smrt, R.D., Kuwabara, T., Nakashima, K., Gage, F.H., Zhao, X., 2006. Identification of astrocyte-expressed factors that modulate neural stem/progenitor cell differentiation. Stem Cells Dev 15, 407-421.

Battista, D., Ferrari, C.C., Gage, F.H., Pitossi, F.J., 2006. Neurogenic niche modulation by activated microglia: transforming growth factor beta increases neurogenesis in the adult dentate gyrus. Eur J Neurosci 23, 83-93.

Ben-Hur, T., Ben-Menachem, O., Furer, V., Einstein, O., Mizrachi-Kol, R., Grigoriadis, N., 2003. Effects of proinflammatory cytokines on the growth, fate, and motility of multipotential neural precursor cells. Mol Cell Neurosci 24, 623-631.

Bengzon, J., Kokaia, Z., Elmer, E., Nanobashvili, A., Kokaia, M., Lindvall, O., 1997. Apoptosis and proliferation of dentate gyrus neurons after single and intermittent limbic seizures. Proc Natl Acad Sci U S A 94, 10432-10437.

Bruccoleri, A., Brown, H., Harry, G.J., 1998. Cellular localization and temporal elevation of tumor necrosis factor-alpha, interleukin-1 alpha, and transforming growth factor-beta 1 mRNA in hippocampal injury response induced by trimethyltin. J Neurochem 71, 1577-1587.

Bruccoleri, A., Harry, G.J., 2000. Chemical-induced hippocampal neurodegeneration and elevations in TNFalpha, TNFbeta, IL-1alpha, IP-10, and MCP-1 mRNA in osteopetrotic (op/op) mice. J Neurosci Res 62, 146-155.

Butovsky, O., Ziv, Y., Schwartz, A., Landa, G., Talpalar, A.E., Pluchino, S., Martino, G., Schwartz, M., 2006. Microglia activated by IL-4 or IFN-gamma differentially induce neurogenesis and oligodendrogenesis from adult stem/progenitor cells. Mol Cell Neurosci 31, 149-160.

Cacci, E., Claasen, J.H., Kokaia, Z., 2005. Microglia-derived tumor necrosis factor-alpha exaggerates death of newborn hippocampal progenitor cells in vitro. J Neurosci Res 80, 789-797.

Choi, Y.S., Cho, H.Y., Hoyt, K.R., Naegele, J.R., Obrietan, K., 2008. IGF-1 receptor-mediated ERK/MAPK signaling couples status epilepticus to progenitor cell proliferation in the subgranular layer of the dentate gyrus. Glia 56, 791-800.

Clark, R.S., Kochanek, P.M., Dixon, C.E., Chen, M., Marion, D.W., Heineman, S., DeKosky, S.T., Graham, S.H., 1997. Early neuropathologic effects of mild or moderate hypoxemia after controlled cortical impact injury in rats. J Neurotrauma 14, 179-189.

Corvino, V., Geloso, M.C., Cavallo, V., Guadagni, E., Passalacqua, R., Florenzano, F., Giannetti, S., Molinari, M., Michetti, F., 2005. Enhanced neurogenesis during trimethyltin-induced neurodegeneration in the hippocampus of the adult rat. Brain Res Bull 65, 471-477.

Ekdahl, C.T., Claasen, J.H., Bonde, S., Kokaia, Z., Lindvall, O., 2003. Inflammation is detrimental for neurogenesis in adult brain. Proc Natl Acad Sci U S A 100, 13632-13637.

Gray, W.P., Sundstrom, L.E., 1998. Kainic acid increases the proliferation of granule cell progenitors in the dentate gyrus of the adult rat. Brain Res 790, 52-59.

Harry, G.J., Funk, J.A., Lefebvre d'Hellencourt, C., McPherson, C.A., Aoyama, M., 2008a. The type 1 interleukin 1 receptor is not required for the death of murine hippocampal dentate granule cells and microglia activation. Brain Res 1194, 8-20.

Harry, G.J., Lefebvre d'Hellencourt, C., 2003. Dentate gyrus: alterations that occur with hippocampal injury. Neurotoxicology 24, 343-356.

Harry, G.J., Lefebvre d'Hellencourt, C., McPherson, C.A., Funk, J.A., Aoyama, M., Wine, R.N., 2008b. Tumor necrosis factor p55 and p75 receptors are involved in chemical-induced apoptosis of dentate granule neurons. J Neurochem 106, 281-298.

Harry, G.J., McPherson, C.A., Wine, R.N., Atkinson, K., Lefebvre d'Hellencourt, C., 2004. Trimethyltin-induced neurogenesis in the murine hippocampus. Neurotox Res 5, 623-627.

Heine, V.M., Maslam, S., Joels, M., Lucassen, P.J., 2004. Increased P27KIP1 protein expression in the dentate gyrus of chronically stressed rats indicates G1 arrest involvement. Neuroscience 129, 593-601.

Iosif, R.E., Ekdahl, C.T., Ahlenius, H., Pronk, C.J., Bonde, S., Kokaia, Z., Jacobsen, S.E., Lindvall, O., 2006. Tumor necrosis factor receptor 1 is a negative regulator of progenitor proliferation in adult hippocampal neurogenesis. J Neurosci 26, 9703-9712.

Jin, K., Minami, M., Lan, J.Q., Mao, X.O., Batteur, S., Simon, R.P., Greenberg, D.A., 2001. Neurogenesis in dentate subgranular zone and rostral subventricular zone after focal cerebral ischemia in the rat. Proc Natl Acad Sci U S A 98, 4710-4715.

Kee, N., Teixeira, C.M., Wang, A.H., Frankland, P.W., 2007. Preferential incorporation of adult-generated granule cells into spatial memory networks in the dentate gyrus. Nat Neurosci 10, 355-362.

Kempermann, G., Jessberger, S., Steiner, B., Kronenberg, G., 2004. Milestones of neuronal development in the adult hippocampus. Trends Neurosci 27, 447-452.

Klassen, H.J., Imfeld, K.L., Kirov, II, Tai, L., Gage, F.H., Young, M.J., Berman, M.A., 2003. Expression of cytokines by multipotent neural progenitor cells. Cytokine 22, 101-106.

Kraft, A.D., McPherson, C.A., Harry, G.J., 2009. Heterogeneity of microglia and TNF signaling as determinants for neuronal death or survival. Neurotoxicology 30, 785-793.

Lefebvre d'Hellencourt, C., Harry, G.J., 2005. Molecular profiles of mRNA levels in laser capture microdissected murine hippocampal regions differentially responsive to TMT-induced cell death. J Neurochem 93, 206-220.

Liu, Y.P., Lin, H.I., Tzeng, S.F., 2005. Tumor necrosis factor-alpha and interleukin-18 modulate neuronal cell fate in embryonic neural progenitor culture. Brain Res 1054, 152-158.

Lu, D., Qu, C., Goussev, A., Jiang, H., Lu, C., Schallert, T., Mahmood, A., Chen, J., Li, Y., Chopp, M., 2007. Statins increase neurogenesis in the dentate gyrus, reduce delayed neuronal death in the hippocampal CA3 region, and improve spatial learning in rat after traumatic brain injury. J Neurotrauma 24, 1132-1146.

Markakis, E.A., Gage, F.H., 1999. Adult-generated neurons in the dentate gyrus send axonal projections to field CA3 and are surrounded by synaptic vesicles. J Comp Neurol 406, 449-460.

McCullers, D.L., Sullivan, P.G., Scheff, S.W., Herman, J.P., 2002. Traumatic brain injury regulates adrenocorticosteroid receptor mRNA levels in rat hippocampus. Brain Res 947, 41-49.

McPherson, C.A., Kubik, J., Wine, R.N., D'Hellencourt, C.L., Harry, G.J., 2003. Alterations in cyclin A, B, and D1 in mouse dentate gyrus following TMT-induced hippocampal damage. Neurotox Res 5, 339-354.

Mehler, M.F., Kessler, J.A., 1997. Hematolymphopoietic and inflammatory cytokines in neural development. Trends Neurosci 20, 357-365.

Micheau, O., Tschopp, J., 2003. Induction of TNF receptor I-mediated apoptosis via two sequential signaling complexes. Cell 114, 181-190.

Monje, M.L., Mizumatsu, S., Fike, J.R., Palmer, T.D., 2002. Irradiation induces neural precursor-cell dysfunction. Nat Med 8, 955-962.

Monje, M.L., Toda, H., Palmer, T.D., 2003. Inflammatory blockade restores adult hippocampal neurogenesis. Science 302, 1760-1765.

Morgan, S.C., Taylor, D.L., Pocock, J.M., 2004. Microglia release activators of neuronal proliferation mediated by activation of mitogen-activated protein kinase, phosphatidylinositol-3-kinase/Akt and delta-Notch signalling cascades. J Neurochem 90, 89-101.

Ogita, K., Nishiyama, N., Sugiyama, C., Higuchi, K., Yoneyama, M., Yoneda, Y., 2005. Regeneration of granule neurons after lesioning of hippocampal dentate gyrus: evaluation using adult mice treated with trimethyltin chloride as a model. J Neurosci Res 82, 609-621.

Parent, J.M., Yu, T.W., Leibowitz, R.T., Geschwind, D.H., Sloviter, R.S., Lowenstein, D.H., 1997. Dentate granule cell neurogenesis is increased by seizures and contributes to aberrant network reorganization in the adult rat hippocampus. J Neurosci 17, 3727-3738.

Shen, Y., Li, R., Shiosaki, K., 1997. Inhibition of p75 tumor necrosis factor receptor by antisense oligonucleotides increases hypoxic injury and beta-amyloid toxicity in human neuronal cell line. J Biol Chem 272, 3550-3553.

Sheng, W.S., Hu, S., Ni, H.T., Rowen, T.N., Lokensgard, J.R., Peterson, P.K., 2005. TNF-alpha-induced chemokine production and apoptosis in human neural precursor cells. J Leukoc Biol 78, 1233-1241.

Spranger, M., Lindholm, D., Bandtlow, C., Heumann, R., Gnahn, H., Naher-Noe, M., Thoenen, H., 1990. Regulation of Nerve Growth Factor (NGF) Synthesis in the Rat Central Nervous System: Comparison between the Effects of Interleukin-1 and Various Growth Factors in Astrocyte Cultures and in vivo. Eur J Neurosci 2, 69-76.

Thorburn, A., 2004. Death receptor-induced cell killing. Cell Signal 16, 139-144.

Thored, P., Heldmann, U., Gomes-Leal, W., Gisler, R., Darsalia, V., Taneera, J., Nygren, J.M., Jacobsen, S.E., Ekdahl, C.T., Kokaia, Z., Lindvall, O., 2009. Long-term accumulation of microglia with proneurogenic phenotype concomitant with persistent neurogenesis in adult subventricular zone after stroke. Glia 57, 835-849.

van Praag, H., Schinder, A.F., Christie, B.R., Toni, N., Palmer, T.D., Gage, F.H., 2002. Functional neurogenesis in the adult hippocampus. Nature 415, 1030-1034.

Widera, D., Mikenberg, I., Elvers, M., Kaltschmidt, C., Kaltschmidt, B., 2006. Tumor necrosis factor alpha triggers proliferation of adult neural stem cells via IKK/NF-kappaB signaling. BMC Neurosci 7, 64.

Wine, R.N., McPherson, C.A., Harry, G.J., 2009. IGF-1 and pAKT Signaling Promote Hippocampal CA1 Neuronal Survival Following Injury to Dentate Granule Cells. Neurotox Res 16, 280-292.

Yamasu, K., Onoe, H., Soma, G., Oshima, H., Mizuno, D., 1989. Secretion of tumor necrosis factor during fetal and neonatal development of the mouse: ontogenic inflammation. J Biol Response Mod 8, 644-655.

Yang, L., Lindholm, K., Konishi, Y., Li, R., Shen, Y., 2002. Target depletion of distinct tumor necrosis factor receptor subtypes reveals hippocampal neuron death and survival through different signal transduction pathways. J Neurosci 22, 3025-3032.

Yu, T.S., Zhang, G., Liebl, D.J., Kernie, S.G., 2008. Traumatic brain injury-induced hippocampal neurogenesis requires activation of early nestin-expressing progenitors. J Neurosci 28, 12901-12912.

Chapter 3

Characterization of the neural progenitor cell microenvironment during injury-induced neurogenesis.

3.1 Introduction

Neurogenesis within the subgranular zone (SGZ) of the dentate gyrus (DG) of the hippocampus is stimulated upon injury to DG neurons including ischemia, traumatic brain injury, seizure activity, and neurotoxicant exposure (Bengzon et al., 1997; Collombet et al., 2005; Keiner et al., 2010; Liu et al., 1998; Rivas-Arancibia et al., 2010). Injury-induced stimulation of neurogenesis in the SGZ suggests a capacity for self-repair of DG following injury, raising questions regarding the specific processes involved in the initiation of proliferation and survival of these new cells (Cho and Kim, 2010; Ming and Song, 2005). In numerous models of injury-induced neurogenesis, there is often a concurrent localized elevation of pro-inflammatory cytokines and microglial activation in response to DG neuronal death. It has been proposed that this localized inflammatory response may modulate neurogenesis.

Early studies suggested the inflammatory response to brain injury hinders neurogenesis. Specifically pro-inflammatory cytokines including interleukin-1α (IL-1α), interleukin-1β (IL-1β), interleukin-6 (IL-6), and tumor necrosis factor-α (TNFα) were demonstrated to adversely affect the proliferation, differentiation and survival of neural progenitor cells (NPCs) (Ajmone-Cat et al., 2010; Das and Basu, 2008;

Mathieu et al., 2010). The adverse effects of neuroinflammation on neurogenesishave been attributed to infiltrating blood-borne monocytes as well as resident microglial cells. This raised questions regarding the potential role of inflammatory factors relative to the cellular source i.e., resident microglia or infiltrating blood-borne macrophages (Cacci et al., 2005; Monje et al., 2003; Nakanishi et al., 2007; Peng et al., 2008). Recent work demonstrated that resident microglia assist in regulating SGZ NPCs by phagocytosis of unhealthy and possibly excess NPCs (Sierra et al., 2010). Additionally, a supportive role for microglia to promote NPC survival and differentiation has been reported (Aarum et al., 2003; McPherson et al., 2011b).

These studies provided evidence that microglia are potentially beneficial to newly generated NPCs. This beneficial role of microglia is consistent with multiple studies providing evidence that activated microglia serve a beneficial neuroprotective function (Batchelor et al., 2002; Choi et al., 2008; Mandrekar et al., 2009). Activated microglia exhibit multiple morphological phenotypes, and possibly, multiple functional profiles in response to their surrounding environment (Kreutzberg, 1996; Streit, 2006). One paradigm proposed to classify microglial functional phenotypes is based on the study of monocyte lineage associated macrophage polarization. Macrophages respond to environmental stimuli by adopting functionally distinct activation states, as manifested by changes in morphology or gene expression profiles. These include the classically activated (M1) or alternatively activated (M2). The M1 activation state is characterized by the production of oxidative metabolites (nitric oxide and superoxide) and the pro-inflammatory IL-1, IL-

6, and, TNFα (Gordon, 2003; Mantovani et al., 2005). M1, pro-inflammatory, macrophages are responsible for destroying foreign organisms, damaged cells, and tumor cells. In order to return damaged tissue to homeostasis, the M1 activation phase is followed by an anti-inflammatory and repair phase. This phase, designated M2, leads to immunoresolution and repair. The anti-inflammatory molecules associated with the M2 phase include arginase 1 (AG-I), IL-4, IL-10, IL-13, and transforming growth factor beta 1 (TGFβ1). In the brain, molecules associated with the repair phase of M2 activation include brain derived neurotrophic factor (BDNF), chitinase 3-like 3 (YM-1), glial cell line derived neurotrophic factor (GDNF), and nerve growth factor (NGF). These activation states may be representative of the differentiation or staging of brain macrophages (Colton and Wilcock, 2010; Mantovani et al., 2005).

The ability of microglia to shift between the M1 and M2 phenotype has been proposed to contribute to neurodegenerative disease and chronic inflammation. Pro-inflammatory factors and excitotoxic molecules released by M1 activated microglia are thought to be detrimental in brain injury and disease (Colton and Wilcock, 2010) while anti-inflammatory molecules associated with the M2 phenotype are considered neuroprotective (Clarke et al., 2008; Dietrich et al., 1999; Lee et al., 2011; Yu et al., 2010). *In vitro*, microglia cells can be stimulated to produce pro-inflammatory M1 cytokines IL-1β, IL-6, and TNF-α (Colton et al., 2006; Michelucci et al., 2009). In these studies the M2 phenotype was also induced, as measured by the expression of anti-inflammatory molecules IL-4, IL-10, AG-I,TGFβ1 (Colton et al., 2006; Michelucci et al., 2009). Hippocampal NPCs express receptors for M1 pro-

inflammatory signaling factors including the 55 kDa type-1 TNF receptor (TNFp55R), 75 kDa type-2 (TNFp75R), IL-6 receptor (IL-6R), gp130, and IL-1 receptor 1 (IL-1R1) suggesting a possible modulatory role of microglia via inflammatory signaling during injury-induced proliferation (Iosif et al., 2006; Koo and Duman, 2008; McPherson et al., 2011a). The differential expression of M1/M2 related factors is likely representative of a well-regulated injury response (Colton et al., 2006; Hung et al., 2002; Ponomarev et al., 2007). Thus, the induction of an injury response in the brain by resident microglia may provide an environment for NPC proliferation, differentiation, and subsequent repair/repopulation in the injured hippocampus.

It has been previously demonstrated that a focal injury to dentate granule cell neurons in young mice prompts proliferation of NPCs within the SGZ (Harry et al., 2004). The localized damage to the dentate granule neurons was induced by the well characterized hippocampal toxicant, trimethyltin (TMT)(Bruccoleri et al., 1998; Geloso et al., 2002; Kassed et al., 2002; Reuhl and Cranmer, 1984). This model of hippocampal damage causes selective death and loss of dentate granule neurons over a 3 day period that is accompanied by a microglia response and activation of a pro-inflammatory cascade (Bruccoleri et al., 1998; Fiedorowicz et al., 2001; Lefebvre d'Hellencourt and Harry, 2005). In the work from our laboratory, we have demonstrated the stimulation of NPC proliferation occurs during the active process of neuronal degeneration, microglia phagocytosis, and under highly inflammatory conditions (Harry et al., 2004; McPherson et al., 2011a). These observations have been confirmed by the work of Ogita et al. (2005). Employing the TMT model of acute and selective neuronal death, the current study builds upon these

observations to further characterize this model and examined the morphological and molecular profile related to microglia morphological activation stages over the course of neuronal death and subsequent neurogenesis. We examined whether the observed morphological change in microglia represents a shift from the M1 (pro-inflammatory) to an M2 (anti-inflammatory/repair) profile over the timecourse of injury and recovery in the DG.

We now provide data demonstrating NPCs are generated and migrate in the GCL during a time that microglia demonstrate morphological characteristics of activation and down regulation to a resing state, astrocytes remain activated throughout this time. The NPC proliferation and migration occurs in a pro-inflammatory microenvironment. At the time of neuronal differentiation microglia and astrocytes did not exhibit morphological characteristics of activation. The DG microenvironment at the time of neuronal differentiation of newly generated cells was characterized by the expression of pro-inflammatory markers and repair-associated markers. The observed proliferative response to TMT injury leads to long-term repopulation of DG granule neurons and functional recovery of the hippocampus.

3.2 Materials and Methods

3.2.1 Mouse model of dentate granule cell death and induced neurogenesis

Postnatal day 21 (PND21) CD-1 male mice (Charles River Laboratories, Raleigh, NC) were individually housed in a dual corridor, semi-barrier animal facility with food (autoclaved NIH 31) and deionized, reverse osmotic-treated water available *ad libitum*. Sentinel animals recorded negative for pathogenic bacteria,

mycoplasma, viruses, ectoparasites, and endoparasites. All procedures were conducted in compliance with NIEHS/NIH Animal Care and Use Committee approved protocol. Mice received an intraperitoneal (i.p.) injection of either saline (SAL) or 2.3 mg/kg trimethyltin hydroxide (TMT; Alfa Products, Danvers, MA)/kg body weight (bwt) in an injection vol of 2 ml/kg bwt. Within 24 h, apoptosis of dentate granule neurons (Bruccoleri et al., 1998; Fiedorowicz et al., 2001; Harry et al., 2008b) was accompanied by microglia activation (Bruccoleri et al., 1998; Harry et al., 2008b). Mice displayed transient clinical signs of seizure at 24 h with no acute morbidity. This localized injury was confirmed to trigger proliferation of NPCs within the SGZ (Harry et al., 2004; Ogita et al., 2005).

3.2.2 Total tin (Sn) levels in the hippocampus

In order to determine the level of injected material that reached the target tissue and clearance, total tin (Sn) was analyzed in hippocampal samples at 1, 3, and 7 d post-TMT. Animals were euthanized by CO_2, the brain excised, the hippocampus dissected, placed in acid-washed glass vials and frozen. Individual samples were digested and Sn analysis was conducted using an inductively coupled plasma-mass spectrometry (ICP-MS; Hewlett-Packard; Palo Alto, CA). This method provided a limit of detection of 0.0032 µg Sn/g and could be reliably used to determine an experimental quantitation limit of 0.025 µg Sn/g. Statistical analyses were performed using the measured Sn concentrations obtained from the study samples and prepared blank samples (solvent, system, and matrix). Each measurement was analyzed in a one-way analysis of variance using PROC GLM (SAS Institute, Inc., Cary, NC).

3.2.3 Histopathology and immunohistochemistry

At 2,5,7 and 14 d post-injection, mice (n=14 per group with age matched controls) were anesthetized with CO_2 and decapitated. Brains were removed from the cranium, bisected in the midsagittal plane, and one hemisphere immersion-fixed in 4% paraformaldehyde/0.1M phosphate buffer (PB; pH 7.2) overnight at room temperature (RT). Brains were rinsed with PB, dehydrated in ethanol, embedded in paraffin, and 8 μm sections cut deparaffinized and ethanol rehydrated and stained with hematoxylin and eosin (H&E). Severity scores (1-4) were assigned for dentate granule cell death based upon number and location (progressing from the inner blade to throughout the blade of the dentate) of $eosin^+$ cells and structural characteristics of dense and collapsed chromatin as described previously (Funk et al., 2011). A score of 1 indicated no evidence of cell death, 2 indicated neuronal death occurring along the inner blade of the dentate to within a 3-cell layer width. A score of 3 indicated cell death throughout the entire blade of the dentate and a score of 4 indicated significant cell loss as indicated by the absence of distinct cellular material as represented by the presence of voids in the granule cell layer (GCL).

Paraffin sections (8 μm) of the hippocampus at 2, 5, 7, and 14 d post-injection were selected within the sagittal plane (0.36-1.95 mm lateral to the brain midline). Cleared and rehydrated sections were subjected to heat induced-epitope retrieval (HIER) in 1X Reveal Decloaker in a decloaking chamber (Biocare Medical, Walnut, CA) for 3 min, rinsed and maintained at RT for 20 min. Microglia were identified with a rabbit polyclonal antibody to ionizing calcium-binding adaptor molecule 1(Iba-1, 1:500; 1 h at RT; Wako Chemicals, Richmond, VA) and astrocytes were identified

with rabbit polyclonal antibody to glial fibrillary acidic protein (GFAP, 1:500; 1 h at 25^{o}C, Dako Corp., Carpenteria, CA). Immunoreactivity was visualized using a Vecastain Elite® ABC goat IgG kit (Vector Laboratories). To detect immature NPCs, sections were incubated (3 h at RT) in 0.1M PB containing 2% normal goat serum and goat anti-doublecortin (DCX) antibody (1:100; Santa Cruz Biotechnology, Santa Cruz, CA). DCX immunoreactivity was visualized using a Vecastain Elite® ABC goat IgG kit. Sections were counterstained with hematoxylin QS (Vector Laboratories).

3.2.4 BrdU immunohistochemistry

To determine peak time of NPC proliferation within the SGZ following TMT injection, mice received 2 injections of 5-bromo-2'-deoxyuridine (BrdU [50 mg/kg i.p.]; Sigma-Aldrich, St. Louis, MO) at 12 h intervals prior to tissue collection on days 1 through 7. Based upon these data and previous reports (Harry et al., 2004), a repeated BrdU dosing regimen [2x day - at the time of TMT dosing, and thereafter every 12 h for up to 3 days (d)] was used to label proliferating cells for quantitation and to determine cell fate over the course of 2 weeks.

At 24 h intervals between 3 and 7 d and at 14 d post-TMT or ^{SAL} injection, mice (n=6) were deeply anesthetized with CO_2, decapitated, the brain rapidly excised, cut in the mid-sagittal plane and one hemisphere immersion fixed in 4%PFA/PB for 18 h then processed for paraffin embedding. From each mouse, six section of the hippocampus were randomly selected within the sagittal plane (0.36-1.95 mm lateral to the brain midline). Cleared and rehydrated sections were incubated in 2N HCl (37℃, 30 min) to denature DNA, rinsed in PBS, and endogenous peroxidase activity quenched with 3% H_2O_2 (10 min). BrdU

incorporation was detected with a rat monoclonal anti-BrdU (1:500; 30 min at RT; Accurate Chemical and Scientific Corp, Westbury, NY) for 1h and visualized using a Vectastain *Elite*® ABC Rat IgG kit and DAB chromagen (Vector Laboratories, Burlingame, CA). To determine co-localization to neurons, BrdU was detected with AlexaFluor® goat anti-rat 594 (Invitrogen, Carlsbad, CA). Sections were then washed in 0.1 M PB, incubated in blocking solution (2% normal goat serum in 0.1 M PB), followed by incubation (90 min) in blocking solution containing mouse anti-NeuN AlexaFluor® 488 conjugated (1:500; Millipore). Sections were coverslipped with ProLong Gold® with DAPI (Invitrogen).

3.2.5 Cell Imaging and Microscopy

H&E and immunohistochemical images of the hippocampus were collected at both 20x and 40x magnification using an Aperio Scanscope T2 Scanner (Aperio Technologies, Inc. Vista, CA) and viewed using Aperio Imagescope v. 6.25.0.1117. Digital fluorescent images were captured as 16-bit monochrome images and pseudo-colored. For co-localization of fluorescent staining, digital images were acquired using a Leica LSM 5 laser-scanning microscope (Wetzlar, Germany).

For cell counting, a region of interest (ROI) was created for the dentate granule cell layer and individual eosin$^+$ positive cells displaying characteristics of cell death, Iba-1 microglia, and BrdU$^+$ cells were counted under a 100x objective using a Leica DMBRE light microscope. For counting of DCX$^+$ cells, two ROI were identified do estimate the migration of cells into the dentate granule cell layer. These included a 2-cell width at the inner blade of the DG representing the SGZ and on the basis of

exclusion of the SGZ, the remaining neuronal width of the GCL representing both the suprapyramidal and infrapyramidal blades of the dentate gyrus.

To examine the physical change in microglia within the GCL over the temporal progression of injury and repair, a rating scale was used to rank morphological phenotype. This rating scale was based upon the works of Wilms et al. (1997) and Heppner et al. (1998) for examining ramifications of microglia and macrophages. The modifications previously employed by Funk et al. (2011) take into consideration the *in vivo* sampling and the range of the cells from fine process bearing (score 1-2), to stellate, process-bearing (score 3-4), or amoeboid and rounded morphology (score 5-6).

3.2.6 Characterization of the mononuclear cell population in the hippocampus

To determine the origin of brain macrophages within the hippocampus following TMT, ^{SAL} and TMT treated mice (n=6) were anesthetized at 2 d post-injection with isoflourane and trans-cardiacally perfused with ice-cold phosphate buffered saline (PBS; pH 7.4). Brains were rapidly excised and the hippocampus mechanically dissociated by forcing through 160 and 70 μm nylon filters and the cell populations examined by flow cytometry for expression levels of CD11b and CD45 (Carson et al., 1998). The resulting individual hippocampal cell suspensions were enzymatically digested with DNase I (28 U/ml; Ambion) and collagenase (0.2 mg/ml; Worthington Biocem. Corp., Lakewood, NJ), in serum free Hank's buffered saline solution (HBSS) for 1 h at 37°C. Following incubation, the enzymatic digestion was quenched with 10% fetal bovine serum (FBS). Cell suspensions were separated on a discontinuous 1.03/1.088 Percoll™ Plus (GE Healthcare; Piscataway, NJ) gradient

(1500g for 20 min). Following centrifugation, myelin and cell debris floated above the gradient and were discarded. Monocytes collected from the interphase and 1.03 Percoll™ Plus fraction were washed 3x in one vol HBSS and cetrifuged at 1500g for 10 min at 4°C. The resuspended cells were incubated in mouse Fc Block (1:1000; BD Biosciences, cat #553141, San Diego, CA) in FACS buffer (HBSS + 10% FBS). Cells were washed with FACS buffer and incubated on ice for 30 min with 1:500 diluted PE-conjugated antibody to CD-45 (BD Biosciences, cat #553081) and FITC-conjugated anti CD-11b (cat #557396) or isotype controls (cat #553989 & 553988; BD Biosciences) in FACS buffer. Cells were washed in FACS buffer and staining was analyzed using Cell Quest 3.1 on a FACSORT instrument (BD Biosciences).

3.2.7 Quantitative real-time polymerase chain reaction (qRT-PCR)

A temporal association between specific transition points of microglia morphology and mRNA levels for genes related to M1 and M2 macrophage phenotypes within the dentate granule cell layer were examined. At 2, 5, 7, and 14 d post-injection, the excised hippocampus (n=4-6) was placed in ice-cold dissection media containing 50% Minimum Essential Medium (MEM; w/Earl's salts, w/o L-Glutamine) and 50% HBSS supplemented with 25mM HEPES, 36mM Glucose (D), and 1μM MK-801 and cut into approximately 10-12, 1 mm sections using a McIlwain Tissue Chopper (Ted Pella, Redding, CA). Sections were then transferred into dissection media and the DG sub-dissected using micro-dissection knife and needle under a dissection microscope (Suppl. Fig. 3.1).

RNA was isolated from the sub-dissected DG of each individual hippocampus with Trizol® Reagent (Invitrogen) and 2.5 μg used for reverse transcription

(SuperScript™II Reverse Transcriptase; Invitrogen). qRT-PCR was carried out on a Perkin Elmer ABI Prism™ 7700 Sequence Detector using 3 μl cDNA as a template, in a final concentrations of 1X Power SYBR® Green Master Mix (Applied Biosystems; Foster City, CA) and optimized forward and reverse primers for genes associated with the various activation stages (Table 3.1). The 50μl reaction mixture was held at 50°C for 2 min, 95°C for 10 min, followed by 40 cycles at 95°C for 15 s, and 1 min at 60°C. Amplification curves from individual qRT-PCR reactions were generated (Sequence Detection System (SDS) 1.9.1 software (Applied Biosystems), threshold cycle values determined, and mean fold changes calculated from each transcript relative to the average age matched ^{SAL} control using the comparative C_T method (Schmittgen and Livak, 2008).

3.2.8 Unbiased stereology of dentate granule neurons

As a measure of long-term neuronal recovery, the total number of dentate neurons was examined at 6 months (m) post-injection. Adult mice previously injected on PND21 with ^{SAL} or TMT (n=6) were deeply anesthetized by Nembutal (52 mg/kg, i.p.) and transcardially perfused with 4°C 0.1M PB followed by 10 ml of 4°C 4% PFA/PB (pH 7.4). Samples were post-fixed overnight, rinsed in PB, cryoprotected in 30% sucrose, embedded in OTC (Ted Pella, Redding, CA), and cryosectioned at 50μm. Total number of cresyl violet stained dentate granule neurons was determined by computerized unbiased stereology (*Stereologer*, Stereology Resource Center, Inc., Chester MD; (Lei et al., 2003; Long et al., 1998; Mouton et al., 2002). Sampling fractions for the optical fractionator method (West et al., 1991) were (a) section sampling fraction (ssf, the number of sections sampled

divided by the total number of sections); (b) the area sampling fraction (asf, the area of the sampling frame divided by the area of the x-y sampling step); and (c) the thickness sampling fraction (tsf, the height of the dissector divided by the section thickness). The dentate granule cell blades on each section were outlined under low power magnification (4X objective) and neurons in granule cell and pyramidal cell layers, respectively, were counted under oil immersion magnification (60X objective). The counting criteria required the presence of a distinct neuronal phenotype, including nuclear membrane, nucleolus, cytoplasm, and cell membrane; and placement within the 3-D virtual counting probe (dissector) or touching the inclusion planes, according unbiased counting rules (Gundersen, 1977). A guard volume of 2-3 µm was used to avoid artifacts (e.g., lost caps) at the sectioning surface. Stereological analysis was conducted on 8-12 sections sampled through the entire rostral-caudual extent of the hippocampus in a systematic random manner, every fifth section with a random start on sections 1-5.

3.2.9 Neurobehavioral assessment of hippocampal deficit and recovery

Hippocampal dependent learning and spatial reference memory were assessed in the Morris water maze. Seven days following injection of TMT or ^{SAL}, each mouse (n=6) was allowed a 1-min water-habituation trial followed by 3, 1 min trials/day (3 min inter-trial interval (ITI)) over 4 d, to learn the location of a submerged platform. On day 5, acquisition training was followed by a 1 min probe trial in the absence of a platform, during which the percent total time spent in the training platform (goal) quadrant was recorded (Any Maze, Stoelting, Wood Dale, IL).

To determine if the observed proliferation of SGZ NPCs following TMT resulted in a functional recovery of hippocampal spatial memory, a cohort of mice (n=6) were examined at 6 months post-injection. Beginning at the time of TMT dosing, mice received BrdU (50 mg/kg i.p.) 2x a day for 3 d. As adults, mice were subjected to 4 d of training for acquisition of the Morris water maze and one probe trial. Ninety min following completion of the probe test, mice were deeply anesthetized with Nembutal (52 mg/kg, i.p.) and transcardially perfused with 4°C 0.1M PB followed by 10 ml of 4°C 4% PFA/PB (pH 7.2). Samples were post-fixed 18 hrs, rinsed in PB, and cryoprotected in 30% sucrose, embedded in OTC (Ted Pella, Redding, CA), and cryosectioned at 50 μm. Cryosections containing the hippocampus were subjected to immunostaining for BrdU and Fos to assess the functional integration of $BrdU^+$ cells, as previously reported (Kee et al., 2007). Sections were incubated in 1N HCl at 37°C for 30 min, washed in 0.1M PB, and incubated in 0.1M PB with 0.3% Triton X-100, 2% normal goat serum, rat monoclonal antibody to BrdU (1:500; Accurate Biochemicals), and rabbit polyclonal anti-Fos (1:1000; Calbiochem, San Diego, CA). Immunoreactive product was detected using AlexaFluor® goat rat-488 and AlexaFluor® goat rabbit-594 (1:500; Invitrogen) secondary antibodies. Sections were coverslipped with Prolong Gold® with DAPI.

3.2.10 Statistical analysis

H&E severity scores and cell counts were analyzed by one-way ANOVA followed by independent group means comparisons by a Dunnett's multiple comparisons test. Microglia phagocytic microglia scores were analyzed by repeated

measures multivariate ANOVA, followed by independent group means comparisons by a Bonferoni test. Fold change in mRNA expression obtained by qRT-PCR were log transformed to obtain homogeneity of variance and analyzed by Student's *t*-test. Total Sn levels, flow cytometry data and unbiased stereology of neuronal counts were analyzed by Student's *t*-test. Acquisition of the Morris water maze was analyzed by a two-way repeated measures ANOVA, followed by independent group means comparisons by a Bonferoni test. Time spent in the goal quadrant in the probe test was analyzed by Student's *t*-test.

3.3 Results

3.3.1 Sn concentration in the hippocampus

Sn concentrations measured in the hippocampus samples from the SAL treated group (0.03 ± 0.008 mg Sn/g tissue; mean ± SD) were within the calibrated range of the instrument. The highest Sn concentration was observed in samples collected 1 d post-TMT (0.9 ± 0.15 mg Sn/g; $p<0.01$), decreasing at 3 d (0.21 ± 0.04 Sn/g; $p<0.05$) and returning to within control levels by 7 d (0.04 ± 0.009 Sn/g).

3.3.2 Histopathology

Consistent with previous reports, the neuropathology of the acute TMT injection involved the death of DG neurons in the hippocampus characteristic of apoptotic death with presence of nuclear fragmentation (i.e., apoptotic bodies) and cytoplasmic acidophilia (Funk et al., 2011; Harry et al., 2008a; Harry et al., 2008b). The pattern of neuronal death expanded through the blades of the DG and, by 2 d post-TMT, pyknotic eosin$^+$ neurons were evident throughout the GCL. The level of degeneration increased in severity to encompass a significant number of the dentate

granule neurons. Morphological evidence of ongoing neuronal death was diminished by 5 d post-TMT and, by 7 d, eosin^{+} cells were rare and the H&E staining was similar to SAL controls (Fig. 3.1A). A similar profile was generated at 2 d and 7 d with TUNEL as a marker of apoptotic cell death (Suppl. Fig. 3.2). Based upon defined severity scores, a significant effect of treatment ($F_{(3,52)}$=33.54; p<0.0001) was detected with a one-way ANOVA. Independent group mean analysis indicated severity score at 2 and 5 d post-TMT (p<0.05; Fig. 3.1B).

3.3.3 BrdU incorporation

Using BrdU uptake, the active period of NPC proliferation was identified to peak at day 2 post-TMT. In the post-weaning SAL control mice, a limited number of BrdU^{+} cells were identified in the SGZ. Upon injury to the dentate granule neurons by TMT, an increase of BrdU^{+} cells birth-dated with BrdU injections every 12 h for 3 d during the time of active cell death was observed in the SGZ and within the DG at 2, 5, and 7 d (Fig. 3.2A). An ANOVA identified a statistically significant effect of treatment ($F_{(7,22)}$=20.92; p<0.0001), with independent group mean analysis indicating significant increases in BrdU^{+} cells observed at 2-7 d post-TMT (p < 0.05; Fig. 3.2B). Mice were given BrdU injections every 12 h for 24 h prior to injection to identify the initiation of the proliferative response. The peak initiation of BrdU incorporation (Fig. 3.2C) was identified at 2 d post-TMT (Fig. 3.2D). BrdU^{+} cells were significantly increased following TMT administration ($F_{(7,21)}$=24.96; p<0.0001). Independent group mean analysis showed a significant increase in the number of BrdU^{+} cells in the DG labeled at either 2 or 3 d (p<0.01) post-TMT. By 5 d and later, the number of cells that incorporated BrdU was similar between TMT dosed and SAL control mice.

3.3.4 Doublecortin cells were increased within the blades of the dentate

Doublecortin (DCX) staining demonstrated that newly generated neurons rapidly migrated from the SGZ to the GCL (Brandt et al., 2003; Brown et al., 2003). In SAL treated mice, DCX^+ cell bodies were limited to within the SGZ. These cells displayed triangular soma and long vertical processes extending through the GCL characteristic of type-3 NPCs of the DG (Brandt et al., 2003; Brown et al., 2003) (Fig. 3.3A). By 5 d post-TMT, DCX^+ cells were present within the granule cell blades often observed in clusters (Fig. 3.3A). The total number of DCX^+ cells within the DG was significant increased following TMT ($F_{(3,8)}$=103.6; p<0.0001) at each time point 5 d (p<0.001; Fig. 3.3B). At 2 d, ≈80% of DCX^+ cells were located in the SGZ. By 5 d post-TMT, the number of DCX^+ cells that had migrated into the GCL was significantly increased to ≈50% of the total number of cells (Fig. 3.3C). By 7 d, the DCX staining pattern was similar to SAL controls, suggesting a return to a normal distribution across the two distinct regions.

3.3.5 Microglia and astrocyte morphology in the GCL during injury-induced proliferation and NPC migration.

In the SAL treated mouse hippocampus, Iba-1^+ microglia extend thin ramified processes throughout the GCL and SGZ (Fig. 3.4A). As expected, with injury to the dentate granule neurons by TMT, the microglia showed a morphological shift to either an amoeboid or stellate process bearing morphology indicative of activation (Fig. 3.4A). This resulted in an increase in the number of microglia compared to SAL controls ($F_{(3,12)}$=9.932; p<0.0014) at 2 d (p<0.001) and 5 d (p<0.05) post-TMT. While the number of $Iba1^+$ microglia remained elevated at day 5, cells shifted from

an activated amoeboid morphology to a morphology charactarized by thick ramified stellate processes. These reactive stellate microglia persisted in the GCL at day 7 and could be observed to extend processes into the SGZ (Fig. 3.4A). Quantitative estimates of the morphological response were conducted using a rating scale for process bearing (score 1-2), stellate process bearing (score 3-4), amoeboid process bearing, and amoeboid (score 5-6) microglia as previously described (Funk et al., 2011) (Table 3.2). In SAL mice, all of the microglia displayed thin ramified processes characteristic of score range of 1-2. Scoring data at 2,5,7 and 14 d post-TMT was analyzed by a repeated measures multivariate ANOVA. A significant main effect of score ($F_{(2,30)} = 8.82$; $p<0.001$), day ($F_{(4,30)} = 6.6$; $p<0.01$), and significant score x day interaction ($F_{(8,36)} = 68.73$; $p<0.0001$) were observed. Independent group mean analyses were then conducted on the TMT treated groups. In the 2 d post-TMT dosed mice, 80.42% ± 5.87% of the cells ranked at a score of 5-6 ($p<0.001$), indicative of a predominant amoeboid morphology. The remaining 20% of the cells displayed stellate, thickened processes, ranking at a score of 3-4 ($p<0.001$). By 5 and 7 d post-TMT, microglia displayed morphological phenotypes ranging across the scoring spectrum with the predominant morphology falling between score 3-4 ($p<0.05$) and a sparse demonstration of amoeboid microglia.

The astrocyte response over the same time period was also examined (Fig. 5), a thickening and retraction of processes was evident at 2 d, as compared to the thin and long fibrous processes projecting through the SGZ and GCL seen in controls. At 5-7 d, astrocyte hypertrophy was observed throughout the hippocampus and not limited to the GCL (Fig. 3.5).

3.3.6 Determination of the macrophage population in the injured hippocampus

Based upon expression of CD11b and a differential level of CD45 expression microglia and infiltrating macrophages in brain tissue can be identified and discriminated by flow cytometry (Babcock et al., 2003; Carson et al., 1998). In the SAL control mice $CD45^{low}/CD11b^{+}$ resident were observed, with very few $CD45^{high}/CD11b^{+}$ infiltrating macrophages observed (Fig. 3.6A). At the peak time of neuronal loss and microglia activation, 2 d post-TMT, a significant increase was observed in the number of $CD45^{low}/CD11b^{+}$ resident microglia ($t = 2.644$; $df=4$; $p<0.05$) with no change seen in $CD45^{high}/CD11b^{+}$ infiltrating macrophages (Fig. 3.6A and C). A direct intracerebral injection of lipopolysaccharide (LPS, 100 ng/ml) into the hippocampus served as positive control tissue (Carson et al., 1998) and resulted in a significant increase in $CD45^{low}/CD11b^{+}$ resident microglia ($t = 2.222$; $df=4$; $p<0.05$) and $CD45^{high}/CD11b^{+}$ infiltrating macrophages ($t = 2.448$; $df=4$; $p<0.05$) as compared to SAL controls.

3.3.7 qRT-PCR of M1 and M2 markers

Across the temporal pattern of neuronal death, microglia response, and NPC proliferation and differentiation, we examined mRNA levels for the M1 and M2 related genes to determine if we could identify a distinct profile associated with the morphological events. The selection of genes represented pro-inflammatory, anti-inflammatory, and repair-associated phenotypes as previously reported (Colton and Wilcock, 2010; Mantovani et al., 2005; Michelucci et al., 2009). With the primary phagocytic microglia response occurring with neuronal death at 2 d post-TMT, mRNA levels were significantly elevated for IL-1α ($t = 2.843$; $df=9$; $p<0.05$), IL-1β ($t =$

3.931; df=9; $p<0.05$), IL-6 (t = 3.096; df=9; $p<0.05$), TNF-α (t = 8.164; df=9; $p<0.05$), and IL-1Ra (t = 3.924; df=9; $p<0.05$), as compared to SAL controls. At this time, a significant decrease was observed in mRNA levels of the anti-inflammatory associated factors, IL-4 (t = 2.620; df=9; $p<0.05$) and IL-13 (t = 5.205; df=9; $p<0.05$), with no change in iNOS, AG-I, TGFβ, and IL-10. For the repair-associated genes, YM-1 was significantly increased (t=5.205; df=9; $p<0.05$), with no change seen in BDNF, GDNF, and NGF mRNA levels (Fig. 3.7A).

At 5 d post-TMT, resolution of the damage was accompanied by a significant elevation in mRNA levels for IL-1α (t = 6.323, $p<0.05$) and TNF-α (t = 4.288; df=10; $p<0.05$; Fig. 3.7B). mRNA levels for IL-6, IL-1β, IL-1Ra, and iNOS were not significantly different from controls. For anti-inflammatory genes, a slight increase was suggested for TGFβ1 mRNA levels but failed to reach statistical significance and AG-1, IL-4, IL-10, and IL-13 were not altered. In the repair related transcripts, BDNF (t = 2.289; df=10; $p<0.05$) mRNA levels were significantly decreased with no difference observed in GDNF and NGF mRNA levels. The earlier elevation in YM-1 was no longer evident at 5 d with mRNA levels falling under ^{SAL} controls.

By 7 d, the active period of neuronal death ceased and the associated microglia activation significantly resolved. mRNA levels for IL-1α remained elevated (t = 6.258; df=6; $p<0.05$) while TNF-α returned to within control levels. These changes were accompanied by a second elevation in IL-1Ra (t = 3.737; df=6; $p < 0.05$) and IL-6 (t=3.628; df=6; $p<0.05$) (Fig. 3.7C). IL-1β levels were increased 4-fold but did not reach statistical significance. mRNA levels for iNOS (t = 3.565; df=6; $p < 0.05$) were significantly lower, as compared to controls. BDNF was the only repair-

related gene significantly elevated (t = 4.971; df=6; $p < 0.05$) with no changes observed for GDNF, NGF, and YM-1 (Fig. 3.7C).

3.3.8 Repair processes at 14 d post-TMT

We previously reported that $BrdU^+$ cells generated during the time of microglia activation migrate into the DG within 14 d of injury and express the mature neuronal marker neuronal nuclei (NeuN) (Harry et. al., 2004). This migration was confirmed in the current study and, by 14 d, $BrdU^+/NeuN^+$ neurons were observed throughout the entire dentate granule cell layer (Fig. 3.8). At this time, Iba-1^+ microglia displayed thin processes throughout the GCL and SGZ, similar to ^{SAL} controls with 100% of microglia falling within the score range of 1-2 (Fig. 3.9A, Table 2). $GFAP^+$ astrocytes extended fibrous processes throughout the SGZ and GCL in both groups (Fig. 3.9B). However, in the TMT-dosed mice, the $GFAP^+$ astrocytes displayed thicker processes through the blade of the dentate and along the SGZ (Fig. 3.9B). When we examined the M1 and M2 related genes at this time of repair, a significant elevations in mRNA levels for IL-1β (t = 2.932; df=8; $p<0.05$), IL-6 (t = 6.991; df=8; $p<0.05$), and iNOS (t = 4.530; df=8; $p<0.05$) were observed. This was accompanied by significant elevations in AG-I (t = 2.648; df=8; $p<0.05$) and IL-1Ra (t = 2.501; df=8; $p<0.05$). A significant increase was observed in mRNA levels for the repair related genes, BDNF (t = 2.633; df=8; $p<0.05$), GDNF (t = 4.398; df=8; $p<0.05$), NGF (t = 3.155; df=8; $p<0.05$), and YM-1 (t = 3.573; df=8; $p<0.05$) (Fig. 3.10).

3.3.9 Unbiased stereology of dentate granule neurons at 6 months post-injury indicated a full replacement of the neuronal population

To determine persistence of the newly generated dentate granule cell, the number of neurons within the dentate granule cell blades 6 months (mo) post-TMT was determined using unbiased stereology. The morphological and structural features of the hippocampus demonstrated no differences between the TMT and ^{SAL} control groups (Fig. 3.11A). The total volume of the superpyramidal and infrapyramidal blades of the dentate was not significantly different in the TMT mice (Fig. 3.11B). In addition, the loss of dentate granule cells following TMT was no longer evident in the adult with a similar total number of dentate granule neurons as observed in the SAL controls (Fig. 3.11B).

3.3.10 Morris Water Maze

To examine the functional deficit and recovery of the hippocampal injury following TMT, mice were assessed in the Morris water maze at 7 d and 6 m post-injection. At 7 d post-TMT, mice displayed adverse clinical signs of acute toxicity. Prior to maze testing, we confirmed no evidence of altered body weight gain, hindlimb strength, activity levels, or swimming speed that could compromise performance on the water maze. Latency data was analyzed by a repeated measures ANOVA and indicated significant main effects of training day ($F_{(3,30)}$ = 13.4; $p<0.0001$), treatment ($F_{(1,30)}=71.42$; $p<0.0001$), and significant training day x treatment interaction ($F_{(3,30)}$ = 3.562; $p<0.025$). Both dose groups showed an acquisition of the task over the 4 days of training (Fig. 3.12A); however, the majority of TMT dosed mice failed to perform the task within the maximum latency period of

60 sec on training days 1 and 2, showed decreased latency on day 3, and, by day 4, performed at a similar latency to ^{SAL} controls. Independent group mean analysis indicated that the deficit in performance on day 2 was statistically significant ($p<0.05$) (Fig. 3.12A). In the probe test to assess memory of the platform location (goal quadrant), TMT dosed mice did not demonstrated a normal preference for the goal quadrant as seen in SAL control mice (t=2,89; df=10; $p<0.01$) (Fig. 3.12B).

In mice that were allowed to recover from the injury over a 6 m period, consistent with the unbiased stereology data, hippocampal functioning, as assessed by the Morris water maze, had returned to within normal control performance. Acquisition of the task was clearly demonstrated over the 4 days of training ($F_{3,42} = 69.41$; $p<0.0001$) (Fig. 3.11C) with no evidence of differences in mice previously injected with TMT. In the probe trial, both groups of mice demonstrated similar preference for the goal quadrant (Fig. 3.12D). The immediate early gene Fos is rapidly induced by performance on the probe trial reflecting circuitry activation (Guzowski et al., 2005). The functional integration of the $BrdU^+$ cells generated during the initial injury response was supported by co-localization of Fos within 90 min following the probe test (Fig. 12E).

3.4 Discussion

Although inflammation is gaining attention with regards to brain injury induced neurogenesis, the role of brain-endogenous inflammatory factors on the injury/repair process is not fully understood nor is the involvement of microglia. In the current study, we examined a broad spectrum of pro-inflammatory (M1) markers and anti-inflammatory/repair (M2) within a framework of neuronal death, microglia activation,

and induction of NPC proliferation. We had several goals for this study. One was to correlate the markers for each inflammatory state with the morphological changes of microglia over the temporal course of the TMT-induced injury. The second was to correlate these changes with the generation, migration, and maturation of newly generated cells induced by neuronal death in the DG. We considered that identification of a link between stages of microglia activation and NPC proliferation and survival would provide a framework for examining neurodegenerative processes and potential repair mechanisms.

Neuroinflammation and elevations in pro-inflammatory cytokines have been largely associated with a detrimental effect upon NPC proliferation and neuronal differentiation (Ajmone-Cat et al., 2010; Das and Basu, 2008; Mathieu et al., 2010). A majority of the supporting studies identified a detrimental effect of microglia *in vitro*, and may not properly model the inflammatory contribution of resident microglia within the neurogenic region. Additional *in vivo* studies utilized brain insults including seizure, ischemia and traumatic brain injury that likely breach the blood brain barrier (BBB) allowing the infiltration of peripheral monocytes into the brain parenchyma (Lehrmann et al., 1997; Stoll et al., 1998; Williams et al., 2006; Zattoni et al., 2011). Compared to resident microglia, cells of the peripheral immune system are strong antigen presenting cells, provide an enriched source of cytokine and inflammatory factors and thus exhibit exaggerated activation phenotypes (Hickey and Kimura, 1988). Thus, brain macrophages derived from infiltrating blood-borne monocytes would represent a source of inflammatory related factors significantly higher than resident microglia and serve as a major confounder. Consistent with this

is the work from Shohami et al. that (1999) suggests the diverging consequences of pro-inflammatory cytokine receptor activation is dependent on subtle differences in the intensity or duration of the stimulus, as well as, the extra/intracellular environment. Recent work has demonstrated infiltrating monocytes as detrimental to NPCs in an *in vivo* model of human immunodeficiency virus infection (Peng et al., 2008). It is possible that infiltrating macrophages produce either different levels of the pro-inflammatory cytokines or different inflammatory molecules altogether than those produced by resident microglia, thereby negatively affecting the endogenous response to injury in the neurogenic region. Using the TMT model, we confirmed previous work demonstrating an absence of recruitment of blood borne monocytes to the injury site (Funk et al., 2011; Harry et al., 2003). We now provide data demonstrating that resident microglia and the pro-inflammatory cytokine elevation occurring following injury are not detrimental to the generation and differentiation of healthy SGZ NPCs.

The distinct morphological response of microglia, as it relates to the state of the neuron, suggests both protective and injurious actions. Functional changes of activated microglia are often accompanied by a morphological transformation leading from cells with thin, ramified processes to cells with larger somata and shorter, coarser cytoplasmic processes. This can eventually progress to amoeboid cells with morphology similar to macrophages. *In vivo*, the transformation of resident microglia into those with a phagocytic phenotype is strictly regulated; however, they retain the capability to shift their phenotype within specific stages of the inflammatory response (Stout and Suttles, 2005) and may not follow a macrophage stereotypic

and linearly graded phenotypic reaction (Hanisch and Kettenmann, 2007; Ransohoff and Perry, 2009). Consistent with previous work using the TMT model, activation of microglia with an amoeboid morphology is evident in the GCL with the presence of apoptotic neurons (Bruccoleri et al., 1998; Harry et al., 2002). However, even within this region a number of microglia maintain a ramified morphology suggesting heterogeneous functions. As active neuronal death dissipates, the local microglia response shifts to a stellate morphology eventually returning to a normal ramified process bearing morphology. This shift temporally and spatially corresponds with the migration of new cells into the region that has been cleared of neuronal debris allowing for repair. An astrocyte response, characterized by increased GFAP immunoreactivity in process bearing cells, follows microglia activation and the initiation of neuronal death consistent with previous reports (Bruccoleri et al., 1998); yet, it continues for a greater period of time extending into the synaptic remodeling of the hippocampus.

Shifts in markers of the M1 and M2 inflammatory states (Colton, 2009; Gordon, 2003) have recently been used in an attempt to discriminate inflammatory status between mouse models of Alzheimer's disease (Wilcock et al., 2011). While the TMT injury/repair model spans a few days to a couple of weeks, we saw a similar profile as reported for these more chronic models (Wilcock et al., 2011). In the APPSw/NOS2-/- mice, a mixed profile of elevated mRNA levels of M2 markers YM1, AG-I, IL-1Ra and M1 markers TNFα, IL-6, and IL-1β occurred at an age of significant hippocampal neuronal loss (Wilcock et al., 2011). While, in the APPSw mouse, the presence of amyloid deposition and absence of neuronal death was

accompanied by elevated mRNA levels for M2 related genes. We considered that these heterogenous patterns were due to the chronic nature of the injury process and that with a more acute and defined injury and microglia response one would be able to detect a clear sequential pattern of inflammatory states. However, we now demonstrate that the heterogeneous pattern of inflammatory states is recapitulated with acute injury and repair and that a clear shift in phenotype from M1 to M2 is not clearly demonstrated. It is known that apoptotic cells can directly stimulate an inflammatory state that can also initiate an acquired deactivation response (Cameron and Landreth, 2010; Ransohoff and Perry, 2009). The pronounced apoptotic death of dentate granule neurons following TMT was accompanied by phagocytic microglia for debris clearance. This coincided with an elevation in M1 cytokines IL-1α, IL-1β, IL-6, and TNFα, as well as the M2 associated genes, IL-1Ra and YM-1. The previous demonstration that TMT-induced dentate granule cell death is a TNF receptor dependent event (Harry et al., 2008b) concurs with the interpretation of TNFα elevation as a detrimental pro-inflammatory event. While IL-1α and IL-1β are also elevated, it is likely that the elevation in IL-1Ra, possible stimulated by TNFα and IL-1 (Watkins et al., 1999), is sufficient to block receptor activation (Seckinger et al., 1987). This would be consistent with the previous report indicating a lack of involvement of IL-1R activation in the TMT-induced neuronal death (Harry et al., 2008a). Of interest is the absence of elevation in iNOS as it is considered to contribute to the classically activated M1 response (Colton and Wilcock, 2010). Thus, from the current study and previous studies (Bruccoleri et al., 1998; Maier et al., 1995) it appears as if the TMT model excludes this component

from the injury pro-inflammatory stage, The early elevation in IL-6, while pro-inflammatory, could reflect anti-inflammatory actions via the downregulation of TNFα and IL-1α signaling through induction of the decoy soluble TNF receptor and IL-1Ra (Petersen and Pedersen, 2006; Tilg et al., 1994). Previous studies identified astrocytes as the primary source for IL-6 following TMT and expression of IL-6R on surviving neurons (Funk et al., 2011) supporting the idea that IL-6 is serving in a neuroprotective capacity. The only clear M2 related gene shown to be elevated in these early stages of injury was YM-1. This protein is expressed in microglia following brain injury (Hung et al., 2002) and has been implicated as a link between the anti-inflammatory and repair process (Raes et al., 2002a; Raes et al., 2002b). While the exact anti-inflammatory mechanism of YM-1 is not known, it is believed to modulate inflammation and leukocyte trafficking by competing for binding sites on the extracellular matrix (Chang et al., 2001). However, in the absence of leukocytes exactly what role YM-1plays is still in question. Thus, during the peak of neuronal death, the region is stimulating the production of classical pro-inflammatory cytokines, which can serve to stimulate the production of anti-inflammatory regulatory factors such as IL-1Ra but also initiate signals toward the resolution of injury.

With the end of the neuronal death phase, microglia showed a progressive return to a ramified morphology suggesting a shift in function. Thus, in the absence of apoptotic signals and presence of cellular debris, the microglia either downregulate to a more quiescent phenotype or totally shift their active functions. However, upon further examination it was found that with the apparent

downregulation of microglia as evidenced by a shift in morphology, elevated mRNA levels of IL-1α, IL-6, and TNFα were maintained. In the full commitment to repair, new neurons were integrated into the dentate granule layer and microglia returned to a normal basal level morphology. As expected, this was accompanied by an increase in arginase 1 and the repair associated genes, BDNF, GDNF, and NGF. YM-1 continued to be elevated similar to levels seen at day 3. However, a second increase in mRNA levels for IL-1β was observed and this was accompanied by an elevation in IL-1Ra. Of interest was the continued elevation in mRNA levels for TNFa and IL-6 but now, with remodeling and repair, iNOS was elevated.

Induction of M2 associated genes is considered to initiate repair following an acute M1 response (Gordon, 2003; Raes et al., 2002b) to ensure proper brain homeostasis and limit the M1 cytotoxicity (Choi et al., 2011; Frieler et al., 2011). The absence of an increase in the classical anti-inflammatory cytokines IL-4, IL-10, and IL-13 suggest that under these conditions IL-1Ra may play a signifcant role in regulation of inflammatory signaling. A further regulatory role for IL-1Ra is implicated subsequent to the resolution of the injury, with a secondary increase in IL-1β mRNA levels. Interestingly, the later time point associated with a return of microglia to a normal morphology and the appearance of healthy dentate granule neurons was the only time at which elevations in mRNA levels for iNOS were observed. iNOS is considered to contribute to the classically activated M1 response (Colton and Wilcock, 2010), however the results of this study and previous work in the TMT model do not implicate it during the early pro-inflammatory response . This was accompanied by an elevation in mRNA levels for AG-I potentially regulating by

competing with iNOS for arginine (Morris, 2004). At the later time point AG-I directly inhibit iNOS, or iNOS may have a neuroprotective role such as has been reported in ischemia (Cho et al., 2005).

Much of the previous work examining the impact of neuroinflammation on NPCs has focused on the regulatory roles of TNFα, IL-1β, and IL-6 and detrimental effects upon various aspects of adult neurogenesis (Cacci et al., 2008; Cacci et al., 2005; Iosif et al., 2006; Koo and Duman, 2008; Monje et al., 2003; Vallieres et al., 2002). Given that the temporal pattern of neuronal death and microglia activation coincided with peak stimulation of NPCs proliferation, we examined the inflammatory profile within the framework of its impact on the newly generated cells. The SGZ is considered the primary regulatory environment for hippocampal NPCs. Within this environment, mRNA levels for IL-1α are elevated with death of dentate granule neurons. This occurs in the absence of elevations in IL-1β, or IL-6 (McPherson et al., 2011) and TNFα (Suppl. Fig 3). In addition to the SGZ, the neighboring GCL can also be viewed as a "neurogenic niche" with regards to secreted factors, as well as a physical environment for fostering the migration, differentiation, and maturation of newly generated cells. In the present study, elevations in IL-1α, IL-1β, IL-6, and TNFα mRNA levels were observed in the subdissected DG, which included both the SGZ and the GCL. It is possible that NPCs in the SGZ could be exposed to these cytokines by diffusion from the neighboring GCL.

As a pro-inflammatory cytokine, TNFα inhibits NPC proliferation *in vitro* (Cacci et al., 2005). Using knockout mice, Iosif et al., (2006) confirmed these effects showing increased NPC proliferation in the absence of TNFp55R and a deficit in

mice deficient for TNFp75R; with a concurrent deficit in migration from the SGZ (McPherson et al., 2011b). In the TMT injury, a differential pattern of TNFp55R and TNFp75R is initiated as the injury progresses. Early in the TMT injury response (6-12 h) neurons predominately express TNFp55R or both TNFp55R/TNFp75R. By 24-48 h there is an equal distribution of neurons expressing TNFp75R and TNFp55R/TNFp75R with the remainder expressing TNFp55R (Harry et al., 2008b). Newly generated cells express TNFp75R during the peak proliferative response in the TMT injury model (McPherson et al., 2011b). Based on these studies the elevation of TNFα in the DG at 5 d may be contributing to the migration and survival of the new cells into the injured GCL.

Newly born cells within the SGZ express IL-1R1 protein (Koo and Duman, 2008), and NPCs isolated from the hippocampus of PND21 mice express mRNA for IL-1R1 and IL-1R accessory protein (IL-1RAcP)(McPherson et al., 2011a). Previous work implicated IL-1R1 signaling, via IL-1α or IL-1β, in the regulation of NPC proliferation (Koo and Duman, 2008; McPherson et al., 2011a; Spulber et al., 2008). Anti-proliferative effects of IL-1β on hippocampal NPC proliferation have been demonstrated *in vivo* and *in vitro* (Koo and Duman, 2008) while, the upregulation of IL-1α and downstream IL-1R1 pathway signaling has been implicated in NPC proliferation (McPherson et al., 2011a). Data in this study suggest a robust proliferative response occurs within the DG in the presence of elevated levels of both IL-1α and IL-1β, supporting the potential pro-neurogenic effects of IL-1R1 signaling. IL-Ra is also elevated at the times of the elevations in IL-1α and IL-1β.

IL-1Ra may serve to minimize the pro-inflammatory effects of IL-1α and the anti-proliferative actions of IL-1β in the TMT injury model.

An elevation in IL-6 mRNA was also observed at day 14 of neuronal differentiation. In the brain, IL-6 has a dual role both as a pro-inflammatory molecule (Bauer et al., 2007) and as a neurotrophic factor. IL-6 can promote neuronal differentiation (Cao et al., 2006) and survival *in vitro* (Cao et al., 2006; Zhang et al., 2007); yet, Monje et al., (2003) reported IL-6 inhibition of neuronal differentiation of adult hippocampal NPCs. Neuronal regeneration *in vivo* can be enhanced with over-expression of IL-6 and soluble IL-6 receptor (Hirota et al., 1996). IL-6 works in concert with BDNF to promote neuronal survival (Murphy et al., 2000) or NGF to promote neuronal differentiation (Kunz et al., 2009; Sterneck et al., 1996) *in vitro*. Thus, it is likely that during the repair stage IL-6 works in concert with BDNF, NGF, and GDNF to promote differentiation and survival of healthy new hippocampal neurons (Frielingsdorf et al., 2007). Given the overall profile at this time, the concurrent increase in YM-1 is likely reflective of efforts to stabilize growth factor signaling by regulating protein degradation (Raes et al., 2002a; Raes et al., 2002b). One could speculate that the increased growth factor signaling coupled with the observed increase in AG-I, IL-1Ra, and YM-1 represents a shift to a pro-neurogenic repair M2 response. Indeed our results demonstrate that the $BrdU^+$ cells generated early in the injury begin expressing the mature neuronal marker NeuN within this environment. The timing of this repopulation is consistent with the birth and differentiation of NPCs in the normal hippocampus where post-mitotic NPCs begin to display characteristics of mature neurons within 14-21 d following birth (Brandt et al.,

2003; Kronenberg et al., 2003). The function of these newly generated neurons was tested in the Morris water maze (MWM). Training mice in the MWM to find the hidden platform produces long-lasting spatial memories dependent on hippocampal circuitry including the DG (McNaughton et al., 1989; Teixeira et al., 2006). While a repopulation of the DG with $BrdU^+/NeuN^+$ cells was observed, it did not ameliorate deficits in hippocampal function as observed in the MWM. Since it takes newly generated neurons 4-8 weeks to become functionally indistinguishable from mature granule neurons (van Praag et al., 2002), the deficits observed at 14 d in the MWM were not unexpected. However, at 6 m post-TMT $BrdU^+$ cells generated in the peak proliferative response expressed Fos following the hippocampal dependent memory task, suggesting these cells repopulate the DG and become functional within the hippocampal circuitry (Kee et al., 2007).

In this study the adolescent brain displays a robust capacity to generate new hippocampal neurons and to utilize a highly inflammatory environment to facilitate the success of this process. The sequence of events associated with M1/M2 signaling suggests that while a number of these molecules are used in brain repair the profile is very heterogenous. In comparison to other injury studies, any differences may be attributed to the reliance on resident microglia alone in the TMT model. While microglia are the primary source of genes associated with the inflammatory related responses, astrocytes and neurons may also be a source for these genes as well as those for the various growth factors. (Colton, 2009; Colton and Wilcock, 2010; Wilcock et al., 2011). Furthermore, it is highly likely that the cellular source of the various markers shifts with the demands of the environment.

While one may consider our data within the framework of progressive neurodegenerative given the similarities to the profile generated in the AD mouse models (Colton et al., 2011) we consider the data, and model, well suited to begin the identification of critical signals and cellular sources for the M1/M2 related proteins at critical periods of brain injury and repair. Gaining further understanding will contribute to identifying therapeutic strategies to enhance successful NPC proliferation and neuronal differentiation to repair brain injury.

Table 3.1. Quantitative real time PCR primer sequences.

Gene	Forward Primer (Concentration)	Reverse Primer (Concentration)
AG-I	TTGGCAAGGTGATGGAAGAGACCT (300 nM)	CGAAGCAAGCCAAGGTTAAAGCCA (300)
BDNF	TCTCAGAATGAGGGCGTTTGCGTA (300 nM)	TGGAACATTGTGGCTTTGCTGTCC (300 nM)
GAPDH	GGGAAGCTCACTGGCATGG (300 nM)	CTTCTTGATGTCATCATACTTGGCAG (300 nM)
GDNF	AGAAGAGGCCCTCCCTCATTGTTT (300 nM)	AGCAGCCACAAAGGGAGTGATACA (300 nM)
IL-1α	TCGGGAGGAGACGACTCTAA (600 nM)	GGCAACTCCTTCAGCAACAC (600 nM)
IL-1β	TGGTGTGTGACGTTCCCATT (300 nM)	CAGCACGAGGCTTTTTTGTTG (300 nM)
IL-1Ra	CTCCCTTCTCATCCTTCTGTTTCATT (300 nM)	CAGCACGAGGCTTTTTTGTTG (300 nM)
IL-4	TCACTGACGGCACAGAGCTATTGA (300 nM)	AATATGCGAAGCACCTTGGAAGCC (300 nM)
IL-6	TCCTACCCCAATTTCCAA (300 nM)	CGTACTAGGGCCCAG (300 nM)
IL-10	TGCTATGCTGCCTGCTCTTACTGA (300 nM)	TCCTTGATTTCTGGGCCATGCTTC (300 nM)
IL-13	ACACAAAGCAACTGTTTCGCCACG (300 nM)	AAGAAATGTGCTCAAGCTGCTGCC (300 nM)
iNOS	TTCACCCAGTTGTGCATCGACCTA (300 nM)	AACTCCAATCTCGGTGCCCATGTA (300 nM)
NGF	AGTGTCAGTGTGTGGGTTGGAGAT (300 nM)	AAGGTGTGAGTCGTGGTGCAGTAT (300 nM)
TGF-β1	GCTCACTGCTCTTGTGACAGCAAA (300 nM)	TGTACTGTGTGTCCAGGCTCCAAA (300 nM)
TNF-α	TGGCCTCCCTCTATCAGTT (300 nM)	GCTTGTCACTCGAAATTTGAGAAG (900 nM)
YM-1	AGGAAGCCCTCCTAAGGACAAACA (300 nM)	ATGCCCATATGCTGGAAATCCCAC (300 nM)

Table 3.2. Quantitative scoring of microglia morphology in the dentate gyrus.

	% Score 1-2	% Score 3-4	% Score 5-6
SAL	100.00 ± 0.00	0.00 ± 0.00	0.00 ± 0.00
2 d	0.00 ± 0.00[a]	19.58 ± 5.87[a]	80.42 ± 5.87[a]
5 d	13.56 ± 6.43[a]	61.24 ± 12.18[a]	25.20 ± 7.86[a]
7 d	3.78 ± 3.14[a]	73.55 ± 8.86[a]	22.67 ± 11.42[a]
14 d	100.00 ± 0.00	0.00 ± 0.00	0.00 ± 0.00

Values represent mean percent of total microglia in each scoring category ± SEM in each treatment group (SAL, 2, 5, 7 and 14 d post-TMT). Data were analyzed by repeated measures multivariate ANOVA, followed by a Bonferoni post-hoc test.

[a] $p < 0.01$, compared SAL in each score group.

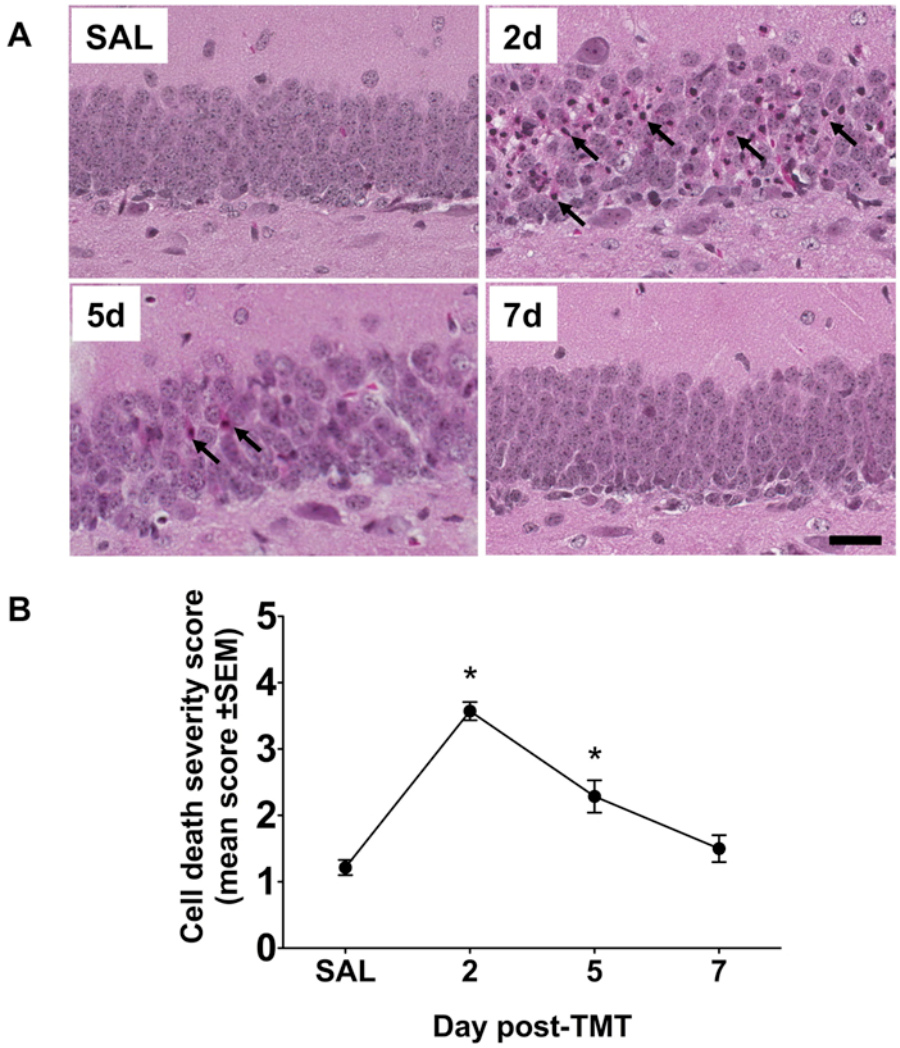

Figure 3.1. Histopathology in the dentate gyrus.
(A) Representative hematoxylin and eosin (H&E) in the DG of SAL control and 2, 5, and 7 d post-TMT (2.3 mg/kg, i.p.). Neuronal death characterized by nuclear and karylosis (arrows) was observed in the dentate gyrus (DG) at 2 and 5 d post-TMT. Scale bar = 30μm. (B) Data represents the mean neuronal death severity score (±SEM) within the DG as described in methods. Data was analyzed by one-way ANOVA followed by a Dunnett's multiple comparison test (*p<0.05).

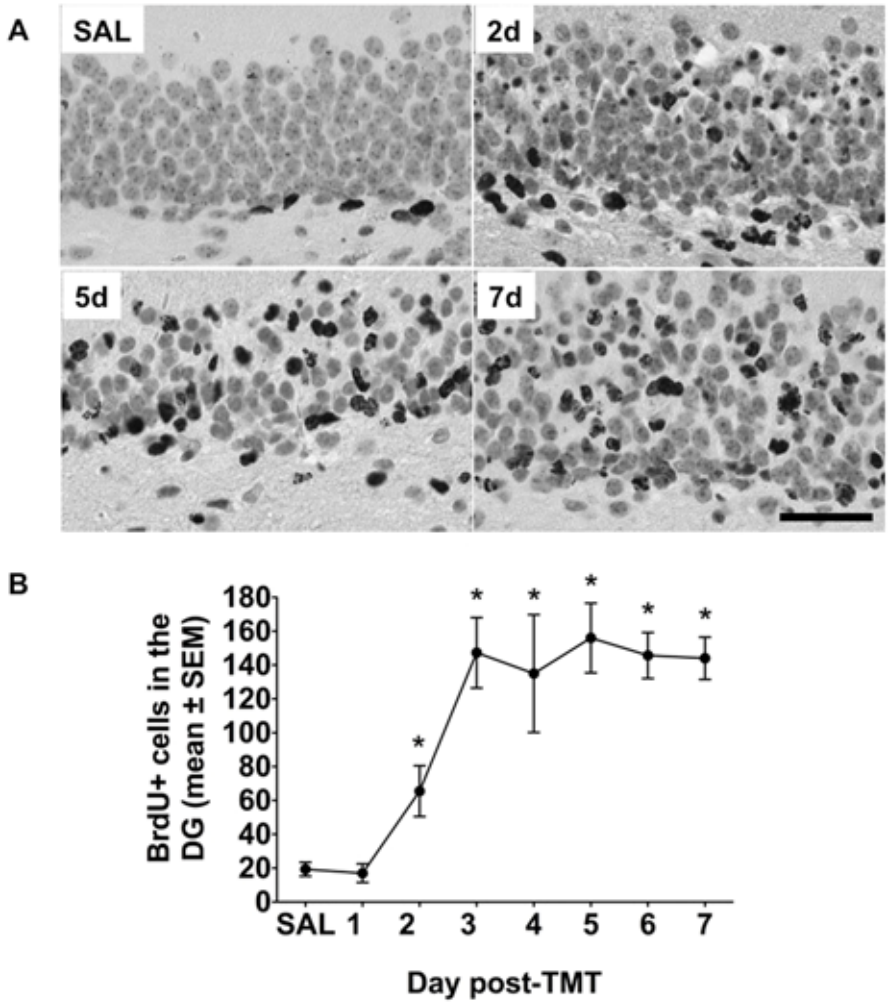

Figure 3.2. Injury-induced proliferative response in the dentate gyrus. (A) Representative images of BrdU immunohistochemistry (dark black product) located in the subgranular zone (SGZ). Mice received BrdU every 12 h for 3 d following SAL or TMT (2 mg/kg, i.p.). $BrdU^+$ cells were observed in the SGZ of SAL treated mice, following TMT and increased number of $BrdU^+$ cells are observed in the SGZ and granule cell layer (GCL) at 2,5, and 7 d. Scale bar = 50 μm. (B) Quantitation of $BrdU^+$ cells in the DG as described in Methods. Data represents mean (±SEM) and was analyzed by one-way ANOVA followed by a Dunnett's multiple comparison test (*p<0.05).

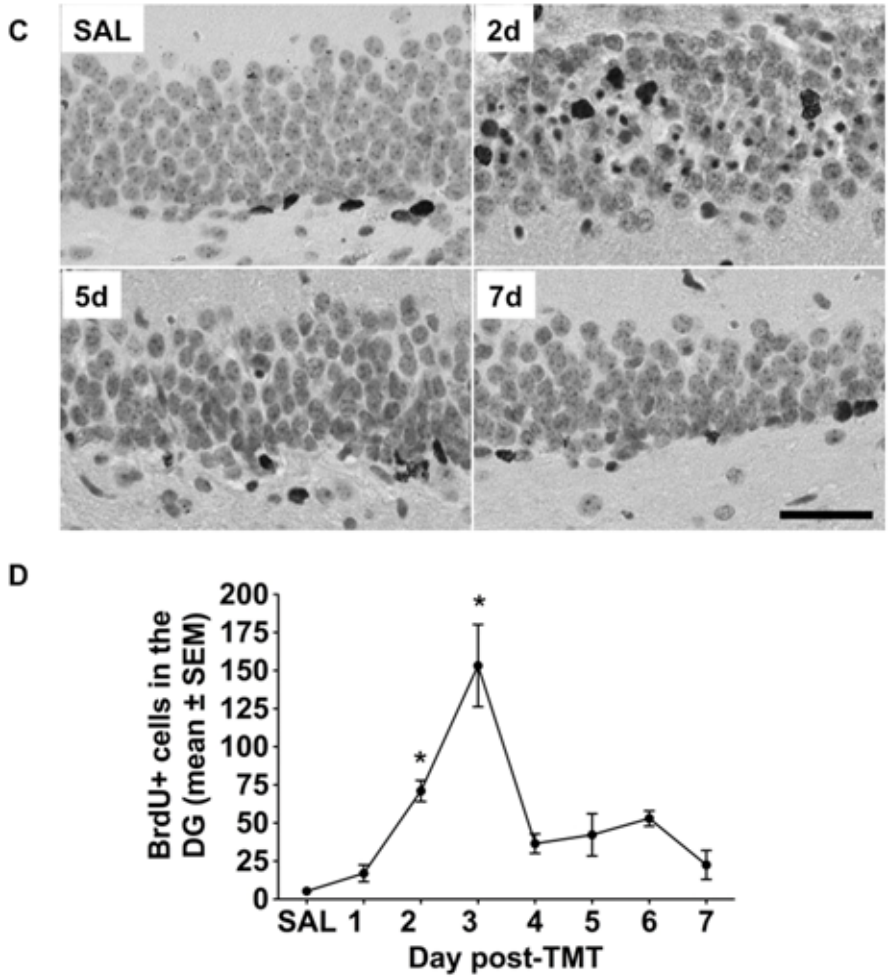

(C) Representative images of BrdU immunohistochemistry (dark black product), mice received BrdU every 12 h for 24 h prior to sacrifice. $BrdU^+$ cells were observed in the SGZ of SAL treated mice, following TMT and increased number of $BrdU^+$ cells are observed in the SGZ and granule cell layer (GCL) at 2 d and 3 d only. Scale bar = 50 μm. (B) Quantitation of $BrdU^+$ cells in the DG as described in Methods. Data represents mean (±SEM) and was analyzed by one-way ANOVA followed by a Dunnett's multiple comparison test (*p<0.05).

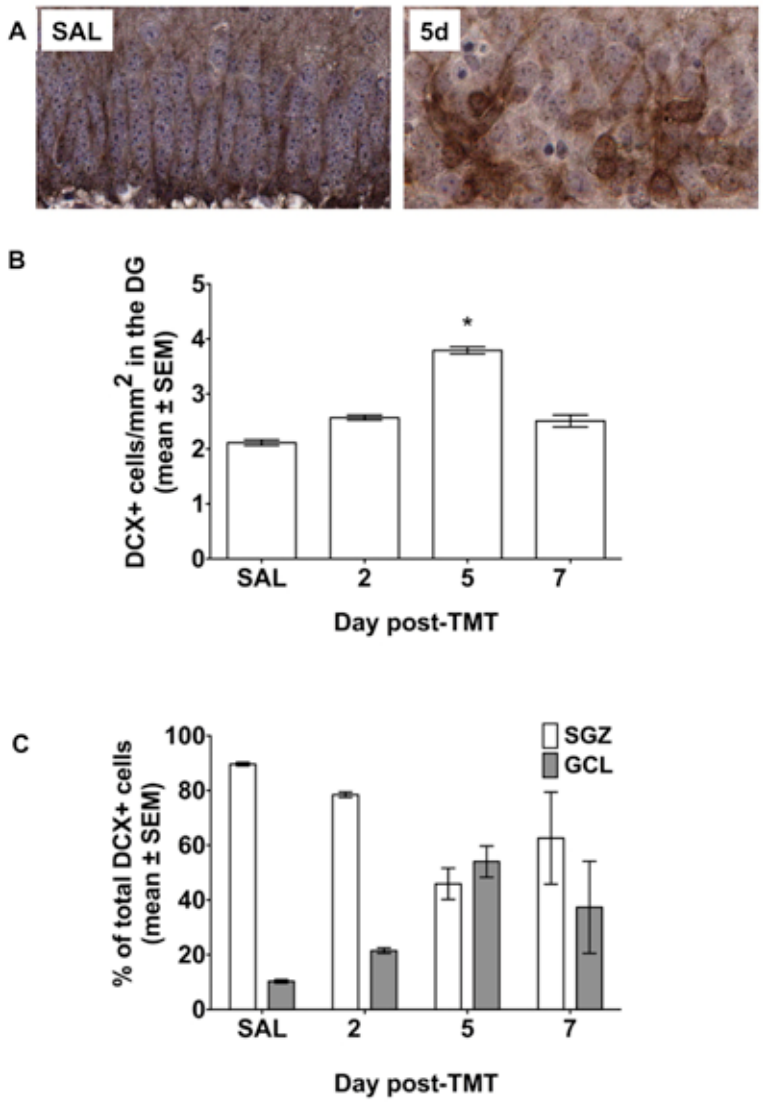

Figure 3.3. Doublecortin immunohistochemistry in the injured dentate gyrus. (A) Representative images of doublecortin (DCX) immunohistochemistry in SAL and 5 d post-TMT (2.3 mg/kg i.p.), scale bar = 50 μm. (B) Quantitation of DCX immunoreactive cells in the dentate gyrus (DG) as described in Methods. Data represents mean DCX^+ cells per mm^2 DG ±SEM and was analyzed by one-way ANOVA followed by a Dunnett's multiple comparison test (*p<0.05). (C) Localization of DCX^+ cells within the subgranular zone (SGZ) and granule cell layer (GCL) of the DG, data represent the mean % DCX^+ cells ±SEM.

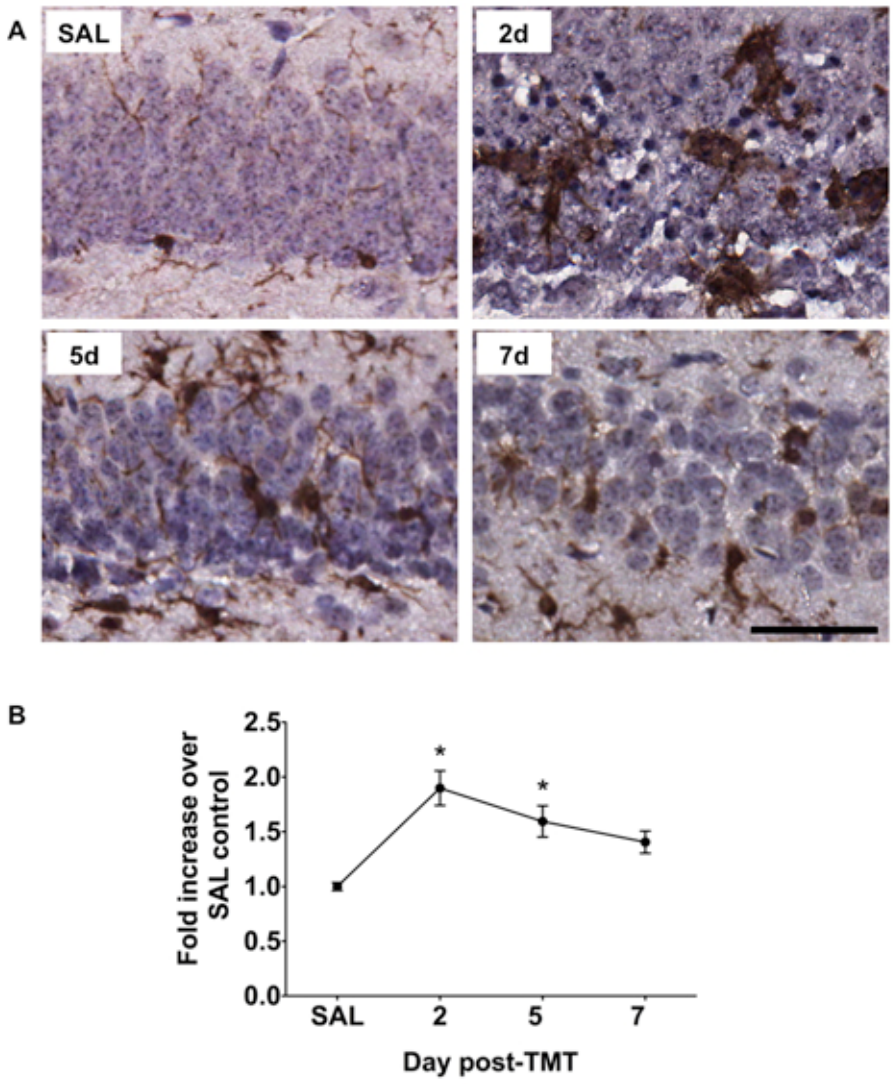

Figure 3.4. Microglia response in the injured dentate gyrus.
(A) Representative images of Iba-1$^+$ microglia in SAL control, 2,5, and 7 d post-TMT. Iba-1$^+$ cells in SAL mice showed thin elongated processes with the subgranular zone (SGZ) and granule cell layer (GCL). At 2 d post-TMT iba-1$^+$ microglia with rounded amoeboid morphology as well as hypertrophied process bearing cells were present within the SGZ and GCL. At 5 and 7 d post-TMT the predominant microglia morphologies were thick ramified process bearing cells within the SGZ and GCL. Scale bar = 50 μm. (B) Fold increase of Iba-1$^+$ cells in the DG at 2, 5, and 7 d post-TMT compared to SAL control. Data represent mean fold increase (±SEM) and were analyzed by one-way ANOVA followed by a Dunnett's multiple comparison test (*p<0.05).

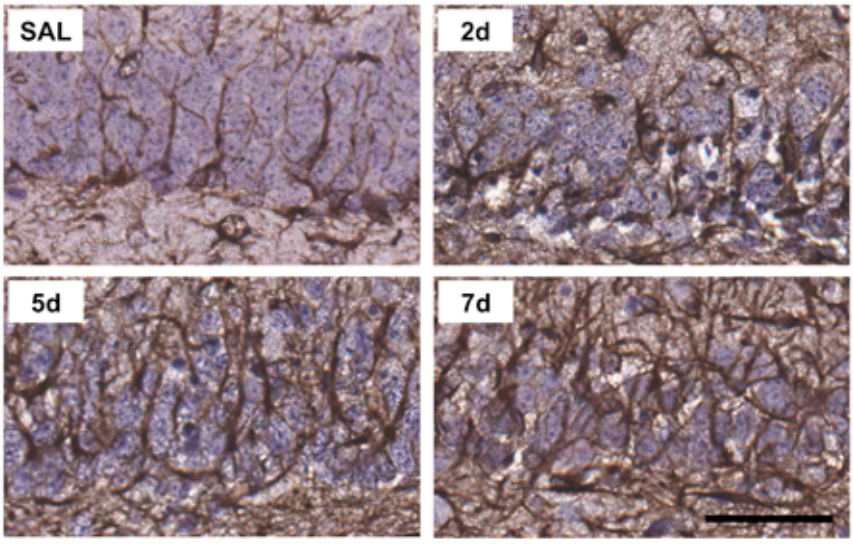

Figure 3.5. Astrocyte morphology in the injured dentate gyrus.
Representative images of $GFAP^+$ astrocytes in dentate gyrus (DG) of SAL control, 2, 5, and 7 d post-TMT. $GFAP^+$ astrocytes displayed long processes that extend through the granule cell layer (GCL) of SAL control mice. At 2 d post-TMT $GFAP^+$ cells demonstrate thickened processes and hypertrophy that persists until 7d post-TMT. Scale bar = 50 μm.

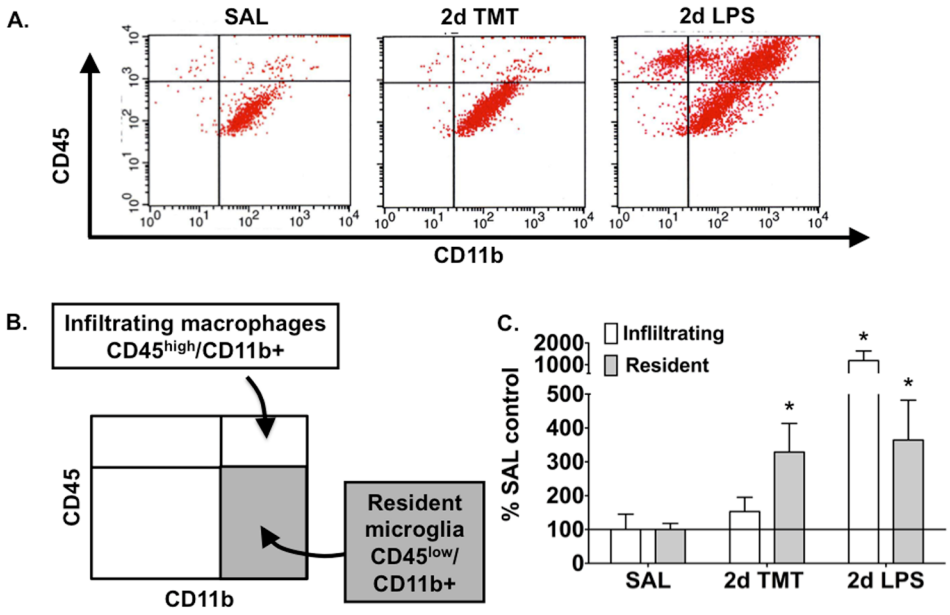

Figure 3.6. Assessment of brain macrophages in the injured dentate gyrus. (A) Flow cytometry for CD45 and CD11b expressing microglia and resident macrophages in SAL control, 2 d TMT, and 2 d LPS injected positive control mice. (B) Resident microglia and peripheral macrophages both express CD11b, resident microglia are $CD45^{low}/CD11b^{+}$ (lower left quadrant), and peripheral macrophages are $CD45^{high}$/CD11b (upper left quadrant). (C) Histogram represents the number of microglia and macrophages in the hippocampus of TMT and LPS treated mice as a % of the SAL control mice. Quadrants were set on the basis of fluorescent levels using isotype-matched control antibodies. Data are representative of pooled hippocampus from 6 mice from each treatment group repeated 3 times and were analyzed by one-way ANOVA followed by a Dunnett's multiple comparison test (*p<0.05).

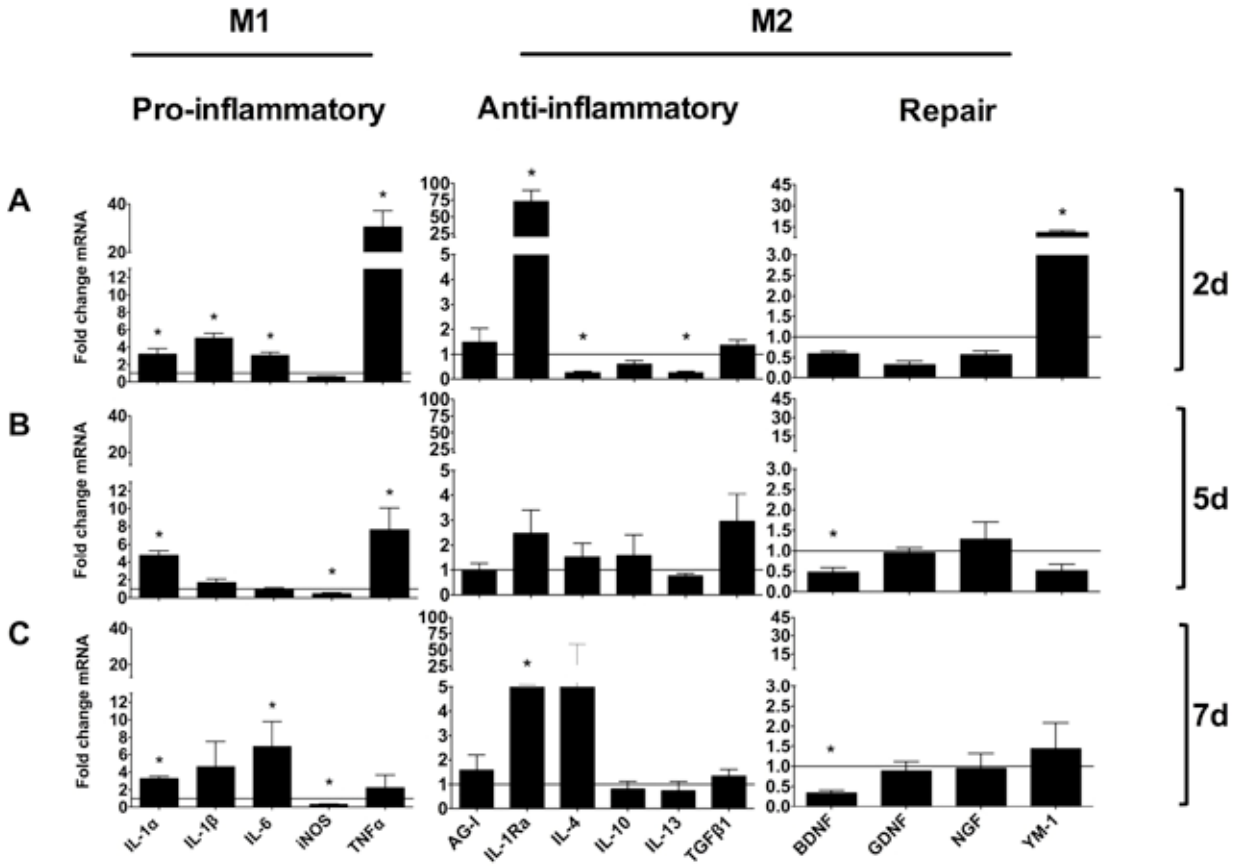

Figure 3.7. qRT-PCR for M1 and M2 related genes in the injured dentate gyrus. qRT-PCR for pro-inflammatory, anti-inflammatory, and repair related genes expressed in the subdissected dentate gyrus at (A) 2d, (B) 5d, and (C) 7d post-TMT. Data are presented as fold change in mRNA expression compared to age-matched SAL control (mean ±SEM). Data were analyzed by two-tailed Student's *t*-test (*p<0.05).

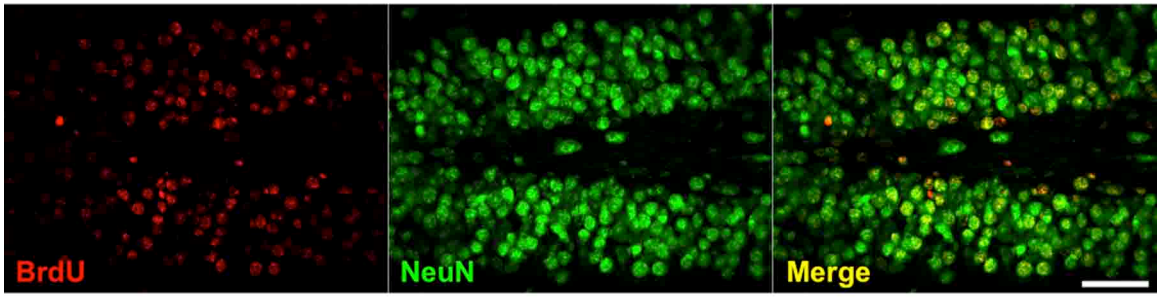

Figure 3.8. Newly-generated cells express NeuN.
Representative image of BrdU (red) and NeuN (green) immunofluorescence in the dentate gyrus (DG) at 14d post-TMT. At 14d post-TMT $BrdU^+$ cells generated during the first 3d of injury migrate into the granule cell layer (GCL) of the DG and merged (yellow) with the mature neuronal marker NeuN. Scale bar = 50 μm.

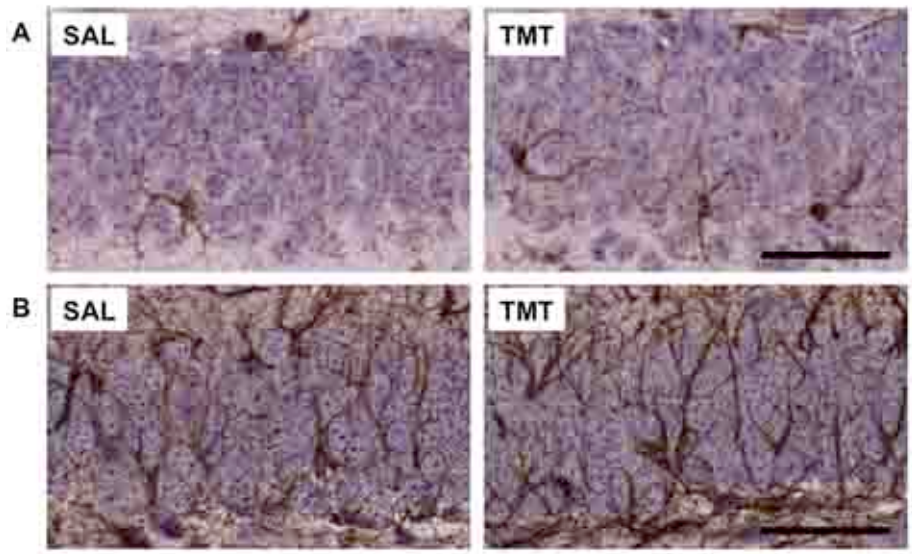

Figure 3.9. Microglia and astrocyte morphology at 14 d post injury.
Figure 8. Representative images of Iba 1^+ microglia (A) and $GFAP^+$ astrocytes (B) at 14 d post-SAL and 14 d post-TMT. (A) Thin ramified process bearing Iba 1^+ microglia were observed in the GCL of both SAL and TMT mice. (B) $GFAP^+$ astrocytes displayed thin processes that extended into GCL in both SAL and TMT mice. Scale bars = 50 μm

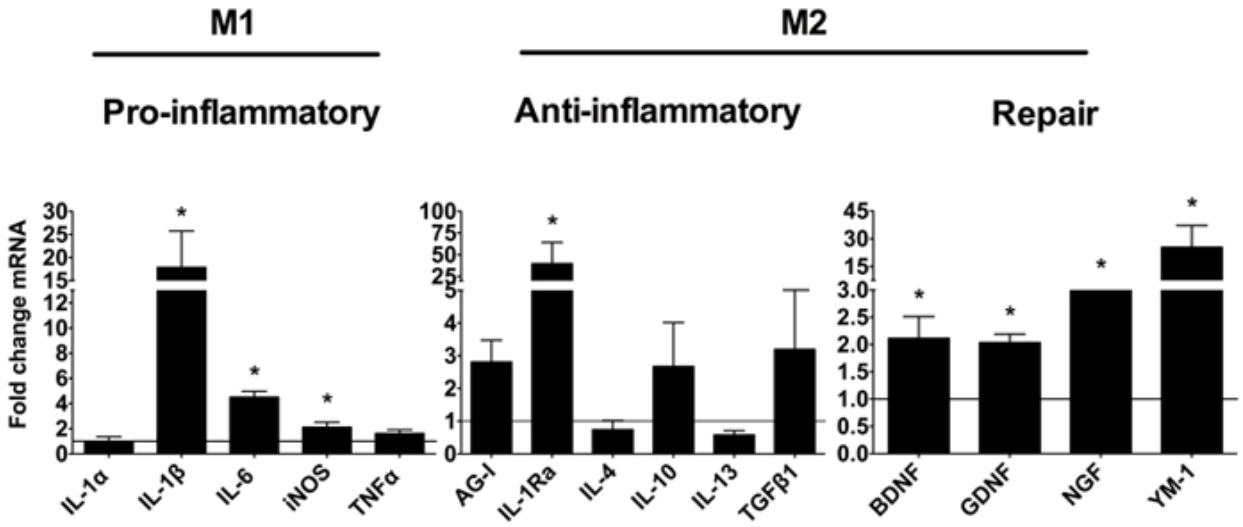

Figure 3.10. qRT-PCR for M1 and M2 related genes in the injured dentate gyrus.

qRT-PCR for pro-inflammatory, anti-inflammatory, and repair related genes expressed in the subdissected DG at 14 d post-TMT and age matched SAL controls (2.3 mg/kg i.p.). Data are presented as fold change compared to age-matched SAL control (mean ±SEM, n = 4-6) analyzed by two-tailed Student's *t-test* (*$p < 0.05$)

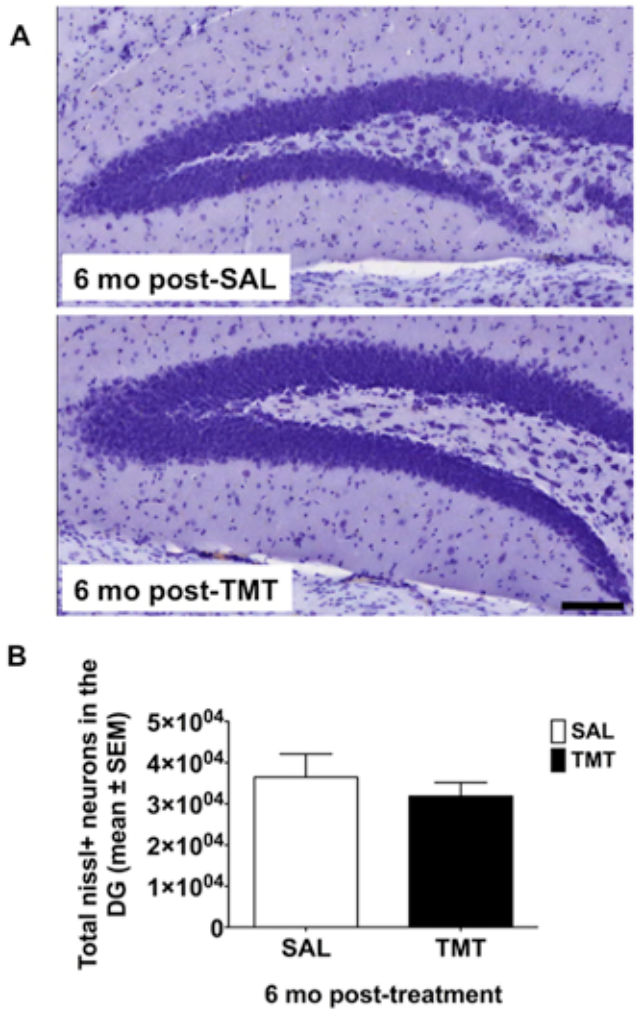

Figure 3.11. Long-term recovery of the dentate gyrus following injury. (A) Representative images of cresyl violet stained coronal sections of the DG at 6 months (mo) post-SAL or TMT (2.3 mg/kg i.p.). (B) Stereological analysis of total neurons in the DG at 6 mo post-SAL and 6 mo post-TMT. Data represent total neurons in the DG (mean ±SEM, n = 6) analyzed by Student's *t-test* (*$p < 0.05$).

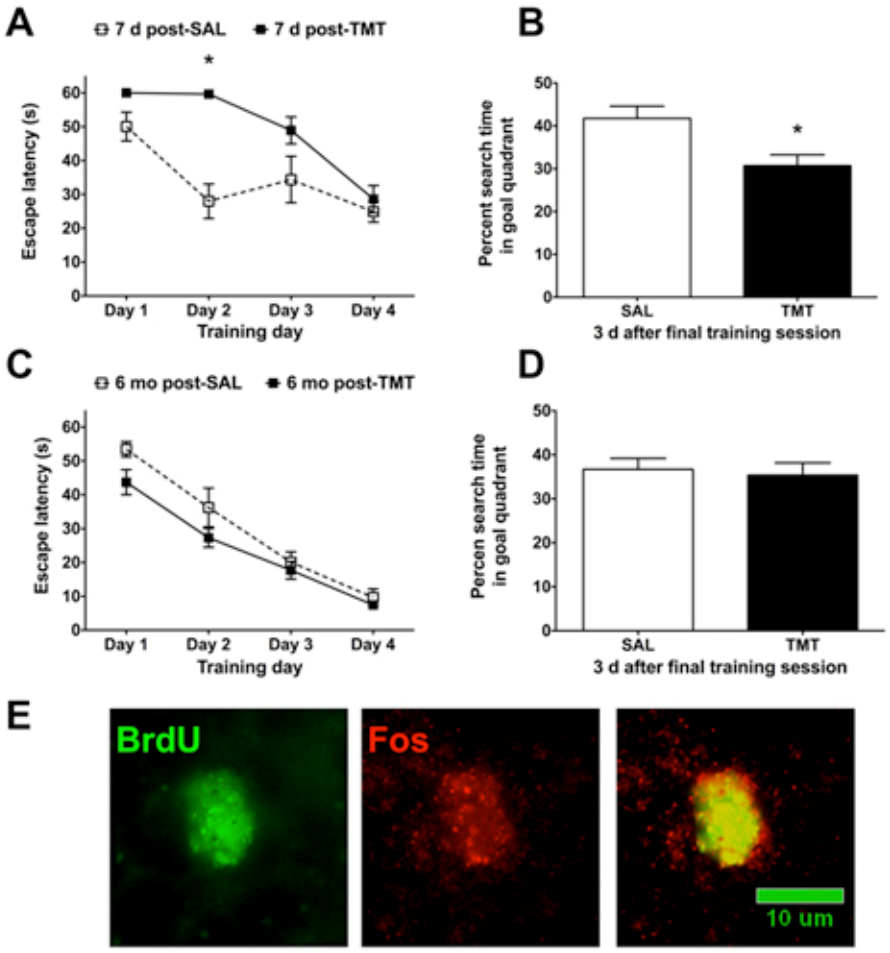

Figure 3.12. Hippocampal function following injury to the dentate gyrus. Comparison of SAL and TMT treated mice in the Morris Water Maze (MWM). (A) At 7 d post-SAL and TMT mice were trained in the MWM (3 trials per day) for 4 d. Mean escape latencies (±SEM) for 7 d post-SAL (open squares) and 7 d post-TMT (closed squares), data were analyzed by one-way ANOVA (*$p < 0.05$, n = 6). (B) Three days after the final training session, mice were given a probe test. In the probe test the percent time spent in the goal quadrant by SAL and TMT mice was calculated (±SEM). Data was analyzed by Student's *t-test* (*$p < 0.05$). (C) At 6 mo post-SAL and TMT mice were trained in the MWM (3 trials per day) for 4 d. Mean escape latencies (±SEM) for 7 d post-SAL (open squares) and 7 d post-TMT (closed squares), data were analyzed by one-way ANOVA (n = 6). (D) Three days after the final training session, mice were given a probe test. In the probe test the percent time spent in the goal quadrant by SAL and TMT mice was calculated (±SEM). Data was analyzed by Student's *t-test* (n = 6). (E) $BrdU^+$ cell in the DG (Green) birthdated during the inflammatory response expresses Fos (Green) following the probe test.

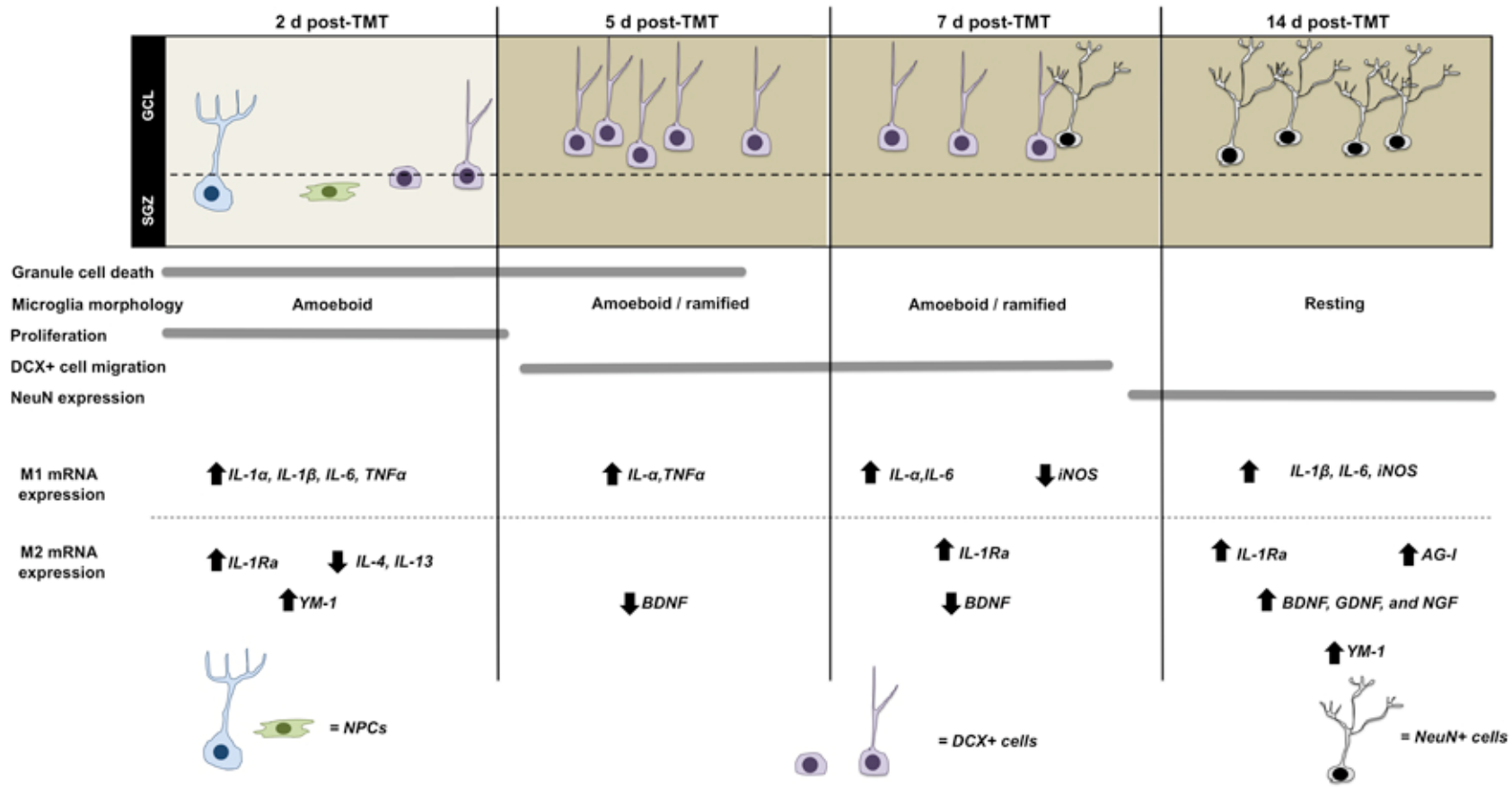

Figure 3.13. Graphical summary of TMT-injury response.

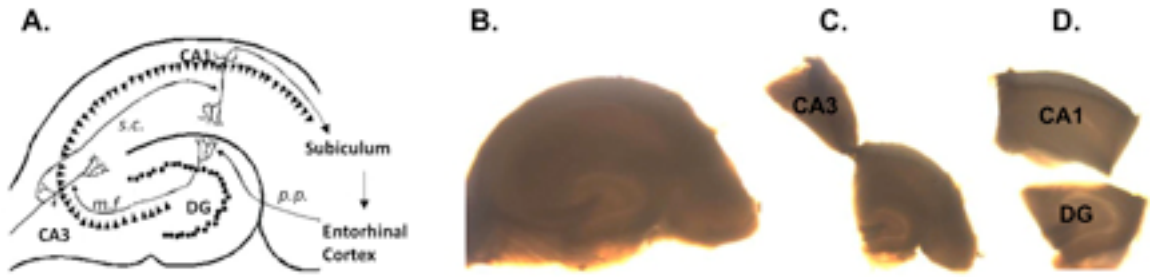

Supplemenatl Figure 3.1. Subdissection of the dentate gyrus.
(A) A schematic representative image of the hippocampal formation was used as a guide to subdissect the DG from other hippocampal regions. (B) One mm sections of the hippocampus were placed under a microscope. (C) One cut was made to separate the CA3 from the CA1 and DG, (D) the DG and CA1 were then separated. RNA was then isolated from the DG.

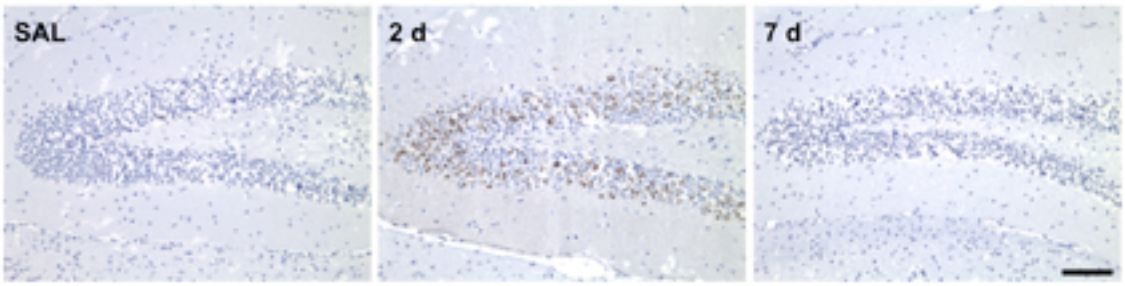

Supplemental Figure 3.2. TUNEL staining in the injured dentate gyrus. Apoptotic cells were identified using terminal deoxynucleotidyl transferasemediated dUTP-biotin in situ end labeling (TUNEL; ApopTag; Intergen, Purchase, NY, USA) and visualized by horseradish peroxidase-conjugated digoxigenin antibodies (diluted 1:1000 in phosphate-buffered saline) and 3,3'-diaminobenzidine (DAB) substrate. Representative images of SAL control and 2, 7 d post-TMT, demonstrate the presence of apoptotic cells (brown) located throughout the granule cell layer (GCL) of the dentate gyrus. Scale bar = 100 μm.

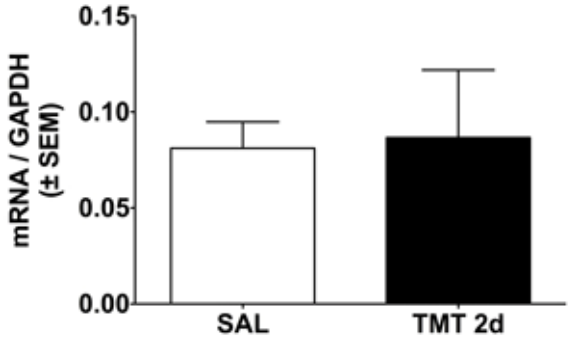

Supplemental Figure 3.1. TNFα mRNA expression in the SGZ.
qRT-PCR mRNA levels of TNFα in the laser-capture microdissected subgranular zone (SGZ) TMT treated mice at 48 h post-TMT (2.3 mg/kg, i.p.). Data represents mean ± SEM mRNA expression relative to GAPDH (n=6) analyzed by a Students *t*-test.

References

Aarum, J., Sandberg, K., Haeberlein, S.L., Persson, M.A., 2003. Migration and differentiation of neural precursor cells can be directed by microglia. Proc Natl Acad Sci U S A 100, 15983-15988.

Ajmone-Cat, M.A., Cacci, E., Ragazzoni, Y., Minghetti, L., Biagioni, S., 2010. Pro-gliogenic effect of IL-1alpha in the differentiation of embryonic neural precursor cells in vitro. J Neurochem 113, 1060-1072.

Babcock, A.A., Kuziel, W.A., Rivest, S., Owens, T., 2003. Chemokine expression by glial cells directs leukocytes to sites of axonal injury in the CNS. J Neurosci 23, 7922-7930.

Batchelor, P.E., Porritt, M.J., Martinello, P., Parish, C.L., Liberatore, G.T., Donnan, G.A., Howells, D.W., 2002. Macrophages and Microglia Produce Local Trophic Gradients That Stimulate Axonal Sprouting Toward but Not beyond the Wound Edge. Mol Cell Neurosci 21, 436-453.

Bauer, S., Kerr, B.J., Patterson, P.H., 2007. The neuropoietic cytokine family in development, plasticity, disease and injury. Nat Rev Neurosci 8, 221-232.

Bengzon, J., Kokaia, Z., Elmer, E., Nanobashvili, A., Kokaia, M., Lindvall, O., 1997. Apoptosis and proliferation of dentate gyrus neurons after single and intermittent limbic seizures. Proc Natl Acad Sci U S A 94, 10432-10437.

Brandt, M.D., Jessberger, S., Steiner, B., Kronenberg, G., Reuter, K., Bick-Sander, A., von der Behrens, W., Kempermann, G., 2003. Transient calretinin expression defines early postmitotic step of neuronal differentiation in adult hippocampal neurogenesis of mice. Mol Cell Neurosci 24, 603-613.

Brown, J.P., Couillard-Despres, S., Cooper-Kuhn, C.M., Winkler, J., Aigner, L., Kuhn, H.G., 2003. Transient expression of doublecortin during adult neurogenesis. J Comp Neurol 467, 1-10.

Bruccoleri, A., Brown, H., Harry, G.J., 1998. Cellular localization and temporal elevation of tumor necrosis factor-alpha, interleukin-1 alpha, and transforming growth factor-beta 1 mRNA in hippocampal injury response induced by trimethyltin. J Neurochem 71, 1577-1587.

Cacci, E., Ajmone-Cat, M.A., Anelli, T., Biagioni, S., Minghetti, L., 2008. In vitro neuronal and glial differentiation from embryonic or adult neural precursor cells are differently affected by chronic or acute activation of microglia. Glia 56, 412-425.

Cacci, E., Claasen, J.H., Kokaia, Z., 2005. Microglia-derived tumor necrosis factor-alpha exaggerates death of newborn hippocampal progenitor cells in vitro. J Neurosci Res 80, 789-797.

Cameron, B., Landreth, G.E., 2010. Inflammation, microglia, and Alzheimer's disease. Neurobiol Dis 37, 503-509.

Cao, Z., Gao, Y., Bryson, J.B., Hou, J., Chaudhry, N., Siddiq, M., Martinez, J., Spencer, T., Carmel, J., Hart, R.B., Filbin, M.T., 2006. The cytokine interleukin-6 is sufficient but not necessary to mimic the peripheral conditioning lesion effect on axonal growth. J Neurosci 26, 5565-5573.

Carson, M.J., Reilly, C.R., Sutcliffe, J.G., Lo, D., 1998. Mature microglia resemble immature antigen-presenting cells. Glia 22, 72-85.

Chang, N.C., Hung, S.I., Hwa, K.Y., Kato, I., Chen, J.E., Liu, C.H., Chang, A.C., 2001. A macrophage protein, Ym1, transiently expressed during inflammation is a novel mammalian lectin. J Biol Chem 276, 17497-17506.

Cho, K.O., Kim, S.Y., 2010. Effects of brain insults and pharmacological manipulations on the adult hippocampal neurogenesis. Arch Pharm Res 33, 1475-1488.

Cho, S., Park, E.M., Zhou, P., Frys, K., Ross, M.E., Iadecola, C., 2005. Obligatory role of inducible nitric oxide synthase in ischemic preconditioning. J Cereb Blood Flow Metab 25, 493-501.

Choi, S.H., Aid, S., Kim, H.W., Jackson, S.H., Bosetti, F., 2011. Inhibition of NADPH oxidase promotes alternative and anti-inflammatory microglial activation during neuroinflammation. J Neurochem.

Choi, Y.S., Cho, H.Y., Hoyt, K.R., Naegele, J.R., Obrietan, K., 2008. IGF-1 receptor-mediated ERK/MAPK signaling couples status epilepticus to progenitor cell proliferation in the subgranular layer of the dentate gyrus. Glia 56, 791-800.

Clarke, R.M., Lyons, A., O'Connell, F., Deighan, B.F., Barry, C.E., Anyakoha, N.G., Nicolaou, A., Lynch, M.A., 2008. A pivotal role for interleukin-4 in atorvastatin-associated neuroprotection in rat brain. J Biol Chem 283, 1808-1817.

Collombet, J.M., Four, E., Bernabe, D., Masqueliez, C., Burckhart, M.F., Baille, V., Baubichon, D., Lallement, G., 2005. Soman poisoning increases neural progenitor proliferation and induces long-term glial activation in mouse brain. Toxicology 208, 319-334.

Colton, C.A., 2009. Heterogeneity of microglial activation in the innate immune response in the brain. J Neuroimmune Pharmacol 4, 399-418.

Colton, C.A., Mott, R.T., Sharpe, H., Xu, Q., Van Nostrand, W.E., Vitek, M.P., 2006. Expression profiles for macrophage alternative activation genes in AD and in mouse models of AD. J Neuroinflammation 3, 27.

Colton, C.A., Wilcock, D.M., 2010. Assessing activation states in microglia. CNS Neurol Disord Drug Targets 9, 174-191.

Das, S., Basu, A., 2008. Inflammation: a new candidate in modulating adult neurogenesis. J Neurosci Res 86, 1199-1208.

Dietrich, W.D., Busto, R., Bethea, J.R., 1999. Postischemic hypothermia and IL-10 treatment provide long-lasting neuroprotection of CA1 hippocampus following transient global ischemia in rats. Exp Neurol 158, 444-450.

Fiedorowicz, A., Figiel, I., Kaminska, B., Zaremba, M., Wilk, S., Oderfeld-Nowak, B., 2001. Dentate granule neuron apoptosis and glia activation in murine hippocampus induced by trimethyltin exposure. Brain Res 912, 116-127.

Frieler, R.A., Meng, H., Duan, S.Z., Berger, S., Schutz, G., He, Y., Xi, G., Wang, M.M., Mortensen, R.M., 2011. Myeloid-specific deletion of the mineralocorticoid receptor reduces infarct volume and alters inflammation during cerebral ischemia. Stroke 42, 179-185.

Frielingsdorf, H., Simpson, D.R., Thal, L.J., Pizzo, D.P., 2007. Nerve growth factor promotes survival of new neurons in the adult hippocampus. Neurobiol Dis 26, 47-55.

Funk, J.A., Gohlke, J., Kraft, A.D., McPherson, C.A., Collins, J.B., Jean Harry, G., 2011. Voluntary exercise protects hippocampal neurons from trimethyltin injury: Possible role of interleukin-6 to modulate tumor necrosis factor receptor-mediated neurotoxicity. Brain Behav Immun.

Geloso, M.C., Vercelli, A., Corvino, V., Repici, M., Boca, M., Haglid, K., Zelano, G., Michetti, F., 2002. Cyclooxygenase-2 and caspase 3 expression in trimethyltin-induced apoptosis in the mouse hippocampus. Exp Neurol 175, 152-160.

Gordon, S., 2003. Alternative activation of macrophages. Nat Rev Immunol 3, 23-35.

Gundersen, H.J.G., 1977. Notes on the estimation of the numerical density of arbitrary profiles: the edge effect. J. Microscopy 111, 219-223.

Guzowski, J.F., Timlin, J.A., Roysam, B., McNaughton, B.L., Worley, P.F., Barnes, C.A., 2005. Mapping behaviorally relevant neural circuits with immediate-early gene expression. Curr Opin Neurobiol 15, 599-606.

Hanisch, U.K., Kettenmann, H., 2007. Microglia: active sensor and versatile effector cells in the normal and pathologic brain. Nat Neurosci 10, 1387-1394.

Harry, G., Bruccoleri, A., Lefebvre d'Hellencourt, C., 2003. Differential modulation of hippocampal chemical-induced injury response by ebselen, pentoxifylline, and TNFalpha-, IL-1alpha-, and IL-6-neutralizing antibodies. J Neurosci Res 73, 526-536.

Harry, G.J., Funk, J.A., Lefebvre d'Hellencourt, C., McPherson, C.A., Aoyama, M., 2008a. The type 1 interleukin 1 receptor is not required for the death of murine hippocampal dentate granule cells and microglia activation. Brain Res 1194, 8-20.

Harry, G.J., Lefebvre d'Hellencourt, C., McPherson, C.A., Funk, J.A., Aoyama, M., Wine, R.N., 2008b. Tumor necrosis factor p55 and p75 receptors are involved in chemical-induced apoptosis of dentate granule neurons. J Neurochem 106, 281-298.

Harry, G.J., McPherson, C.A., Wine, R.N., Atkinson, K., Lefebvre d'Hellencourt, C., 2004. Trimethyltin-induced neurogenesis in the murine hippocampus. Neurotox Res 5, 623-627.

Harry, G.J., Tyler, K., d'Hellencourt, C.L., Tilson, H.A., Maier, W.E., 2002. Morphological alterations and elevations in tumor necrosis factor-alpha, interleukin (IL)-1alpha, and IL-6 in mixed glia cultures following exposure to trimethyltin: modulation by proinflammatory cytokine recombinant proteins and neutralizing antibodies. Toxicol Appl Pharmacol 180, 205-218.

Heppner, F.L., Roth, K., Nitsch, R., Hailer, N.P., 1998. Vitamin E induces ramification and downregulation of adhesion molecules in cultured microglial cells. Glia 22, 180-188.

Hickey, W.F., Kimura, H., 1988. Perivascular microglial cells of the CNS are bone marrow-derived and present antigen in vivo. Science 239, 290-292.

Hirota, H., Kiyama, H., Kishimoto, T., Taga, T., 1996. Accelerated Nerve Regeneration in Mice by upregulated expression of interleukin (IL) 6 and IL-6 receptor after trauma. J Exp Med 183, 2627-2634.

Hung, S.I., Chang, A.C., Kato, I., Chang, N.C., 2002. Transient expression of Ym1, a heparin-binding lectin, during developmental hematopoiesis and inflammation. J Leukoc Biol 72, 72-82.

Iosif, R.E., Ekdahl, C.T., Ahlenius, H., Pronk, C.J., Bonde, S., Kokaia, Z., Jacobsen, S.E., Lindvall, O., 2006. Tumor necrosis factor receptor 1 is a negative regulator of progenitor proliferation in adult hippocampal neurogenesis. J Neurosci 26, 9703-9712.

Kassed, C.A., Willing, A.E., Garbuzova-Davis, S., Sanberg, P.R., Pennypacker, K.R., 2002. Lack of NF-kappaB p50 exacerbates degeneration of hippocampal neurons after chemical exposure and impairs learning. Exp Neurol 176, 277-288.

Kee, N., Teixeira, C.M., Wang, A.H., Frankland, P.W., 2007. Preferential incorporation of adult-generated granule cells into spatial memory networks in the dentate gyrus. Nat Neurosci 10, 355-362.

Keiner, S., Walter, J., Oberland, J., Redecker, C., 2010. Contribution of constitutively proliferating precursor cell subtypes to dentate neurogenesis after cortical infarcts. BMC Neurosci 11, 146.

Koo, J.W., Duman, R.S., 2008. IL-1beta is an essential mediator of the antineurogenic and anhedonic effects of stress. Proc Natl Acad Sci U S A 105, 751-756.

Kreutzberg, G.W., 1996. Microglia: a sensor for pathological events in the CNS. Trends Neurosci 19, 312-318.

Kronenberg, G., Reuter, K., Steiner, B., Brandt, M.D., Jessberger, S., Yamaguchi, M., Kempermann, G., 2003. Subpopulations of proliferating cells of the adult hippocampus respond differently to physiologic neurogenic stimuli. J Comp Neurol 467, 455-463.

Kunz, D., Walker, G., Bedoucha, M., Certa, U., Marz-Weiss, P., Dimitriades-Schmutz, B., Otten, U., 2009. Expression profiling and Ingenuity biological function analyses of interleukin-6- versus nerve growth factor-stimulated PC12 cells. BMC Genomics 10, 90.

Lee, C.H., Park, O.K., Yoo, K.Y., Byun, K., Lee, B., Choi, J.H., Hwang, I.K., Kim, Y.M., Won, M.H., 2011. The role of peroxisome proliferator-activated receptor gamma, and effects of its agonist, rosiglitazone, on transient cerebral ischemic damage. J Neurol Sci 300, 120-129.

Lefebvre d'Hellencourt, C., Harry, G.J., 2005. Molecular profiles of mRNA levels in laser capture microdissected murine hippocampal regions differentially responsive to TMT-induced cell death. J Neurochem 93, 206-220.

Lehrmann, E., Christensen, T., Zimmer, J., Diemer, N.H., Finsen, B., 1997. Microglial and macrophage reactions mark progressive changes and define the penumbra in the rat neocortex and striatum after transient middle cerebral artery occlusion. J Comp Neurol 386, 461-476.

Lei, D.L., Long, J.M., Hengemihle, J., O'Neill, J., Manaye, K.F., Ingram, D.K., Mouton, P.R., 2003. Effects of estrogen and raloxifene on neuroglia number and morphology in the hippocampus of aged female mice. Neuroscience 121, 659-666.

Liu, J., Solway, K., Messing, R.O., Sharp, F.R., 1998. Increased neurogenesis in the dentate gyrus after transient global ischemia in gerbils. J Neurosci 18, 7768-7778.

Long, J.M., Kalehua, A.N., Muth, N.J., Calhoun, M.E., Jucker, M., Hengemihle, J.M., Ingram, D.K., Mouton, P.R., 1998. Stereological analysis of astrocyte and microglia in aging mouse hippocampus. Neurobiol Aging 19, 497-503.

Maier, W.E., Brown, H.W., Tilson, H.A., Luster, M.I., Harry, G.J., 1995. Trimethyltin increases interleukin (IL)-1 alpha, IL-6 and tumor necrosis factor alpha mRNA levels in rat hippocampus. J Neuroimmunol 59, 65-75.

Mandrekar, S., Jiang, Q., Lee, C.Y., Koenigsknecht-Talboo, J., Holtzman, D.M., Landreth, G.E., 2009. Microglia mediate the clearance of soluble Abeta through fluid phase macropinocytosis. J Neurosci 29, 4252-4262.

Mantovani, A., Sica, A., Locati, M., 2005. Macrophage polarization comes of age. Immunity 23, 344-346.

Mathieu, P., Battista, D., Depino, A., Roca, V., Graciarena, M., Pitossi, F., 2010. The more you have, the less you get: the functional role of inflammation on neuronal differentiation of endogenous and transplanted neural stem cells in the adult brain. J Neurochem 112, 1368-1385.

McNaughton, B.L., Barnes, C.A., Meltzer, J., Sutherland, R.J., 1989. Hippocampal granule cells are necessary for normal spatial learning but not for spatially-selective pyramidal cell discharge. Exp Brain Res 76, 485-496.

McPherson, C.A., Aoyama, M., Harry, G.J., 2011a. Interleukin (IL)-1 and IL-6 regulation of neural progenitor cell proliferation with hippocampal injury: Differential regulatory pathways in the subgranular zone (SGZ) of the adolescent and mature mouse brain. Brain Behav Immun 25, 850-862.

McPherson, C.A., Kraft, A.D., Harry, G.J., 2011b. Injury-induced neurogenesis: consideration of resident microglia as supportive of neural progenitor cells. Neurotox Res 19, 341-352.

Michelucci, A., Heurtaux, T., Grandbarbe, L., Morga, E., Heuschling, P., 2009. Characterization of the microglial phenotype under specific pro-inflammatory and anti-inflammatory conditions: Effects of oligomeric and fibrillar amyloid-beta. J Neuroimmunol 210, 3-12.

Ming, G.L., Song, H., 2005. Adult neurogenesis in the mammalian central nervous system. Annu Rev Neurosci 28, 223-250.

Monje, M.L., Toda, H., Palmer, T.D., 2003. Inflammatory blockade restores adult hippocampal neurogenesis. Science 302, 1760-1765.

Morris, S.M., Jr., 2004. Recent advances in arginine metabolism. Curr Opin Clin Nutr Metab Care 7, 45-51.

Mouton, P.R., Long, J.M., Lei, D.L., Howard, V., Jucker, M., Calhoun, M.E., Ingram, D.K., 2002. Age and gender effects on microglia and astrocyte numbers in brains of mice. Brain Res 956, 30-35.

Murphy, P.G., Borthwick, L.A., Altares, M., Gauldie, J., Kaplan, D., Richardson, P.M., 2000. Reciprocal actions of interleukin-6 and brain-derived neurotrophic factor on rat and mouse primary sensory neurons. Eur J Neurosci 12, 1891-1899.

Nakanishi, M., Niidome, T., Matsuda, S., Akaike, A., Kihara, T., Sugimoto, H., 2007. Microglia-derived interleukin-6 and leukaemia inhibitory factor promote astrocytic differentiation of neural stem/progenitor cells. Eur J Neurosci 25, 649-658.

Ogita, K., Nishiyama, N., Sugiyama, C., Higuchi, K., Yoneyama, M., Yoneda, Y., 2005. Regeneration of granule neurons after lesioning of hippocampal dentate gyrus: evaluation using adult mice treated with trimethyltin chloride as a model. J Neurosci Res 82, 609-621.

Peng, H., Whitney, N., Wu, Y., Tian, C., Dou, H., Zhou, Y., Zheng, J., 2008. HIV-1-infected and/or immune-activated macrophage-secreted TNF-alpha affects human fetal cortical neural progenitor cell proliferation and differentiation. Glia 56, 903-916.

Petersen, A.M., Pedersen, B.K., 2006. The role of IL-6 in mediating the anti-inflammatory effects of exercise. J Physiol Pharmacol 57 Suppl 10, 43-51.

Ponomarev, E.D., Maresz, K., Tan, Y., Dittel, B.N., 2007. CNS-derived interleukin-4 is essential for the regulation of autoimmune inflammation and induces a state of alternative activation in microglial cells. J Neurosci 27, 10714-10721.

Raes, G., De Baetselier, P., Noel, W., Beschin, A., Brombacher, F., Hassanzadeh Gh, G., 2002a. Differential expression of FIZZ1 and Ym1 in alternatively versus classically activated macrophages. J Leukoc Biol 71, 597-602.

Raes, G., Noel, W., Beschin, A., Brys, L., de Baetselier, P., Hassanzadeh, G.H., 2002b. FIZZ1 and Ym as tools to discriminate between differentially activated macrophages. Dev Immunol 9, 151-159.

Ransohoff, R.M., Perry, V.H., 2009. Microglial physiology: unique stimuli, specialized responses. Annu Rev Immunol 27, 119-145.

Reuhl, K.R., Cranmer, J.M., 1984. Developmental neuropathology of organotin compounds. Neurotoxicology 5, 187-204.

Rivas-Arancibia, S., Guevara-Guzman, R., Lopez-Vidal, Y., Rodriguez-Martinez, E., Zanardo-Gomes, M., Angoa-Perez, M., Raisman-Vozari, R., 2010. Oxidative stress caused by ozone exposure induces loss of brain repair in the hippocampus of adult rats. Toxicol Sci 113, 187-197.

Schmittgen, T.D., Livak, K.J., 2008. Analyzing real-time PCR data by the comparative C(T) method. Nat Protoc 3, 1101-1108.

Seckinger, P., Lowenthal, J.W., Williamson, K., Dayer, J.M., MacDonald, H.R., 1987. A urine inhibitor of interleukin 1 activity that blocks ligand binding. J Immunol 139, 1546-1549.

Shohami, E., Ginis, I., Hallenbeck, J.M., 1999. Dual role of tumor necrosis factor alpha in brain injury. Cytokine Growth Factor Rev 10, 119-130.

Sierra, A., Encinas, J.M., Deudero, J.J., Chancey, J.H., Enikolopov, G., Overstreet-Wadiche, L.S., Tsirka, S.E., Maletic-Savatic, M., 2010. Microglia shape adult hippocampal neurogenesis through apoptosis-coupled phagocytosis. Cell Stem Cell 7, 483-495.

Sterneck, E., Kaplan, D.R., Johnson, P.F., 1996. Interleukin-6 induces expression of peripherin and cooperates with Trk receptor signaling to promote neuronal differentiation in PC12 cells. J Neurochem 67, 1365-1374.

Stoll, G., Jander, S., Schroeter, M., 1998. Inflammation and glial responses in ischemic brain lesions. Prog Neurobiol 56, 149-171.

Stout, R.D., Suttles, J., 2005. Immunosenescence and macrophage functional plasticity: dysregulation of macrophage function by age-associated microenvironmental changes. Immunol Rev 205, 60-71.

Streit, W.J., 2006. Microglial senescence: does the brain's immune system have an expiration date? Trends Neurosci 29, 506-510.

Teixeira, C.M., Pomedli, S.R., Maei, H.R., Kee, N., Frankland, P.W., 2006. Involvement of the anterior cingulate cortex in the expression of remote spatial memory. J Neurosci 26, 7555-7564.

Tilg, H., Trehu, E., Atkins, M.B., Dinarello, C.A., Mier, J.W., 1994. Interleukin-6 (IL-6) as an anti-inflammatory cytokine: induction of circulating IL-1 receptor antagonist and soluble tumor necrosis factor receptor p55. Blood 83, 113-118.

Vallieres, L., Campbell, I.L., Gage, F.H., Sawchenko, P.E., 2002. Reduced hippocampal neurogenesis in adult transgenic mice with chronic astrocytic production of interleukin-6. J Neurosci 22, 486-492.

van Praag, H., Schinder, A.F., Christie, B.R., Toni, N., Palmer, T.D., Gage, F.H., 2002. Functional neurogenesis in the adult hippocampus. Nature 415, 1030-1034.

Watkins, L.R., Hansen, M.K., Nguyen, K.T., Lee, J.E., Maier, S.F., 1999. Dynamic regulation of the proinflammatory cytokine, interleukin-1beta: molecular biology for non-molecular biologists. Life Sci 65, 449-481.

West, M.J., Slomianka, L., Gundersen, H.J., 1991. Unbiased stereological estimation of the total number of neurons in thesubdivisions of the rat hippocampus using the optical fractionator. Anat Rec 231, 482-497.

Wilcock, D.M., Zhao, Q., Morgan, D., Gordon, M.N., Everhart, A., Wilson, J.G., Lee, J.E., Colton, C.A., 2011. Diverse inflammatory responses in transgenic mouse models of AD and the effect of immunotherapy on these responses. ASN Neuro.

Williams, A.J., Hartings, J.A., Lu, X.C., Rolli, M.L., Tortella, F.C., 2006. Penetrating ballistic-like brain injury in the rat: differential time courses of hemorrhage, cell death, inflammation, and remote degeneration. J Neurotrauma 23, 1828-1846.

Wilms, H., Hartmann, D., Sievers, J., 1997. Ramification of microglia, monocytes and macrophages in vitro: influences of various epithelial and mesenchymal cells and their conditioned media. Cell Tissue Res 287, 447-458.

Yu, J.T., Lee, C.H., Yoo, K.Y., Choi, J.H., Li, H., Park, O.K., Yan, B., Hwang, I.K., Kwon, Y.G., Kim, Y.M., Won, M.H., 2010. Maintenance of anti-inflammatory cytokines and reduction of glial activation in the ischemic hippocampal CA1 region preconditioned with lipopolysaccharide. J Neurol Sci 296, 69-78.

Zattoni, M., Mura, M.L., Deprez, F., Schwendener, R.A., Engelhardt, B., Frei, K., Fritschy, J.M., 2011. Brain infiltration of leukocytes contributes to the pathophysiology of temporal lobe epilepsy. J Neurosci 31, 4037-4050.

Zhang, P.L., Levy, A.M., Ben-Simchon, L., Haggiag, S., Chebath, J., Revel, M., 2007. Induction of neuronal and myelin-related gene expression by IL-6-receptor/IL-6: a study on embryonic dorsal root ganglia cells and isolated Schwann cells. Exp Neurol 208, 285-296.

Chapter 4

Interleukin (IL)-1 and IL-6 regulation of neural progenitor cell proliferation with hippocampal injury: Differential regulatory pathways in the subgranular zone (SGZ) of the adolescent and mature mouse brain.[2]

4.1 Introduction.

Adult hippocampal neurogenesis is initiated with the proliferation of neural progenitor cells (NPCs) within the subgranular zone (SGZ) of the dentate gyrus leading to the formation of new dentate granule neurons. Regulation of this process in the normal control brain and following injury occurs via numerous secreted factors such as hormones (Cameron and Gould, 1994), neurotransmitters (Banasr et al., 2004; Yoshimizu and Chaki, 2004), growth factors (Aberg et al., 2000; Larsson et al., 2002), and cytokines (Das and Basu, 2008; Kaneko et al., 2006; Mathieu et al., 2010; Taupin, 2008). Though not fully understood at this time, regulation of this process through either cellular components such as microglia and astrocytes (Alvarez-Buylla and Lim, 2004) or secreted factors is known to be critical for hippocampal neurogenesis following brain injury, and is thought to contribute to the capacity for "self-repair" of the dentate granule neurons (Ming and Song, 2005).

Associated with the regulation of NPCs in the hippocampus following injury is often the concurrent activation of microglia. Microglia serve as the resident immune

[2] McPherson, C.A., Aoyama, M., and Harry, G.J. 2011. *Brain Behav. Immun.* 25:850-62>

cells of the brain and upon injury they shift to a reactive phenotype (Davalos et al.2005; Nimmerjahn et al., 2005). Upon activation these cells produce pro-inflammatory cytokines including interleukin-1β (IL-1β), interleukin-1α (IL-1α), and interleukin-6 (IL-6) (Mrak and Griffin, 2005). Overall, the literature indicates IL-1β, IL-1α, and IL-6 adversely affects neurogenesis by altering proliferation, survival, differentiation, and functional aspects of NPCs (Ajmone-Cat et al., 2010; Das and Basu, 2008; Mathieu et al., 2010). Recent studies examining the specificity of these effects on NPC proliferation support the critical modulatory effects of neuroinflammation (Monje et al., 2003) and targeted effects of IL-1 and IL-6 signaling (Monje et al., 2003; Spulber et al., 2008). Upon activation of microglia by lipopolysaccharride (LPS) to release pro-inflammatory cytokines, a direct inhibition of NPC proliferation has been observed (Cacci et al., 2005; Monje et al., 2003). In addition, this inhibition is associated with an enhanced differentiation of NPC to the glial lineage. A similar decline in NPC proliferation has been demonstrated in the hippocampus *in vivo* in transgenic mice over-expressing IL-6 in astrocytes (Vallieres et al., 2002). Further examination of the modulation effects of IL-1β showed that the inhibition of NPC proliferation is the result of downstream signaling events occurring following the activation of IL-1 receptor 1 (IL-1R1) (Koo and Duman, 2008). These effects of IL-1R1 activation have not necessarily been translated *in vivo* in that transgenic mice over-expressing IL-1 receptor antagonist (IL-1Ra) demonstrated diminished NPC proliferation following an excitotoxic injury (Spulber et al., 2008). The work of Spulber et al (2008) was the first to suggest that the effect of IL-1R1 signaling on NPCs was conditional on the age of the animal. Under non-injury

conditions, the basal level of hippocampal NPC proliferation was significantly diminished in 5 month-old IL-1Ra transgenic mice and by 22 months-of-age, this difference was no longer evident.

Studies have demonstrated diminished hippocampal NPC proliferation as a function of aging from the adolescent/young adult to the adult rodent (Hattiangady et al., 2008; He and Crews, 2007; Kuhn et al., 1996) and brain insult (Hattiangady et al., 2008; Shetty et al., 2010). These studies clearly demonstrate an ontogeny in the level of hippocampal NPC proliferation that has only been marginally examined within the framework of a coordinated development of the proliferative SGZ, the dentate granule cell layer, and microglia. The proliferative zone of the hippocampus is established between the 2nd and 4th week following birth when precursor cells of dentate granule neurons populate the SGZ of the rodent (Schlessinger et al., 1975). The dentate granule cell layer (GCL) is also established during this same age period. Concurrent with these developmental processes, microglia are proliferating rapidly and establishing a unique nervous system identity primarily between postnatal days 5 to 20 (Lawson et al., 1990). The impact of these coordinated development events on the response of hippocampal NPC to injury and the associated elevation of pro-inflammatory cytokines due to maturing microglia has not been adequately examined.

To address these questions, we compared changes in the SGZ in the adolescent (21 day-old) and the adult (1 yr-old) CD-1 male mouse following a localized damage to the dentate granule neurons. We utilized the hippocampal toxicant, trimethyltin (TMT) to produce hippocampal damage, elevate pro-

inflammatory cytokines, and induce the proliferation of NPC within the SGZ (Harry and Lefebvre d'Hellencourt, 2003; Harry et al., 2004; McPherson et al., 2010). Using this injury model, an elevation of IL-1α signaling via IL-1R1 and downstream genes within the IκB/NFkB1 signaling pathway were observed in the SGZ of 21 day-old mice. An alternative pathway was activated in 1 yr-old mice, with an upregulation of IL-6/gp130 signaling via the Ras/MAPK pathway. When we compared the effects of IL-1α and IL-6 on the *in vitro* proliferation of NPCs obtained from the hippocampus of adolescent and adult mice, an induction of NPC proliferation was observed with IL-1α and a specific inhibition of NPC proliferation was seen in the 1 yr-old mice. Thus, our data demonstrates an age-related shift in IL-1α and IL-6 signaling within the SGZ supporting a differential effect of pro-inflammatory cytokines on hippocampal NPC self-renewal following injury.

4.2 Materials and Methods

4.2.1 Animals

Male adolescent (21 day-old) and adult (1 yr-old) CD-1 mice were obtained from Charles River Laboratories (Raleigh, NC). Mice were individually housed in a dual corridor, semi-barrier animal facility with food (autoclaved NIH 31 rodent chow) and deionized, reverse osmotic-treated water available *ad libitum*. Sentinel animals recorded negative for pathogenic bacteria, mycoplasma, viruses, ectoparasites, and endoparasites. All procedures were conducted in compliance with NIEHS/NIH Animal Care and Use Committee approved animal protocol.

4.2.2 Model of dentate granule cell death

Mice received a single intraperitoneal (i.p.) injection of either 2.3 mg/kg trimethyltin hydroxide (TMT; Alfa Products, Danvers, MA) or vehicle (saline), in a dosing volume of 2 ml/kg body weight using a 50 μl Hamilton syringe. Tremor was evident at 24 h post-TMT with no acute morbidity. All endpoints were examined at 48 h post-dosing time point.

4.2.3 Tissue fixation and sectioning

Mice were anesthetized with CO_2 and decapitated. Brains were excised, bisected in the midsagittal plane, and one hemisphere immersion-fixed in 4% paraformaldehyde(PFA)/0.1M phosphate buffer (PB; pH 7.2) overnight at room temperature (RT). Within 24 h, the brains were rinsed with PB and dehydrated in ethanol, embedded in paraffin, and sections were cut at 8 μm.

For unbiased stereology and immunostaining, mice from each treatment and age group were deeply anesthetized by Nembutal (52 mg/kg, i.p.) at 48 h post-injection of saline or TMT and perfused transcardially with 4˚C 0.1 M phosphate buffer (PB) followed by 10 ml of 4˚C 4% PFA/PB (ph 7.4). Brains post-fixed with 4% PFA/PB for 18 h, cryoprotected in 30% sucrose/PB, and frozen. Serial cryostat sections (≈70) were cut at an instrument setting of 50 μm through the entire hippocampus. Based upon sampling requirements for unbiased stereology, one section was selected from each block of 8 sections and stained for Nissl to visualize neuronal architecture.

4.2.4 Histological assessment of neuronal death

From each mouse, six H&E stained sections at systematic-random location

were selected and the severity of dentate granule cell death scored by three independent observers according to an *a priori* defined severity scale (0-4), as previously described (Harry et al., 2008). Apoptotic cell death was detected with immunostaining for fractin, the product of beta actin cleavage by active caspase 3 (Oo et al., 2002). Sections were incubated (72 h at 4°C) in 0.3% Triton X-100, 2% normal goat serum, and rabbit polyclonal antibody to fractin (1:500; Invitrogen), rinsed, then incubated in 0.1M PB containing 0.3% Triton X-100, 2% normal goat serum and AlexaFluor® goat anti-rabbit 594 (1:500; Invitrogen) for 30 min at RT. Sections were coverslipped with ProLong Gold® with DAPI (Invitrogen). Digitized images of were acquired using a Leica LSM 5 laser-scanning microscope.

4.2.5 Immunohistochemistry for microglia and astrocyte response

Cryostat sections were incubated (72 h at 4°C) in 0.3% Triton X-100, 2% normal goat serum, and either rabbit polyclonal antibody to rabbit polyclonal anti-ionized calcium-binding adaptor molecule-1 (Iba-1 1:500; Wako Chemicals, Japan) or GFAP (1:500; Dako Corp., Carpenteria, CA). Sections were washed, incubated in AlexaFluor® goat anti-rabbit 594 (1:500; Invitrogen) as described above. Sections were coverslipped with ProLong Gold® with DAPI (Invitrogen) as a nuclear counterstain. Digitized images were acquired using a Leica LSM 5 laser-scanning microscope.

4.2.6 Immunofluorescent staining and unbiased stereology of $BrdU^+$ cells within the GCL/SGZ

Mice, at both ages, were injected with 5-bromo-2'-deoxyuridine (BrdU [50 mg/kg i.p]; Sigma-Aldrich, St. Louis, MO) at the time of TMT or saline dosing, and

four injections thereafter every 12 h for 48 h allowing for incorporation at discrete intervals during the peak interval of NPC proliferation. Based upon sampling requirements for unbiased stereology, from the ~70 sagittal cryostat sections representing the entire hippocampus, a set of 8 sequential sections was sampled in a systemic-random manner, i.e., every eighth section with a random start on sections 1-8. Sections were incubated at 37°C in 1N HCL for 30 min, washed in PBS (30 min), and incubated in 0.1M PB with 0.3% Triton X-100, 2% normal goat serum and rat monoclonal antibody to BrdU (1:500; Accurate Biochemicals; Westbury, NY). Sections were washed, incubated in AlexaFluor® goat rat-488 (1:500; Invitrogen) as previously described, and coverslipped with ProLong Gold® with DAPI. Digitized images of immunofluorescence were acquired using a Leica DMBRE laser-scanning microscope.

To determine the number of newly generated $BrdU^+$ cells, a fractionator, sampling scheme for rare events was used (Kempermann et al., 2002). The sum of objects counted was multiplied by the reciprocal of the fraction of reference space sampled. The sampling fractions were defined as follows: (a) section sampling fraction (ssf), the number of sections sampled divided by the total number of sections for each hippocampus; (b) area sampling fraction (asf), the area of the sampling frame divided by the area of the x-y sampling step; and (c) thickness sampling factor (tsf), the height of the dissector divided by the section thickness. $BrdU^+$ cells co-stained with DAPI were identified throughout the latero-medial extension of the GCL and SGZ under 100x using a Leica DMRBE fluorescent microscope. In this procedure, the uppermost and lowermost 5 μm focal planes of

the section were eliminated to avoid artifacts created by the knife blade. The number of $BrdU^+$ cells was estimated as $N = \Sigma Q^-(1/ssf)(1asf)(1tsf)$, where N = number of total estimated $BrdU^+$ cells and ΣQ^- = the number of counted $BrdU^+$ cells. All analysis was conducted with the observer blinded to the treatment conditions.

4.2.7 Confirmation of immature NPC phenotype in $BrdU^+$ cells by nestin immunofluorescent staining

A set of three sections was selected out of ~70 sagittal cryostat sections at random from animals in each age and treatment group. Sections were immunostained for BrdU as described with the addition of rabbit polyclonal anti-nestin (1:500; Abcam, Cambridge, MA) as a marker for immature NPCs. Immunoreactive product was detected with AlexaFluor® goat rat- 488 and AlexaFluor® goat rabbit-594 (1:500; Invitrogen) secondary antibodies. Sections were coverslipped with Prolong Gold® with DAPI. Digital images were acquired throughout the latero-medial extension of the GCL and SGZ under 60x magnification using a Leica LSM 5 laser-scanning microscope. A series of 1 mm sections throughout the entire z-plane was analyzed. To ensure that all $nestin^+$ cells were captured regardless of location within the hippocampal dentate, either the GGL or the SGZ, cells were counted across both regions and data was expressed as the total number of $BrdU^+$ cells co-expressing nestin.

4.2.8 qRT-PCR of hippocampal glial activation and pro-inflammatory cytokines

Total RNA was isolated from the hippocampus (n=6) using the RNeasy® Mini Kit (Qiagen, Valencia, CA) and 2.5 μg used for reverse transcription (SuperScript™II Reverse Transcriptase; Invitrogen). Quantitative real-time PCR (qRT-PCR) was

carried out on a Perkin Elmer ABI Prism™ 7700 Sequence Detector using 3 μl cDNA as a template, combined with a reaction mixture to give final concentrations of 1X Power SYBR® Green Master Mix (Applied Biosystems; Foster City, CA) and optimized forward and reverse primers (Table 1). The 50 μl reaction mixtures were held at 50°C for 2 min, 95°C for 10 min, followed by 40 cycles at 95°C for 15 s, and 1 min at 60°C. Amplification curves from individual qRT-PCR reactions were generated (Sequence Detection System (SDS) 1.9.1 software (Applied Biosystems)). Relative mRNA amounts were calculated using a normalized standard curve and expressed as ratios of target gene to GAPDH.

4.2.9 Laser capture microdissection (LCM) of the SGZ

Cryostat sagittal brain sections (12 μm) were collected on uncoated glass slides and fixed for 1 min in 70% ethanol. Sections were rinsed in RNase-free water for 30 s, stained with Histogene® Staining Solution (Arcturus, Mountain View, CA) for 15 s, rinsed in RNase-free water for 30 s, dehydrated in 95% ethanol for 30 s, 100% ethanol for 30 s and xylene for 5 min, and air-dried for 5 min in a laminar flow hood. A two-cell width at the inner-blade edge of the GCL, representative of the SGZ, was excised using a PixCell Laser Capture Microscope with an infrared diode laser (Arcturus) within 2 h of cryosectioning. A total of 100 sections from each brain hemisphere provided 60000 μm^2 x 100 total area from the SGZ using 7500 laser pulses, 15 μm beam diameter, 75 mW power, 2.5 ms pulse. Total RNA from LCM samples was isolated on an individual animal basis (n = 6) using the PicoPure® RNA Isolation Kit (Arcturus) within 12 h of cyrosectioning. RNA on the column was subjected to RNase-Free DNase Set (Qiagen) then eluted with Elution Buffer. qRT-

PCR was conducted as described for hippocampal tissues.

4.2.10 Generation of Primary Neurospheres

Two mm thick coronal sections containing the hippocampus were collected from three 21 day-old or 1 yr-old mice, as previously described (Bull and Bartlett, 2005). The hippocampus was dissected from the coronal slice excluding the corpus callosum, lateral ventricle, and cortex. Minced tissue was dissociated using the NeuroCult® Enzymatic Dissociation Kit for Adult Mouse and Rat CNS Tissue (Stemcell Technologies, Vancouver, BC). Single cell suspensions were sequentially filtered through 70 μm and 40 μm strainers into proliferation medium (PM) consisting of mouse NeuroCult® NSC Basal Medium (mouse) plus NeuroCult® NSC Proliferation Supplement (Stemcell Technologies) with the addition of 20 ng/ml recombinant human epidermal growth factor (rhEGF), 10 ng/ml recombinant human fibroblast growth factor basic (rhFGFb), and 2 μg/ml heparin (StemCell Technologies). Single cell suspensions were plated at a density of 3500 cells/cm^2 in T-75 tissue culture flasks (BD Falcon) in PM, and incubated at 37°C in 5% CO_2/5% O_2, forming neurospheres by 7 days *in vitro* (DIV).

4.2.10.1 Neural colony forming-cell assay (NCFCA)

The NeuroCult® Neural Colony-Forming Cell Assay Kit (NCFCA; StemCell Technologies) was used to discriminate between stem and progenitor cells on the basis of their proliferative capability and size of colony formed. At 7 DIV, neurospheres generated from the hippocampus of each age and each dosing group were dissociated into single cell suspensions (NeuroCult® Chemical Dissociation Kit; StemCell Technologies) for use in NCFCA as previously described (Louis et al.,

2008). Briefly 2.5 x 10^3 cells were plated in 35 mm tissue culture dishes in a semi-solid collagen matrix containing NeuroCult® NCFC media, supplemented with 20 ng/ml rhEGF, 10 ng/ml rhFGFb and 2 μg/ml heparin. Cultures were incubated at 37°C in 5% CO_2/5% O_2 and fed with 60 μl of PM every 7 days, until 21 days. At 21 days post-plating, the total number of colonies was counted from each experimental group, and categorized by size, as imaged by an inverted Nikon TE-2000 microscope using a 2 mm x 2 mm gridded scoring dish (StemCell Technologies).

4.2.10.2 qRT-PCR for IL-1R1, IL-1RAcP, IL-6Rα, gp130 in neurospheres

To measure mRNA expression, total RNA was isolated from neurospheres at 7 DIV (RNeasy® Mini Kit; Qiagen). qRT-PCR for each transcript (Table 1) was conducted as described for hippocampal samples. Amplification curves were generated and relative mRNA amounts were calculated using a normalized standard curve and expressed as ratio of target gene to GAPDH.

4.2.11 NCFCA in the presence of IL-1α or IL-6

The NCFCA was used to determine the effects of IL-1α or IL-6 on the formation of neural cell colonies**.** Based upon previous work (Harry et al., 2002; Monje et al., 2003) a dose range of recombinant IL1α and IL-6 was selected. At initial plating of single cell suspensions, media (NeuroCult® NCFC Serum Free Media without Cytokines; 20 ng/ml rhEGF, 10 ng/ml rhFGFb and 2 μg/ml heparin) was supplemented with either recombinant mouse IL-6 (rmIL-6, [5, 10, or 15 ng/ml]) or recombinant mouse IL-1α (rmIL-1α [75, 150, or 150 pg/ml]) (R&D Systems; Chicago, IL). In NPCs obtained from adolescent hippocampus, a linear dose response pattern was evident with a stimulation of proliferation observed with IL-1a

and an inhibition with IL-6 (Suppl. Fig. 1). From this dose response, dose levels of IL-1a (150 pg/ml) and IL-6 (10ng/ml) were selected for a direct comparison of proliferation across age of NPCs. An additional comparison was conducted with a combined dosing of rm IL-6 [10 ng/ml and rm IL-1α [150 ng/ml]. Cells were incubated at 37°C in 5% CO_2/5% O_2. Cultures were fed with 60 μl of PM every 7 days until 21 days. At 21 days post-plating, the total number of colonies was counted from each experimental group, and categorized by size.

4.2.12 Statistical analysis

Data for cell number determination and each mRNA transcript displaying a homogenous distribution of variance were analyzed by ANOVA. Group differences between 21 day-old and 1 year-old mice with and without TMT were assessed using a 2 × 2 multi-factorial ANOVA with age and treatment as major factors. Subsequent independent group mean comparisons were conducted using the Bonferroni test. Student t-tests were conducted to determine the effect of combined cytokine exposure and mRNA levels within NPCs obtained from control mice at each age. All statistical significance levels for independent group mean analyses were set at $p < 0.05$.

4.2.13 Microarray analysis

To examine changes induced in genes related to the IL-1 and IL-6 pathways, total RNA (10-20 ng) from LCM samples of the SGZ (n=3) was amplified (Affymetrix One-Cycle cDNA Synthesis Protocol). Fifteen µg of amplified biotin-cRNAs were fragmented and hybridized to Affymetrix Mouse Genome 430 2.0 GeneChip® array for 16 h at 45ºC in a rotating hybridization oven using the Affymetrix Eukaryotic

Target. Slides were stained with steptavidin/phycoerythrin using a double-antibody staining procedure and washed utilizing the EukGE-WS2v5 protocol of the Affymetrix Fluidics Station FS450 for antibody amplification. Arrays were scanned with an Affymetrix Scanner 3000 and data obtained using the GeneChip® Operating Software (GCOS; Version 1.2.0.037). Data were processed with an Affymetrix-specific error model for estimating measurement variance, using Rosetta Resolver, as described (Weng et al., 2006). Biological replicates were combined through error-weighted averaging and comparison ratios were built between samples. Statistical significance was set at $p < 0.001$ and a minimum fold change of 1.2 was set as criteria.

Genes that were differentially regulated in 21 day-old versus 1 yr-old TMT exposed mice, taking into account differences in baseline expression in naïve mice, were analyzed using PathwayArchitect (Stratagene) software. This software uses the KEGG, DIP, and BIND databases and natural language scans of Medline to identify functional associations among differentially expressed genes. Gene interactions and associations (binding, expression, metabolism, promoter binding, protein modification and regulation) were represented graphically as a network. In this analysis, age was considered a mediator of injury related differential expression patterns using ANOVA.

4.3 Results

4.3.1 TMT induced an equivalent level of localized dentate granule neuron apoptosis at 21 days and 1 yr of age

We examined severity of neuronal apoptosis in the GCL and determined a uniform level and timing of hippocampal neuronal death induced by TMT across both ages. No evidence of cell death was observed by H&E staining in saline treated control (severity scores = 0-1; Fig. 1A,B). At 48 h post-TMT, dentate granule neurons displayed nuclear pyknosis and karyolysis (severity scores = 3-4; Fig. 1C,D). No indication of apoptosis was detected in saline control mice by immunostaining for fractin (Fig. 1E,F); fractin^{+} neurons were prominent following TMT (Fig. 1G,H).

4.3.2 TMT injury-induced proliferation is greater in the adolescent versus mature hippocampus

In the 21 day-old and 1 yr-old control mice, BrdU^{+} cells were sparse and restricted to the GCL inner blade/SGZ (Fig. 2A,B**).** An increase in BrdU^{+} cells was observed at 48 h post-TMT in the SGZ, as well as within the GCL in both 21 day-old (Fig. 2C) and the 1 yr-old mice (Fig. 2D). These visual observations were confirmed by unbiased stereology (Fig. 2E). Two-way ANOVA revealed a significant effect of treatment ($F_{(1,8)}$=49.58; p=0.0001), age ($F_{(1,8)}$=43.43; p=0.0002), and treatment x age interaction on BrdU^{+} cell number in the GCL/SGZ ($F_{(1,8)}$=27.20; p=0.0008). The number of BrdU^{+} cells within the GCL/SGZ was significantly higher in the 21 day-old control mice than in 1 yr-old control mice (p<0.05). In both age groups, TMT exposure resulted in a significant increase in the number of BrdU^{+} cells within the

GCL/SGZ (p<0.05). In 21 day-old mice, the increase in $BrdU^+$ cells was approximately 7-fold higher than the basal level observed in controls. In 1 yr-old mice, the increase in $BrdU^+$ cells was significantly less, at an estimated 3.5-fold elevation (p<0.05).

We then confirmed the proliferation of NPC by examining immunostaining for nestin and co-localization with BrdU (Fig. 2F-H). To capture any changes in the distribution of NPCs as a function age or injury, the distribution of $BrdU^+$ cells across the entire GCL was examined. The percent total #$BrdU^+$ cells throughout the GCL that co-expressed nestin was determined within controls and TMT-dosed mice for each age group (Fig. 2I). A two-way ANOVA indicated a significant main effect of age ($F_{(1,8)}$=36.41; p=0.0003) with the 21 day-old mice showing a higher percentage of co-localized immunostaining as compared to 1 yr-old, across both conditions. A significant main effect of TMT treatment ($F_{(1,8)}$=49.04; p=0.0001) was observed with an increase in co-localization at 48 h following TMT injection. No significant interaction of age and TMT was detected with the adolescent mice showing an approximate 30% increase over the higher basal level and the mature mice demonstrating an approximate 50% increase over the lower basal level.

4.3.3 Microglia demonstrate different morphological responses to injury as a function of age

In the normal 21 day-old mouse hippocampus, microglia displayed thin, ramified processes within the SGZ, hilus, and the densely packed dentate GCL (Fig 3A). Similar to the Iba-1 staining pattern in the 21 day-old, microglia within the 1 yr-old hippocampus were prominent within the hilus and molecular layer. In addition,

Iba-1^{+} microglia displayed an increased staining in processes within the SGZ, hilus, and GCL (Fig. 3B), suggestive of a lower threshold for activation (Sparkman and Johnson, 2008).

In the 21 day-old mice, neuronal injury and loss following TMT induced an activation of microglia displaying an amoeboid morphology within proximity to dying neurons showing dense collapsed nuclei (Fig. 3C). In addition, process-bearing responsive microglia were evident throughout the GCL and in the hilus, occasionally extending into the SGZ. In 1 yr-old mice, a comparable level of neuronal death did not result in the localization of amoeboid microglia with dying neurons. Rather, prominent reactive microglia within the GCL displayed thick ramified processes. Similar to the 21 day-old mice, process-bearing reactive microglia were observed throughout the GCL and hilus occasionally extending into the SGZ (Fig. 3D). The morphological response of microglia was supported by qRT-PCR of Iba-1 (Fig. 3E). Two-way ANOVA of Iba-1 mRNA levels revealed a significant effect of treatment ($F_{(1,20)}$=8.438; p<0.0088) and higher levels seen in the 21 day-old TMT dosed mice. (p<0.05). No significant main effects of age or interaction between age and treatment were observed.

4.3.4 GFAP^{+} astrocytes demonstrate similar morphological responses to injury across ages

In control mice, minimal differences in GFAP staining were observed as a function of age. At both ages, astrocytes displayed fibrous processes projecting thorough the SGZ and GCL (Fig. 3F,G). Within 48 h post-TMT a retraction and moderate thickening of GFAP processes, was evident throughout the GCL (Fig.

3H,I). The increase in GFAP immunoreactivity with TMT was supported by qRT-PCR for GFAP mRNA levels (Fig. 3J). Two-way ANOVA revealed a significant effect of treatment ($F_{(1,20)}$=14.82; p=0.001) with a significant increase observed following TMT in both ages, as compared to controls (p<0.05). No significant main effects of age or age x treatment interaction were observed.

4.3.5 IL-1α and IL-6 mRNA levels are differentially elevated in the hippocampus following TMT as a function of age

Given the differential activation of microglia in 21 day-old, as compared to 1 yr-old mice, additional characterization of the microglial response was conducted based on proposed pro-inflammatory (MI) or anti-inflammatory (M2) phenotypes (Colton and Wilcock, 2010; Michelucci et al., 2009). Gene expression associated with the M1 phenotype was examined (IL-1β, IL-6) as well as the pro-inflammatory cytokine IL-1α. Expression of anti-inflammatory M2 phenotype associated genes: arginase I (AG-I), chitinase 3-like-3 (YM-1), IL-10, and transforming growth factor beta (TGFβ1) were also examined. Consistent with our previous work (Bruccoleri et al., 1998), we did not observe an elevation in mRNA levels for TGFβ1 in the hippocampus at this early time point (Fig. 4A). IL-10 and AG-I mRNA levels were not significantly altered in the hippocampus (Fig. 4A) following TMT. No signal for YM-1 mRNA was detected (data not shown). IL-1β mRNA expression was not significantly elevated by TMT in either age group (Fig. 4A). Two-way ANOVA for IL-1α mRNA expression showed significant main effects of treatment ($F_{(1,20)}$=45.41; p=<0.0001), age ($F_{(1,20)}$=19.91; p<0.0001), and treatment x age interaction ($F_{(1,20)}$=24.67; p=<0.0001). A significant TMT-induced elevation was observed in 21

day-old mice (p<0.001). IL-6 mRNA levels in the hippocampus were significantly elevated following TMT ($F_{(1,20)}$=7.755; p=<0.05) in 1 yr-old mice (p<0.001).

4.3.6 TMT-induced injury selectively elevated IL-6 mRNA in SGZ of mature mice

To further examine whether the differential inflammatory cytokine response observed in the hippocampus was observed within the SGZ, mRNA levels were determined from LCM samples. A slight elevation in mRNA levels for TGFβ1 within the SGZ following TMT was noted at both ages but failed to reach statistical significance (Fig. 4B). IL-10 and AG-I mRNA levels in the SGZ were not significantly altered by TMT (Fig. 4B). No signal for YM-1 mRNA was detected (data not shown). mRNA levels for IL-1β showed no significant differences as a function of age or TMT injection (Fig. 4B). IL-1α mRNA levels (Fig. 4B) were significantly elevated with TMT ($F_{(1,20)}$=42.50; p<0.0001) in both age groups (p<0.01). No significant effect was observed as a function of age. IL-6 mRNA levels (Fig. 4B) were significantly elevated by TMT ($F_{(1,20)}$=8.595; p<0.005) and with age ($F_{(1,20)}$=5.304; p<0.05). A significant treatment x age interaction ($F_{(1,20)}$=5.036; p<0.05) was detected with TMT-induced elevations in IL-6 mRNA levels occurring in 1 yr-old mice (p<0.05).

4.3.7 *In vivo* TMT exposure induced neural colony cell formation *in vitro*

Neurogenic cells within the SGZ are primarily progenitor cells that maintain the capability to differentiate into neurons or glia (Bull and Bartlett, 2005; Seaberg and van der Kooy, 2002); however, with localized neuronal activation, a latent stem cell population has also been identified (Walker et al., 2008). Using the NCFCA to discriminate between colonies of neural stem and progenitor cells, we examined

alterations in the size of colonies formed from hippocampal cells as a function of age and *in vivo* neuronal activation/injury by TMT. We found no difference in culturing success of NPC from young and mature brains, consistent with similar published work (Blackmore et al., 2009). Colonies >2.0 mm were not observed in either age or treatment group, suggesting origination from progenitor cells, rather than stem cells. The mean total number of colonies generated *in vitro* was greater in 21 day-old as compared to the 1 yr-old saline control mice (Fig. 5A; $p<0.005$). TMT treatment induced colony formation from both 21 day-old and 1 yr-old mice. The number of colonies generated from the hippocampus of mice injected with TMT was greater at 21 days of age compared to the 1 yr-old; however, the fold increase over saline control was similar in both ages (1.8 fold for 21 day-old and 1.9 fold for the 1 yr-old).

4.3.8 NPCs from the adolescent and mature hippocampus express IL-1R1, IL-1RAcP, IL-6Rα, and gp130

To confirm that NPC displayed the capability to respond to the *in vivo* elevations in IL-1α and IL-6 within the SGZ, IL-1R1, IL-1RAcP, IL-6Rα, and gp130 mRNA levels were determined in isolated NPCs generated from each age group. A basal level of each transcript was detected (Fig. 5D). No differences as a function of age were seen for IL-1R1, IL-1RAcP, or gp130. Hippocampal NPCs derived from 1 year-old mice expressed higher levels of IL-6Rα, compared to NPCs from 21 day-old mice ($t = 4.871$, $p < 0.05$).

4.3.9. IL-1α stimulated colony formation of adolescent NPCs and IL-6 inhibited colony formation of adolescent and mature NPCs

Given the expression of IL-1 and IL-6 receptors on NPCs, we examined the proliferative response to exogenous recombinant IL-1α, IL-6, or a combination of IL-1α and IL-6 proteins in the NCFCA. Following a 21 DIV exposure to rmIL-1α, two-way ANOVA revealed a significant effect of treatment ($F_{(1,8)}$=14.64; *p*=0.005), age ($F_{(1,8)}$=127.3; *p*=<0.0001), and treatment x age interaction on total colony formation ($F_{(1,8)}$=7.029; *p*=0.02). Treatment with rmIL-1α significantly increased formation of colonies obtained from the hippocampus of 21 day-old mice (p<0.05; Fig. 6A). rmIL-1α did not stimulate colony proliferation in cultures obtained from the hippocampus of 1 yr-old mice. Following 21 DIV, exposure to rmIL-6 produced a significant effect of treatment ($F_{(1,8)}$=14.64; *p*=0.005), age ($F_{(1,8)}$=127.3; *p*=<0.0001), and treatment x age interaction on total colony formation ($F_{(1,8)}$=7.029; *p*=0.02). Decreased colony formation with rmIL-6 was observed in hippocampal NPC from both ages (p<0.05; Fig. 6B). In NPCs from 21 day-old mice, concurrent exposure to IL-1α and IL-6 did not result in a significant increase in colony formation thus, inhibiting the stimulatory properties of IL-1α. (Fig. 6C) In NPCs from 1-yr-old mice, concurrent exposure to both cytokines resulted in a significant decrease (t=3.113, *p*<0.05) in colony formation similar to the effects observed with IL-6 alone.

4.3.10 Differential activation of the IL-1 pathway in the adolescent and the IL-6 pathway in the mature SGZ following TMT injury

Based upon our observations that hippocampal NPCs isolated from both age groups 1) expressed IL-1 and IL-6 receptors for downstream signaling activation, 2)

expressed both cytokines *in vivo* within the SGZ, and 3) demonstrated age related proliferative responses in isolated NPC, we examined the molecular profiles associated with both receptor pathways as a function of age and injury. Microarray profiles generated from LCM SGZ tissue identified a total of 109 unique transcripts changed in the 21 day-old samples, 54 unique transcripts in the 1 yr-old samples, with a total of 88 similarly changed at both ages as a function of TMT (Fig. 7A). While a full analysis of the microarray data is outside the scope of this manuscript, a number of genes were identified in support of the speculation that a greater level of "immune" activation occurs in the adolescent SGZ. For example, CD44 antigen transcript was elevated 10.9-fold ($p<0.0001$) in the adolescent with only a 2-fold ($p=0.23$) elevation in the adult. Similar patterns were seen for Mmd (monocytes to macrophage differentiation-associated) transcripts with a 2.8-fold increase in the adolescent ($p<0.00001$) and a 1.4 fold increase in the adult ($p=0.0005$) and for Msr2 (macrophage scavenger receptor 2) with a 3.4-fold increase ($p<0.000001$) in the adolescent and a 1.08-fold non-significant increase in the adult.

We used PathwayArchitect software to examine the differential expression of IL-1α and IL-6 related genes in the SGZ as a function of age and TMT injury. The transcript expression pattern generated from the SGZ suggested a primary involvement with injury of the IL-1 signaling pathway in the 21 day-old mice with IL-6 serving a primary role in the SGZ of 1 yr-old mice (Fig. 7B). Using this approach, statistical significance was set at $p<0.001$ and a minimum fold change of 1.2 was set as criteria. IL-1α and IL-1R1 were induced at a greater level in the adolescent SGZ compared with the mature SGZ. A specific alternative pathway for neurogenesis has

yet to be reported. We now report a network association between IL-1α and signaling genes downstream of IL-1R1 including: myeloid differentiation primary response gene-88 (Myd88), IκB, and NFκB1 in the SGZ with higher levels in the 21 day-old injured SGZ as compared to the 1 yr-old mice.

With TMT injury, IL-6 mRNA levels were significantly elevated in the SGZ of 1 yr-old with a minimal induction in 21 day-old mice. The IL-6/IL-6R complex initiates signaling through the gp130 receptor (Jones et al., 2005) leading to activation of either Janus kinase (JAK) or Ras-mediated signaling (Heinrich et al., 1998; Hirano et al., 2000) regulating cell growth, proliferation, differentiation, and apoptosis. We noted a concurrent upregulation of IL-6 and a number of Ras-mediated signaling genes in the SGZ of adult mice following injury. Ras- Genes elevated in the Ras/MAPK signaling pathway included SHC, the gene encoding a signaling and transforming protein Src homology 2 and 3 that are involved in mitogenic signal transduction and facility the activation of Ras proteins. Growth factor receptor bound protein-2 (Grb-2), an adaptor protein involved in epidermal growth factor receptor tyrosine kinase for the activation of Ras and downstream kinases, ERK1,2. Elevations were noted in v-raf-1, murine leukemia viral oncogene homolog 1 (Raf-1), the gene encoding MAP3K that functions downstream of Ras membrane associated GTPases. Raf-1 phosphorylates MEK1 and MEK2 to activate ERK1 and ERK2, controlling gene expression involved in cell division, differentiation, migration, and apoptosis. Elevations were seen in mitogen-activate protein kinase kinase-1 (MAP2K1) for which the associated protein product, MEK1 protein kinase is essential for normal development before and survival after birth.

4.4 Discussion

In the current study, we examined microglia activation, IL-1α and IL-6 mRNA levels, and NPC proliferation within the SGZ in mice exposed to the hippocampal toxicant, TMT. Based upon the adolescent establishment of the proliferative SGZ (Schlessinger et al., 1975) and active NPC proliferation in the hippocampus, we further compared differences in the response to TMT-induced injury as a function of age. These comparisons incorporated differences in the SGZ of the normal adolescent hippocampus as compared to an adult age showing a decline in NPC proliferation. Our data confirmed previous reports of a greater number of NPCs in the SGZ of adolescent, as compared to adult mice under normal conditions (Ben Abdallah et al., 2010; He and Crews, 2007; Kuhn et al., 1996), as well as with brain injury (Hattiangady et al., 2008; Shetty et al., 2010). The novel findings of these studies include age-related differences in the response of isolated NPCs to IL-1α or IL-6 and the molecular profiles generated from the injured SGZ. First, we report that the age-related level of NPC proliferation *in vivo* following TMT-induced injury correlates with elevations in IL-1α mRNA levels in the adolescent hippocampus and IL-6 within the adult. We show that proliferation of NPCs isolated from the hippocampus of mice at both ages was inhibited by IL-6. Proliferation of NPCs by IL-1α was observed only in cells derived from the hippocampus of adolescent mice and not from NPCs from the mature hippocampus. Third, we examined the molecular profile of the SGZ from each age and treatment and identified distinct signaling pathway activations as a function of age. TMT injury selectively induced an activation of IL-1α signaling via IL-1R1 and downstream genes within the

IkB/NFkB1 signaling pathway in the 21 day-old and IL-6Rα/gp130 signaling via the Ras/MAPK pathway in the 1 yr-old mice. From these data, we conclude that the age related expression of IL-1α and subsequent signaling pathway activation in the adolescent fosters NPC proliferation. In comparison, activation of the IL-6Rα/gp130 pathway in the adult contributes to maintaining a tight regulatory control on NPC proliferation, thus serves as a basis for an age-dependent level of NPC self-renewal following injury.

Both IL-1β and IL-α induce signaling via binding to IL-R1 followed by a sequence of protein-protein interactions forming a complex to recruit IL-1RAcP (Greenfeder et al., 1995). Myeloid differentiation primary response gene-88 (Myd88) is then recruited to the IL-1α/IL-R1 complex activating the interleukin-1 receptor associated kinase (IRAK) (Wesche et al., 1997), for activation either of ERK, p38MAPK, c-jun, or NFκB signaling (Dunne and O'Neill, 2003; O'Neill, 2002; O'Neill and Greene, 1998). Previous studies have demonstrated that IL-1R1 is expressed *in vitro* in NPCs isolated from the rat embryonic forebrain (Wang et al., 2007) and in the adult rat hippocampus *in vivo* (Koo and Duman, 2008). This receptor expression suggests the potential for direct effect of receptor action via IL-1β or IL-1α (Greenfeder et al., 1995). Wang et al., (2007) demonstrated that the treatment of rat embryonic forebrain NPCs with IL-1β and upon IL1-R1 activation of the SAP/JNK pathway inhibited proliferation. Additionally, activation of the NFκB pathway by IL-1β binding to IL-1R1 decreased proliferation but not differentiation of adult hippocampal NPCs both *in vivo* and *in vitro* (Koo and Duman, 2008). Inhibition of proliferation, observed by Wang et al. (2007), was accompanied by a normal pattern of cell

differentiation; but a lower level of GFAP protein expression in differentiated NPCs. A direct effect of IL-1β on the differentiation of NPCs to neurons has been suggested by the work of Kuzumaki et al., (2010) indicating a decrease in β-tubulin^{+} neurons differentiated from mouse whole brain embryonic NPCs.

While the majority of the work on IL-1 signaling in NPCs has focused on IL-1β, IL-1α also activates the IL-1R1 and direct effects on NPCs have been observed. Using mouse embryonic cortical NPCs, IL-1α exposure was reported to direct differentiation to the astrocyte lineage (Ajmone-Cat et al., 2010). The effect of IL-1R1 signaling on NPC proliferation has been supported by the studies of Spulber et al. (2008) utilizing transgenic mice overexpressing IL-1 receptor antagonist (IL-1ra). In these animals, the overexpression of IL-1ra was sufficient to inhibit *in vivo* excitotoxicity-induced hippocampal progenitor cell proliferation. Further observations from this study suggested that the effect of IL-1ra on the *in vivo* basal level of hippocampal progenitor cell proliferation was influenced by the age of the animal. In 5 month-old mice, the IL-1ra transgenic mice demonstrated a decrease in basal proliferation for which no such effects were observed in mice at ~22 months of age. Our current data supports the work of Spulber et al. (2008) suggesting that the effect of IL-1R1 activation on NPCs can be dependent upon the age of the animal. In the isolated SGZ, a significant elevation was observed for IL-1α in both age groups; however, activation of the IkB/NFkB signaling cascade was restricted to the adolescent. Consistent with this *in vivo* observation, IL-1α stimulated *in vitro* proliferation of NPCs isolated from adolescent hippocampus; while, no such effects were observed in cells isolated from the adult. Activated microglia provide the

earliest source of IL-1α and IL-1ra after injury (Eriksson et al., 2000; Eriksson et al., 1999) and in the TMT-induced injury model (Bruccoleri et al., 1998). Thus, the age related changes we observed in the current study with regards to IL-1R1 activation are likely influenced by the maturation of microglia and differences in activation. Just as the functional capability of microglia change in the aged brain (Streit, 2006), microglia during the postnatal period represent a more immature phenotype (Kuzumaki et al., 2010; Rezaie and Male, 1999; Yokoyama et al., 2004). TMT induced a similar severity of neuronal death in both age groups but a pronounced activation of microglia within the GCL was seen only in the adolescent, as evidenced by the morphological phenotype and the elevation in IL-1α. In the adult, a more blunted hypertrophic process-bearing microglia response was observed. No elevation was observed the in microglia M2 associated genes, AG-I, TGFβ1, IL-10, and chitinase-3-like-3 (YM-1) (Colton and Wilcock, 2010; Michelucci et al., 2009) suggesting the absence of an alternatively activated microglia phenotype at both ages following TMT exposure. Thus, as a source of IL-1α in this injury model (Bruccoleri et al., 1998), activated microglia could serve as a major influence not only on the NPC *in vivo* but also on the surrounding astrocytes, resulting in an environment promoting differences observed as a function of age.

The prominent cytokine response observed in the adult GCL and SGZ following TMT-induced injury was the up-regulation of IL-6. We also showed a slight elevation in mRNA levels of IL-6 in the normal adult hippocampus as compared to the adolescent. This finding is consistent with the report of an increase in IL-6 protein expression in the hippocampus of aged, as compared to juvenile mice (Ye and

Johnson, 1999, 2001). While a body of literature exists demonstrating the ability of multiple neural cell types to express IL-6 mRNA or protein, there is limited available data in the literature demonstrating the cellular source of IL-6 within the brain. Recent work suggests the expression of IL-6 protein in cortical lesions from patients with either tuberous sclerosis complex (TSC) or focal cortical dysplasia type IIb (FCDIIb)(Shu et al., 2010). Within the TSC tubers cortical tubers, IL-6 immunoreactivity co-localized to dysmorphic neurons and giant neurons with no evidence of localization to GFAP astrocytes. In FCDIIb, balloon cells expressed both IL-6 and GFAP. Additional work suggests the expression of IL-6 in neurons of the cerebral cortex and hypothalamus with trinitrobenzene sulfonic acid-induced colitis (Wang et al., 2010). Further work has demonstrated that the combination of neuronal depolarization and activation of IL-1R1 with IL-1β can induce neurons to synthesize and release IL-6 (Juttler et al., 2002; Ringheim et al., 1995; Tsakiri et al., 2008a, b). It is possible that the production of IL-1a by microglia, coinciding with the stimulation of neurons by TMT, could lead to the increased neuronal production of IL-6. Microglial production of IL-6 has also been demonstrated in non-pathological conditions *in vivo* (Schobitz et al., 1992) and classically activated M1 microglia are also identified to produce IL-6 (Colton and Wilcock, 2010; Monje et al., 2003). We attempted to identify the cellular source of IL-6 within the current study however, a consistent staining pattern was not observed across various antibody sources. With a monoclonal antibody we were able to identify localization to neurons; yet, with a polyclonal antibody, a similar pattern of neuronal expression was lacking and the overall impression was of localization to microglia. In neither case did we identify

immunoreactivity within $GFAP^+$ astrocytes. However, to identify the cellular source will require additional studies to verify specificity of the antibodies and confirmation of a consistent pattern of immunostaining. Whatever the source, the effects of IL-6 upon NPCs were clearly demonstrated.

IL-6 binds to IL-6Rα then to the gp130 receptor to initiate signal transduction via the Janus tyrosine kinase /signal transducers and activators of transcription 3 (JAK/STAT3) and phosphatidylinositol (PI)-3 kinase/Akt pathways. It is known that these pathways can then be employed as a mechanism for cell survival (Reich, 2007). Recent studies report that, while rat embryonic neural stem cells respond *in vitro* to IL-6 (Nakanishi et al., 2007), NPCs from the embryonic subventricular zone (SVZ) do not express a functional membrane IL-6R (Islam et al., 2009). In this latter case, exposure to hyper IL-6 (the complex of IL-6/IL-6R) was required to stimulate gp130 signaling and cell differentiation (Islam et al., 2009). IL-6 has been shown to promote astrocytic differentiation of embryonic neural stem cells derived from the rat SVZ (Nakanishi et al., 2007) via the Janus tyrosine kinase/signal transducers and activators of transcription 3 (JAK/STAT3) signaling pathway (Bromberg and Darnell, 2000). Monje et al., (2003) reported that, *in vitro*, IL-6 inhibits neuronal differentiation of adult hippocampal NPCs; however, recent work demonstrated that while gliogenesis due to IL-6 receptor activation is related to signaling via the JAK/STAT pathway, neuronal differentiation occurs via activation of the RAS-MAPK signaling pathway (Islam et al., 2009; Taga and Fukuda, 2005). Within the SGZ of the adult brain, we now report elevations in genes associated with both IL-6Rα and gp130, as well as genes associated with downstream signaling through Ras to

activate Raf-1 or MAP2K1. The prevailing hypothesis that acute exposure to IL-6 is detrimental to NPCs (Ekdahl et al., 2003; Ekdahl et al., 2009; Monje et al., 2003; Vallieres et al., 2002), is further supported by our finding that IL-6 inhibited proliferation of hippocampal NPCs, regardless of age. While the inhibition of proliferation may be a direct effect, further studies may determine a correlation with an earlier onset of differentiation. In light of the work of Islam et al. (2009), a possible role for IL-6 in promoting neurogenesis for replacement of dentate granule cells following hippocampal injury with TMT requires consideration.

In the early work identifying the sustained neuro-proliferative capability of the hippocampus, Altman et al., (1973) proposed the idea that changes occurring with maturation from the adolescent to the adult hippocampus represented selective stabilization of the structure. Consistent with this idea, and similar ones proposed by Changeux and Dauchin (1976), is the idea that the higher levels of NPC proliferation observed in the adolescent brain reflect a greater level of hippocampal plasticity. Lower levels observed in the adult appear to reflect a system focused on maintaining cellular homeostasis and survival. We now propose that the contribution of pro-inflammatory cytokines, and possibly neuroinflammation in general, varies as a function of maturational stage and can assume different regulatory roles with regards to the self-renewal of NPCs within the injured hippocampus. One could speculate that the upregulation of IL-1α, as an initiator, and the lack of corresponding upregulation of IL-6, as a down-regulator, serve to enhance the neurogenic proliferative response to injury in the adolescent SGZ. In comparison, in the adult hippocampus, the GCL is a more developed and compacted region and the

induction of IL-6 and absence of IL-1 signaling with injury may represent these maturational differences. The dynamic neurogenic response in the adolescent hippocampus following the death of dentate granule neurons as a result of a systemic injection of TMT provides a model to identify critical factors delineating the adolescent SGZ and the transition to an adult profile.

Table 4.1 Quantitative real-time PCR sequences

Gene	Forward Primer (Concentration)	Reverse Primer (Concentration)
GFAP	ACCGCTTTGCTAGCTACATCGAGA (900 nM)	TTCTCTCCAAATCCACACGCCA (900 nM)
Iba-1	TGTGGAAGTGATGCCTGGGAGTTA (50 nM)	TCAAGTTTGGACGGCAGATCCTCA (300 nM)
IL-1α	TCGGGAGGAGACGACTCTAA (600 nM)	GGCAACTCCTTCAGCAACAC (600 nM)
IL-1β	TGGTGTGTGACGTTCCCATT (300 nM)	CAGCACGAGGCTTTTTTGTTG (300 nM)
IL-6	TCCTACCCCAATTTCCAA (300 nM)	CGTACTAGGGCCCAG (300 nM)
IL-1R1	CGGCGCATGTGCAGTTAA (300 nM)	GCCCCCGATGAGGTAATT (300 nM)
IL-1RAcP	TTGGATACAAGGTGTGCATCTTC (300 nM)	GCTGAGGGTCTCATCTGTGAC (300 nM)
IL-6R	GGTGGCCCAGTACCAATG (300 nM)	GGACCTGGACCACGTGCT (300 nM)
gp130	ATTTGTGTGCTGAAGGAGGC (300 nM)	AAAGGACAGGATGTTGCAGG (300 nM)
GAPDH	GGGAAGCTCACTGGCATGG (300 nM)	CTTCTTGATGTCATCATACTTGGCAG (300 nM)

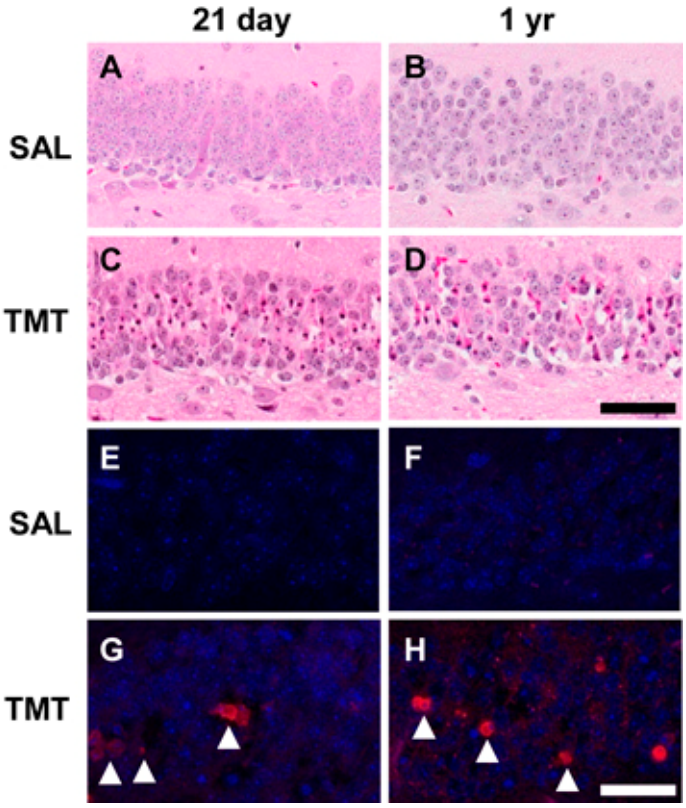

Figure 4.1. Cell death in the DG.
(A-D) Representative hematoxylin and eosin (H&E) staining in the subgranular zone (SGZ) and granule cell layer (GCL) of the dentate gyrus (DG) in CD-1 male mice. Twenty one day-old (A) and 1 yr-old (B) saline control, or 21 day-old (C) and 1 yr-old (B) at 48 h post-TMT (2.3 mg/kg i.p.). (C & D) $Eosin^{+}$ staining (deep pink) of neurons displaying nuclear pyknosis and karyolysis indicated an equivalent level of neuronal death (represented by a severity score of 3-4 as defined in Methods). (E-H) Representative immunofluorescent staining for fractin (red; arrowheads) and DAPI (blue) in the GCL. Scale bar = 50 μm

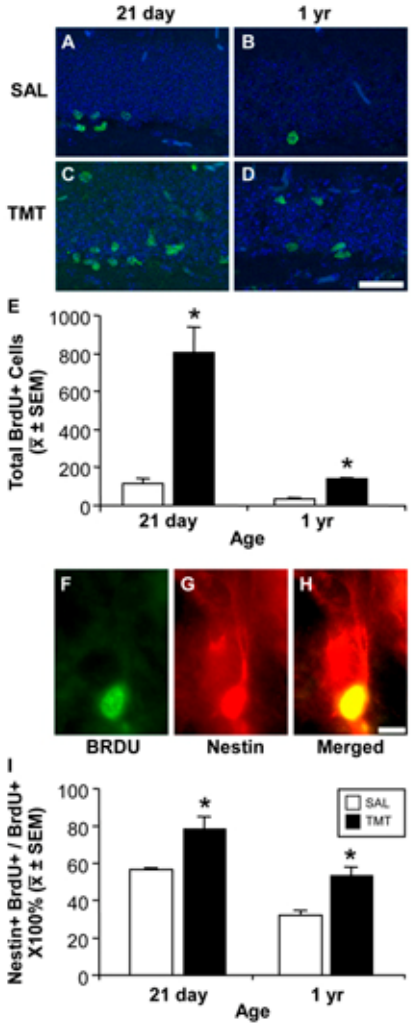

Figure 4.2. NPC proliferation in the DG.
(A-D) Representative immunofluorescent images of 5'-bromo-2'-deoxyuridine (BrdU) (green) and DAPI (blue) in the SGZ and GCL (A, B) along the inner cell layer of saline control mice and (C, D) within the GCL 48 h post- TMT (2.3 mg/kg i.p.). Scale bar = 50 μm. (E) Unbiased stereology of the number of $BrdU^+$ determined by rare events protocol as described in Methods. Data represents mean ± SEM as defined in Methods and analyzed by a 2x2 ANOVA followed Bonferonni post hoc test (*p < 0.05). (F-H) Representative immunostaining of $BrdU^+$ cells co-localized with nestin at 48 h post-TMT. Scale bar = 10 μm (I) Mean $^+$ SEM number of $BrdU^+$ cells that co-stained with nestin within the SGZ and GCL. Data analyzed by a 2x2 ANOVA followed by Bonferonni post hoc test (*p < 0.05).

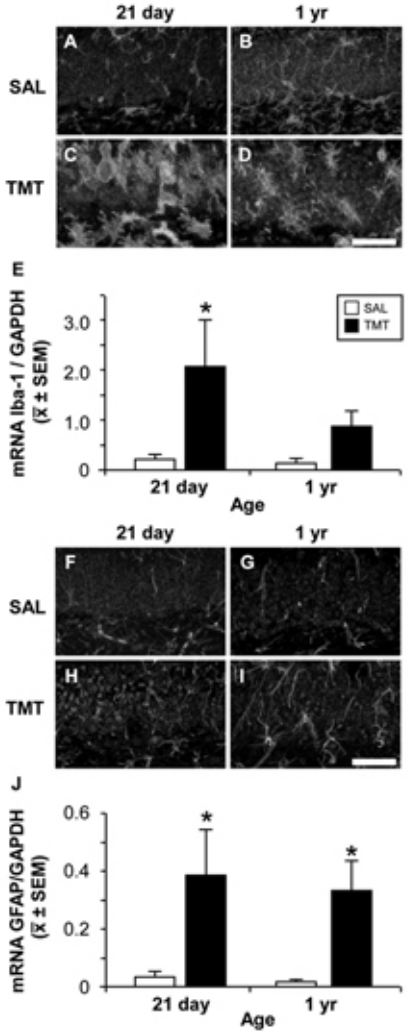

Figure 4.3. Gliosis in the DG.
Representative images of Iba-1$^+$ microglia (A-D, red) and GFAP$^+$ astrocytes (F-I, red), DAPI (A-D, F-I, blue), in the GCL and SGZ (lower portion of each image) in saline control and 48 h post-TMT CD-1 male 21 day-old or 1 yr-old mice. (A) Iba-1$^+$ cells in control 21 day-old mice showed thin elongated processes with distal ramifications. (B) Iba-1$^+$ cells (red) in 1 yr-old mice showed increased staining thickened processes with proximal arborization. With TMT (C) Iba-1$^+$ cells differentiated to a rounded amoeboid morphology in the GCL and cells with enlarged cell bodies and retracted processes in the hilus in the 21 day-old and (D) process bearing cells showing thickened and retracted processes in the 1 yr-old. (F-I) GFAP$^+$ astrocytes (red) showing thin processes through the GCL in (F, G) control and an increased staining at 48 h post-TMT in both (H) 21 day-old and 1 yr-old (I). Scale bar = 50 μm. (E, J) qRT-PCR mRNA levels for Iba-1 and GFAP relative to GAPDH. (E) mRNA levels for Iba-1 were significantly elevated in the 21 day-old at 48 h post-TMT. (J) mRNA levels for GFAP were significantly elevated in the 21 day-old and 1 yr-old mice 48 h post-TMT. Data represents mean ± SEM. Data analyzed by a 2x2 ANOVA followed by Bonferonni post hoc test (*p<0.05).

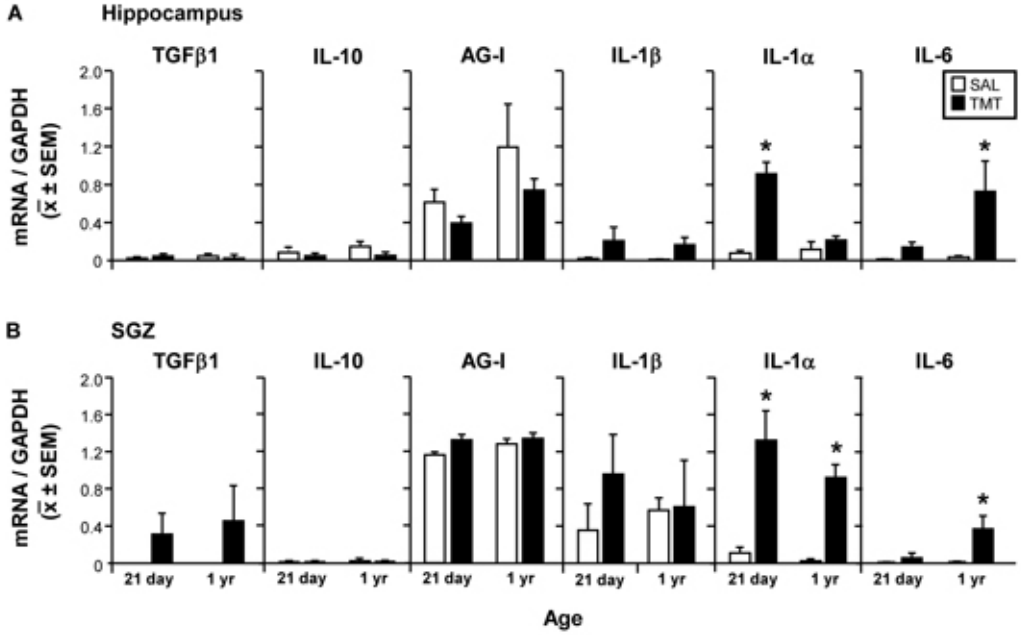

Figure 4.4. qRT-PCR of pro-inflammatory and anti-inflammatory markers. qRT-PCR mRNA levels of TGFβ1, IL-10, AG-I, IL-1β, IL-α, and IL-6 in the (A) hippocampus and (B) laser-capture microdissected subgranular zone (SGZ) of 21 day-old and 1 yr-old saline and TMT treated mice at 48 h post-TMT (2.3 mg/kg, i.p.). Data represents mean ± SEM mRNA expression relative to GAPDH (n=6) analyzed by a 2x2 ANOVA followed by Bonferonni post hoc test (*p<0.05).

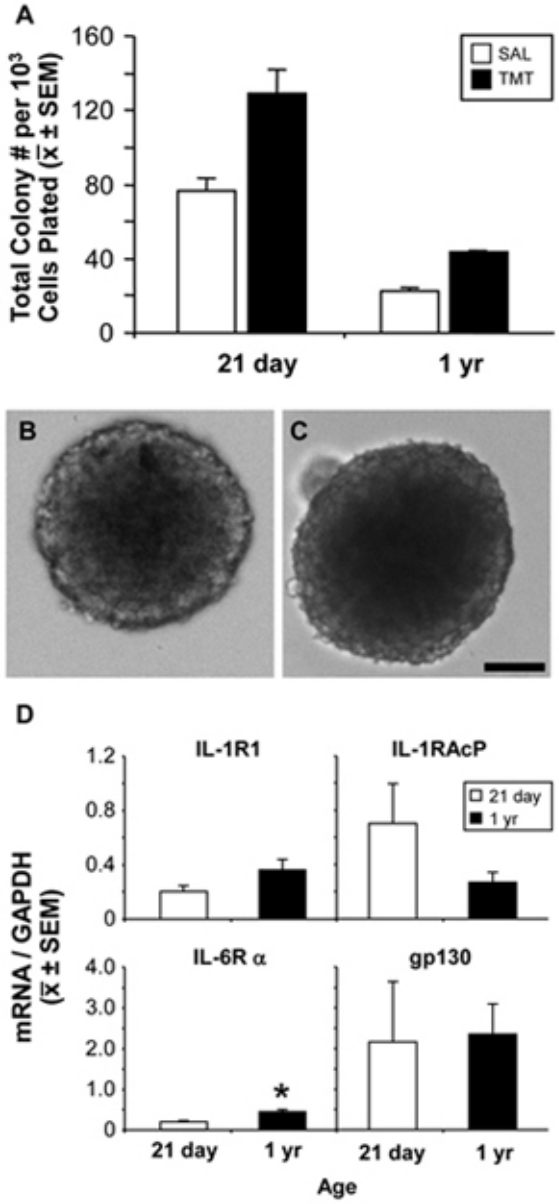

Figure 4.5. Neurosphere proliferation following TMT.
(A) Proliferation of neurospheres as indicated by determining the mean total numbers of colonies formed per 10^3 cells plated from the hippocampus of 21 day-old and 1 yr-old mice 48 h post-TMT (2.3 mg/kg, i.p.) or saline. Data represents mean ± SD (n=2). (B-C) Representative images of neurospheres obtained from the hippocampus of (B) 21 day-old or (C) 1 yr-old mice. Scale bar = 100 µm.
(D) qRT-PCR for mRNA levels of IL-1R1, IL-RAcP, IL-6Rα, and gp130 within neurospheres isolated from the hippocampus of 21 day or 1 yr-old mice. Data represents mean ± SEM transcript level relative to GAPDH (*p<0.05).

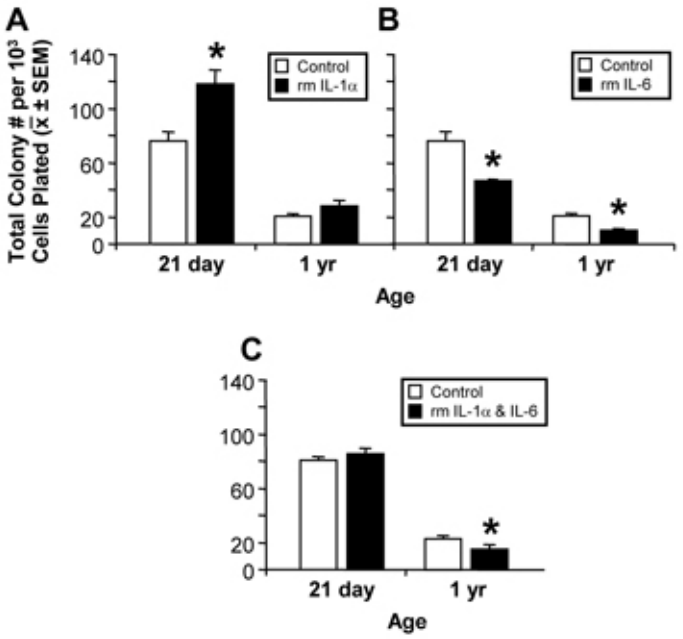

Figure 4.6. Effects of cytokines on proliferation of NPCs

Differential effects of 21 day exposure to recombinant mouse (A) IL-1α [150 pg/ml], (B) IL-6 [10 ng/ml], or (C) IL-1α [150 pg/ml] and IL-6 [10 ng/ml] protein on neural colony formation. Data represents the mean total colony number per 10^3 cells plated $\pm$ SEM. Data (A,B) was analyzed by a 2x2 ANOVA followed by Bonferonni post hoc test or (C) Student t-test (*$p < 0.05$).

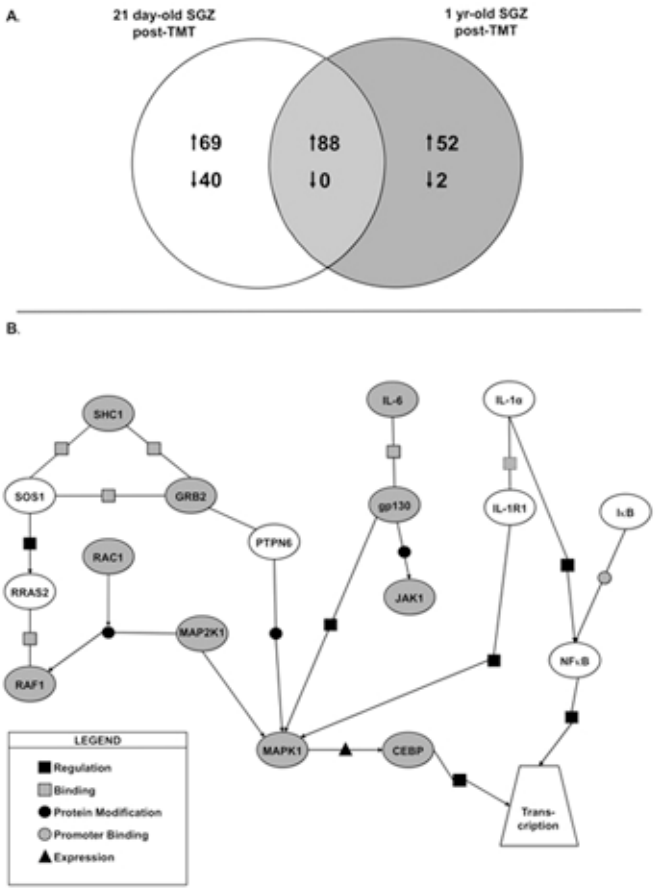

Figure 4.7. Expression of inflammatory pathway genes in the SGZ.
ANOVA was used to identify genes differentially expressed in TMT-treated versus saline-treated SGZs while taking into account the age-related interaction. (A) Venn diagram represents differentially expressed genes (1.2-fold or greater) by two-way error weighted ANOVA (ANOVA $p<0.001$ with Benjamini-Hochberg FDR $p<0.05$). (B) Graphical representation of differentially expressed genes following TMT-induced injury in 21 day-old versus 1 yr-old mice created using Pathway Archictect. Genes were then further analyzed using the categories of binding, expression, metabolism, promoter binding, protein modification and regulation (see legend). In this analysis, age was considered a mediator of injury related differential expression patterns using ANOVA. These data suggest key molecules in the IL-6 signaling pathway are upregulated (grey ovals) in the 1 yr-old SGZ following injury. Alternatively, IL-1α pathway genes are upregulated (white ovals) in the young SGZ following injury.

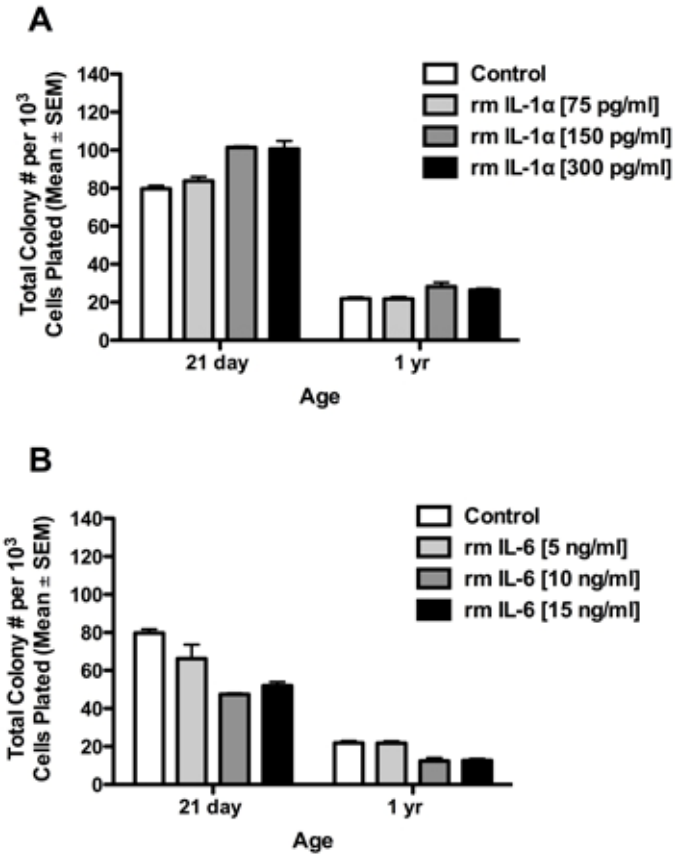

Supplemental Figure 4.1. Neurosphere proliferation.
(A) Proliferation of neurospheres as indicated by determining the mean total numbers of colonies formed per 10^3 cells plated from the hippocampus of 21 day-old and 1 following a 21 day exposure to recombinant mouse (A) IL-1α [75, 150, or 300 pg/ml] or (B) IL-6 [5, 10, or 15 ng/ml], Data represents mean $\pm$ SD.

References

Aberg, M.A., Aberg, N.D., Hedbacker, H., Oscarsson, J., Eriksson, P.S., 2000. Peripheral infusion of IGF-I selectively induces neurogenesis in the adult rat hippocampus. J Neurosci 20, 2896-2903.

Ajmone-Cat, M.A., Cacci, E., Ragazzoni, Y., Minghetti, L., Biagioni, S., 2010. Pro-gliogenic effect of IL-1alpha in the differentiation of embryonic neural precursor cells in vitro. J Neurochem 113, 1060-1072.

Alvarez-Buylla, A., Lim, D.A., 2004. For the long run: maintaining germinal niches in the adult brain. Neuron 41, 683-686.

Banasr, M., Hery, M., Printemps, R., Daszuta, A., 2004. Serotonin-induced increases in adult cell proliferation and neurogenesis are mediated through different and common 5-HT receptor subtypes in the dentate gyrus and the subventricular zone. Neuropsychopharmacology 29, 450-460.

Ben Abdallah, N.M., Slomianka, L., Vyssotski, A.L., Lipp, H.P., 2010. Early age-related changes in adult hippocampal neurogenesis in C57 mice. Neurobiol Aging 31, 151-161.

Blackmore, D.G., Golmohammadi, M.G., Large, B., Waters, M.J., Rietze, R.L., 2009. Exercise increases neural stem cell number in a growth hormone-dependent manner, augmenting the regenerative response in aged mice. Stem Cells 27, 2044-2052.

Bromberg, J., Darnell, J.E., Jr., 2000. The role of STATs in transcriptional control and their impact on cellular function. Oncogene 19, 2468-2473.

Bruccoleri, A., Brown, H., Harry, G.J., 1998. Cellular localization and temporal elevation of tumor necrosis factor-alpha, interleukin-1 alpha, and transforming growth factor-beta 1 mRNA in hippocampal injury response induced by trimethyltin. J Neurochem 71, 1577-1587.

Bull, N.D., Bartlett, P.F., 2005. The adult mouse hippocampal progenitor is neurogenic but not a stem cell. J Neurosci 25, 10815-10821.

Cacci, E., Claasen, J.H., Kokaia, Z., 2005. Microglia-derived tumor necrosis factor-alpha exaggerates death of newborn hippocampal progenitor cells in vitro. J Neurosci Res 80, 789-797.

Cameron, H.A., Gould, E., 1994. Adult neurogenesis is regulated by adrenal steroids in the dentate gyrus. Neuroscience 61, 203-209.

Colton, C.A., Wilcock, D.M., 2010. Assessing activation states in microglia. CNS Neurol Disord Drug Targets 9, 174-191.

Das, S., Basu, A., 2008. Inflammation: a new candidate in modulating adult neurogenesis. J Neurosci Res 86, 1199-1208.

Davalos, D., Grutzendler, J., Yang, G., Kim, J.V., Zuo, Y., Jung, S., Littman, D.R., Dustin, M.L., Gan, W.B., 2005. ATP mediates rapid microglial response to local brain injury in vivo. Nat Neurosci 8, 752-758.

Dunne, A., O'Neill, L.A., 2003. The interleukin-1 receptor/Toll-like receptor superfamily: signal transduction during inflammation and host defense. Sci STKE 2003, re3.

Ekdahl, C.T., Claasen, J.H., Bonde, S., Kokaia, Z., Lindvall, O., 2003. Inflammation is detrimental for neurogenesis in adult brain. Proc Natl Acad Sci U S A 100, 13632-13637.

Ekdahl, C.T., Kokaia, Z., Lindvall, O., 2009. Brain inflammation and adult neurogenesis: the dual role of microglia. Neuroscience 158, 1021-1029.

Eriksson, C., Nobel, S., Winblad, B., Schultzberg, M., 2000. Expression of interleukin 1 alpha and beta, and interleukin 1 receptor antagonist mRNA in the rat central nervous system after peripheral administration of lipopolysaccharides. Cytokine 12, 423-431.

Eriksson, C., Van Dam, A.M., Lucassen, P.J., Bol, J.G., Winblad, B., Schultzberg, M., 1999. Immunohistochemical localization of interleukin-1beta, interleukin-1 receptor antagonist and interleukin-1beta converting enzyme/caspase-1 in the rat brain after peripheral administration of kainic acid. Neuroscience 93, 915-930.

Greenfeder, S.A., Nunes, P., Kwee, L., Labow, M., Chizzonite, R.A., Ju, G., 1995. Molecular cloning and characterization of a second subunit of the interleukin 1 receptor complex. J Biol Chem 270, 13757-13765.

Harry, G.J., Funk, J.A., Lefebvre d'Hellencourt, C., McPherson, C.A., Aoyama, M., 2008. The type 1 interleukin 1 receptor is not required for the death of murine hippocampal dentate granule cells and microglia activation. Brain Res 1194, 8-20.

Harry, G.J., Lefebvre d'Hellencourt, C., 2003. Dentate gyrus: alterations that occur with hippocampal injury. Neurotoxicology 24, 343-356.

Harry, G.J., McPherson, C.A., Wine, R.N., Atkinson, K., Lefebvre d'Hellencourt, C., 2004. Trimethyltin-induced neurogenesis in the murine hippocampus. Neurotox Res 5, 623-627.

Harry, G.J., Tyler, K., d'Hellencourt, C.L., Tilson, H.A., Maier, W.E., 2002. Morphological alterations and elevations in tumor necrosis factor-alpha, interleukin (IL)-1alpha, and IL-6 in mixed glia cultures following exposure to trimethyltin: modulation by proinflammatory cytokine recombinant proteins and neutralizing antibodies. Toxicol Appl Pharmacol 180, 205-218.

Hattiangady, B., Rao, M.S., Shetty, A.K., 2008. Plasticity of hippocampal stem/progenitor cells to enhance neurogenesis in response to kainate-induced injury is lost by middle age. Aging Cell 7, 207-224.

He, J., Crews, F.T., 2007. Neurogenesis decreases during brain maturation from adolescence to adulthood. Pharmacol Biochem Behav 86, 327-333.

Heinrich, P.C., Behrmann, I., Muller-Newen, G., Schaper, F., Graeve, L., 1998. Interleukin-6-type cytokine signalling through the gp130/Jak/STAT pathway. Biochem J 334 (Pt 2), 297-314.

Hirano, T., Ishihara, K., Hibi, M., 2000. Roles of STAT3 in mediating the cell growth, differentiation and survival signals relayed through the IL-6 family of cytokine receptors. Oncogene 19, 2548-2556.

Islam, O., Gong, X., Rose-John, S., Heese, K., 2009. Interleukin-6 and neural stem cells: more than gliogenesis. Mol Biol Cell 20, 188-199.

Jones, S.A., Richards, P.J., Scheller, J., Rose-John, S., 2005. IL-6 transsignaling: the in vivo consequences. J Interferon Cytokine Res 25, 241-253.

Juttler, E., Tarabin, V., Schwaninger, M., 2002. Interleukin-6 (IL-6): a possible neuromodulator induced by neuronal activity. Neuroscientist 8, 268-275.

Kaneko, N., Kudo, K., Mabuchi, T., Takemoto, K., Fujimaki, K., Wati, H., Iguchi, H., Tezuka, H., Kanba, S., 2006. Suppression of cell proliferation by interferon-alpha through interleukin-1 production in adult rat dentate gyrus. Neuropsychopharmacology 31, 2619-2626.

Kempermann, G., Gast, D., Gage, F.H., 2002. Neuroplasticity in old age: sustained fivefold induction of hippocampal neurogenesis by long-term environmental enrichment. Ann Neurol 52, 135-143.

Koo, J.W., Duman, R.S., 2008. IL-1beta is an essential mediator of the antineurogenic and anhedonic effects of stress. Proc Natl Acad Sci U S A 105, 751-756.

Kuhn, H.G., Dickinson-Anson, H., Gage, F.H., 1996. Neurogenesis in the dentate gyrus of the adult rat: age-related decrease of neuronal progenitor proliferation. J Neurosci 16, 2027-2033.

Kuzumaki, N., Ikegami, D., Imai, S., Narita, M., Tamura, R., Yajima, M., Suzuki, A., Miyashita, K., Niikura, K., Takeshima, H., Ando, T., Ushijima, T., Suzuki, T., 2010. Enhanced IL-1beta production in response to the activation of hippocampal glial cells impairs neurogenesis in aged mice. Synapse.

Larsson, E., Mandel, R.J., Klein, R.L., Muzyczka, N., Lindvall, O., Kokaia, Z., 2002. Suppression of insult-induced neurogenesis in adult rat brain by brain-derived neurotrophic factor. Exp Neurol 177, 1-8.

Lawson, L.J., Perry, V.H., Dri, P., Gordon, S., 1990. Heterogeneity in the distribution and morphology of microglia in the normal adult mouse brain. Neuroscience 39, 151-170.

Louis, S.A., Rietze, R.L., Deleyrolle, L., Wagey, R.E., Thomas, T.E., Eaves, A.C., Reynolds, B.A., 2008. Enumeration of neural stem and progenitor cells in the neural colony-forming cell assay. Stem Cells 26, 988-996.

Mathieu, P., Battista, D., Depino, A., Roca, V., Graciarena, M., Pitossi, F., 2010. The more you have, the less you get: the functional role of inflammation on neuronal differentiation of endogenous and transplanted neural stem cells in the adult brain. J Neurochem 112, 1368-1385.

McPherson, C.A., Kraft, A.D., Harry, G.J., 2010. Injury-Induced Neurogenesis: Consideration of Resident Microglia as Supportive of Neural Progenitor Cells. Neurotox Res.

Michelucci, A., Heurtaux, T., Grandbarbe, L., Morga, E., Heuschling, P., 2009. Characterization of the microglial phenotype under specific pro-inflammatory and anti-inflammatory conditions: Effects of oligomeric and fibrillar amyloid-beta. J Neuroimmunol 210, 3-12.

Ming, G.L., Song, H., 2005. Adult neurogenesis in the mammalian central nervous system. Annu Rev Neurosci 28, 223-250.

Monje, M.L., Toda, H., Palmer, T.D., 2003. Inflammatory blockade restores adult hippocampal neurogenesis. Science 302, 1760-1765.

Mrak, R.E., Griffin, W.S., 2005. Glia and their cytokines in progression of neurodegeneration. Neurobiol Aging 26, 349-354.

Nakanishi, M., Niidome, T., Matsuda, S., Akaike, A., Kihara, T., Sugimoto, H., 2007. Microglia-derived interleukin-6 and leukaemia inhibitory factor promote astrocytic differentiation of neural stem/progenitor cells. Eur J Neurosci 25, 649-658.

Nimmerjahn, A., Kirchhoff, F., Helmchen, F., 2005. Resting microglial cells are highly dynamic surveillants of brain parenchyma in vivo. Science 308, 1314-1318.

O'Neill, L.A., 2002. Signal transduction pathways activated by the IL-1 receptor/toll-like receptor superfamily. Curr Top Microbiol Immunol 270, 47-61.

O'Neill, L.A., Greene, C., 1998. Signal transduction pathways activated by the IL-1 receptor family: ancient signaling machinery in mammals, insects, and plants. J Leukoc Biol 63, 650-657.

Oo, T.F., Siman, R., Burke, R.E., 2002. Distinct nuclear and cytoplasmic localization of caspase cleavage products in two models of induced apoptotic death in dopamine neurons of the substantia nigra. Exp Neurol 175, 1-9.

Reich, N.C., 2007. STAT dynamics. Cytokine Growth Factor Rev 18, 511-518.
Rezaie, P., Male, D., 1999. Colonisation of the developing human brain and spinal cord by microglia: a review. Microsc Res Tech 45, 359-382.

Ringheim, G.E., Burgher, K.L., Heroux, J.A., 1995. Interleukin-6 mRNA expression by cortical neurons in culture: evidence for neuronal sources of interleukin-6 production in the brain. J Neuroimmunol 63, 113-123.

Schlessinger, A.R., Cowan, W.M., Gottlieb, D.I., 1975. An autoradiographic study of the time of origin and the pattern of granule cell migration in the dentate gyrus of the rat. J Comp Neurol 159, 149-175.

Schobitz, B., Voorhuis, D.A., De Kloet, E.R., 1992. Localization of interleukin 6 mRNA and interleukin 6 receptor mRNA in rat brain. Neurosci Lett 136, 189-192.

Seaberg, R.M., van der Kooy, D., 2002. Adult rodent neurogenic regions: the ventricular subependyma contains neural stem cells, but the dentate gyrus contains restricted progenitors. J Neurosci 22, 1784-1793.

Shetty, A.K., Hattiangady, B., Rao, M.S., Shuai, B., 2010. Deafferentation enhances neurogenesis in the young and middle aged hippocampus but not in the aged hippocampus. Hippocampus.

Shu, H.F., Zhang, C.Q., Yin, Q., An, N., Liu, S.Y., Yang, H., 2010. Expression of the interleukin 6 system in cortical lesions from patients with tuberous sclerosis complex and focal cortical dysplasia type IIb. J Neuropathol Exp Neurol 69, 838-849.

Sparkman, N.L., Johnson, R.W., 2008. Neuroinflammation associated with aging sensitizes the brain to the effects of infection or stress. Neuroimmunomodulation 15, 323-330.

Spulber, S., Oprica, M., Bartfai, T., Winblad, B., Schultzberg, M., 2008. Blunted neurogenesis and gliosis due to transgenic overexpression of human soluble IL-1ra in the mouse. Eur J Neurosci 27, 549-558.

Streit, W.J., 2006. Microglial senescence: does the brain's immune system have an expiration date? Trends Neurosci 29, 506-510.

Taga, T., Fukuda, S., 2005. Role of IL-6 in the neural stem cell differentiation. Clin Rev Allergy Immunol 28, 249-256.

Taupin, P., 2008. Adult neurogenesis, neuroinflammation and therapeutic potential of adult neural stem cells. Int J Med Sci 5, 127-132.

Tsakiri, N., Kimber, I., Rothwell, N.J., Pinteaux, E., 2008a. Interleukin-1-induced interleukin-6 synthesis is mediated by the neutral sphingomyelinase/Src kinase pathway in neurones. Br J Pharmacol 153, 775-783.

Tsakiri, N., Kimber, I., Rothwell, N.J., Pinteaux, E., 2008b. Mechanisms of interleukin-6 synthesis and release induced by interleukin-1 and cell depolarisation in neurones. Mol Cell Neurosci 37, 110-118.

Vallieres, L., Campbell, I.L., Gage, F.H., Sawchenko, P.E., 2002. Reduced hippocampal neurogenesis in adult transgenic mice with chronic astrocytic production of interleukin-6. J Neurosci 22, 486-492.

Walker, T.L., White, A., Black, D.M., Wallace, R.H., Sah, P., Bartlett, P.F., 2008. Latent stem and progenitor cells in the hippocampus are activated by neural excitation. J Neurosci 28, 5240-5247.

Wang, K., Yuan, C.P., Wang, W., Yang, Z.Q., Cui, W., Mu, L.Z., Yue, Z.P., Yin, X.L., Hu, Z.M., Liu, J.X., 2010. Expression of interleukin 6 in brain and colon of rats with TNBS-induced colitis. World J Gastroenterol 16, 2252-2259.

Wang, X., Fu, S., Wang, Y., Yu, P., Hu, J., Gu, W., Xu, X.M., Lu, P., 2007. Interleukin-1beta mediates proliferation and differentiation of multipotent neural precursor cells through the activation of SAPK/JNK pathway. Mol Cell Neurosci 36, 343-354.

Weng, L., Dai, H., Zhan, Y., He, Y., Stepaniants, S.B., Bassett, D.E., 2006. Rosetta error model for gene expression analysis. Bioinformatics 22, 1111-1121.

Wesche, H., Korherr, C., Kracht, M., Falk, W., Resch, K., Martin, M.U., 1997. The interleukin-1 receptor accessory protein (IL-1RAcP) is essential for IL-1-induced activation of interleukin-1 receptor-associated kinase (IRAK) and stress-activated protein kinases (SAP kinases). J Biol Chem 272, 7727-7731.

Ye, S.M., Johnson, R.W., 1999. Increased interleukin-6 expression by microglia from brain of aged mice. J Neuroimmunol 93, 139-148.

Ye, S.M., Johnson, R.W., 2001. Regulation of interleukin-6 gene expression in brain of aged mice by nuclear factor kappaB. J Neuroimmunol 117, 87-96.

Yokoyama, A., Yang, L., Itoh, S., Mori, K., Tanaka, J., 2004. Microglia, a potential source of neurons, astrocytes, and oligodendrocytes. Glia 45, 96-104.

Yoshimizu, T., Chaki, S., 2004. Increased cell proliferation in the adult mouse hippocampus following chronic administration of group II metabotropic glutamate receptor antagonist, MGS0039. Biochem Biophys Res Commun 315, 493-496.

Chapter 5

Overall discussion and future directions.

In the years since the discovery of the neurogenic region in the adult hippocampus, investigators have focused on identifying molecules responsible for regulating the endogenous proliferation and differentiation of NPCs. While this is a continuous process over the life of the organism it varies with age and other endogenous changes such as stress, exercise, and hormonal balance. Modulation of adult neurogenesis by a diverse array of factors has lead to an intensive research effort to determine signaling molecules associated with proliferation, migration, and differentiation of NPCs as well as the functional integration of the neurons into the brain circuitry (Cho and Kim, 2010; Ming and Song, 2005). While much advancement has been made identifying signaling factors that modulate NPCs, questions remain regarding the nature of this pool of progenitor cells and their fate. Of primary interest for the field of neurotoxicology and neurodegeneration is the fact that neurogenesis is rapidly upregulated with brain injury or insult. The ability of this response to serve in a repair/replacement function has been implicated in a number of studies; however, the level at which the neurogenic process can provide new neurons for repair has not been clearly delineated.

Data from the current series of studies clearly demonstrate a robust neurogenic response in the SGZ to fully replace the large number of dentate granule neurons that are lost with TMT exposure. This is the first study to demonstrate such a capacity both in cell numbers and integration into the hippocampal circuitry for functional recovery of learning and memory. In addition a robust neurogenic response appears prominent in the adolescent brain while a slightly diminished response is observed in the mature brain. While this may be due to an "aging" of the NPC, the current study (Chapter 4), suggested a relationship to a change or aging of the regulatory processes of the SGZ neurogenic "niche". One hypothesis is based upon the generalized increase in inflammatory factors in the brain with aging, and proposes that the inflammatory state hinders the successful production and differentiation of NPCs. Data from the current studies demonstrated that the influence of pro-inflammatory cytokines on NPCs changes as a function of age. In addition to inflammatory factors, microglia of the adolescent brain appear to shepherd the newly generated neurons through the dentate granule cell layer to their final mature location. Overall the data suggest that microglia play a critical role in hippocampal injury-induced neurogenesis both in cell-cell contact and secreted factors. These data set the stage for an extended observation into staging the characteristics of the cells during the course of neuronal death and replacement.

Along with NPCs, astrocytes, oligodendroglia, and microglia contribute to the cellular composition of the intact SGZ. While there are numerous reports of microglia clusters in the normal SGZ, it was not until the work of Sierra et al.

(2010) that the unique role for these cells with regards to regulation of NPCs became appreciated. Neurogenesis in the SGZ appears to be a rather prominent event with hundreds of $BrdU^+$ progenitor cells reported to be generated over a 24 h period (Kronenberg et al., 2003). The normal life of $BrdU^+$ cells is rather short with apoptotic death in the first 1-4 days of their life, representative of the transition from amplifying NPC to neuroblasts (Kempermann et al., 2003; Steiner et al., 2004). A majority of these cells are eliminated, with a small number of cells recruited into the functional circuitry (Biebl et al., 2000; Young et al., 1999) becoming indistinguishable from mature neurons within 4-6 weeks of birth (Kee et al., 2007; van Praag et al., 2002). Given the fact that a comparable level of cell death in the GCL has not been reported, one can not assume that the cells serve in a replacement function for dentate granule neurons. This then raised the issue of the mechanism for clearing the excess or unhealthy cells to maintain homeostasis of the region (Mattocks and Tropepe, 2010). The work of Sierra et al. (2010) demonstrated that within the SGZ, microglia display a functional morphology that allows for the clearance of unhealthy NPCs by microglial phagocytosis. In this case rather than the microglia differentiating to an amoeboid macrophage as is normally seen with brain injury, SGZ microglia extend their processes to contact NPCs and, in the case of unhealthy NPC, they engulf and clear the small NPCs. While neurogenesis decreases as a function of age, the efficiency of this clearance process is maintained across the lifespan suggesting that it is a tightly regulated event (Sierra et al., 2010).

While the work of Sierra et al. (2010) demonstrated a clearance role for SGZ microglia, additional work suggests that microglia can play a beneficial role to stimulate neurogenesis and to support the newly generated cells through a high inflammatory environment (McPherson et al., 2011b). In the first set of experiments conducted within this dissertation project, amoeboid microglia were identified in the dentate granule cell layer actively engulfing apoptotic neurons. However microglia displaying a non-amoeboid morphology were also observed, often in contact with healthy surviving dentate granule neurons. This suggested that the microglia, as a population performed various functions within a localized injury site. Upon further examination a prominent physical contact was identified between microglia and newly proliferating $BrdU^+$ cells (McPherson et al., 2011b)(Fig. 5.1). Consistent with the work of Sierra et al. (2010), contact between the two cell types in the normal hippocampus was predominant within the SGZ; however, these cells were not engulfing dying cells. The spatial distribution of the cell-cell contact suggested a primary location closest to the SGZ, with contact relationship diminishing as $BrdU^+$ cells migrated to the outer layers of the dentate blades. As these $BrdU^+$ cells showed normal morphological features of healthy cells, it was speculated that contact with microglia had a supportive role, not only for cell survival, but also for migration into the GCL. Upon migration, the $BrdU^+$ cell-glia contact relationship appeared to shift from the microglia to a predominant contact relationship with astrocytes. This shift occurred as the NPC matured and migrated into the outer layer of the DG.

These data suggested a spatial shift for the supportive glial cells and a potentially coordinated effort to ensure the success of neurogenesis.

Previous work showed that astrocytes within the SGZ “cradle” newborn progenitors (Plumpe et al., 2006). In comparison in the TMT damaged hippocampus, this “cradling” appeared to be performed by microglia, shifting to the astrocyte only upon migration into the blades of the dentate. In support of the observation of a more prominent role for astrocyte contact in the outer GCL, Shapiro et al. (2005) reported a contact relationship between newborn DCX^+ cells and $GFAP^+$ astrocyte processes as the cells migrate into the GCL. Thus in the TMT model it appears as if the glial cells hand-off the newly generated neurons from microglia to astrocytes for full migration and maturation of the neurons. It is also speculated from the current data that the microglia cells may serve to maintain the new cells in a less differentiated form to facilitate their migration across the entire width of the dentate blades. The pattern of microglia morphology and NPC proliferation and maturation to neurons suggests the potential for a shift in the environment to support the different cellular development stages. Thus one could visualize two distinct neurogenic “niches”. One niche, existing within the SGZ, responsible for the proliferation of NPCs and the other, within the neighboring GCL responsible for the migration, differentiation, and integration of new neurons into the hippocampus. In addition this secondary niche may also serve to regulate proliferation within the neighboring SGZ with the production and secretion of various inflammatory or neurotrophic factors.

Within the brain parenchyma microglia rapidly respond to changes in the environment often resulting in the release of pro-inflammatory cytokines. One would assume that a similar response of microglia occurs within the SGZ. Overall the body of published literature suggests that the mode of activation, the context of the injury, and the intensity of the response serve to determine whether microglia will exert a beneficial or detrimental effect on injury-induced neurogenesis. Previous studies suggested that the production of pro-inflammatory cytokines by brain macrophages, both resident microglia and infiltrating peripheral macrophages, serve to down regulate hippocampal neurogenesis (Ekdahl et al., 2003; Monje et al., 2003). These studies contributed to establishing a prevailing hypothesis that microglial-derived inflammatory factors are detrimental to neurogenesis. However this would not necessarily be consistent with the wealth of data demonstrating with injury and the associated pro-inflammatory cytokine response neurogenesis is upregulated. One point for consideration is the nature of the stimuli. For example in the original Monje et al. (2003) and Ekhdal et al. (2003) studies, microglia were stimulated by LPS. However if the microglia are stimulated *in vitro* with pro- and anti-inflammatory cytokines rather than with LPS, the effects are quite different and there is neuronal survival (Butovsky et al., 2006). Further work *in vivo* using an ischemic injury model demonstrated that ED-1 activated microglia did not compromise BrdU uptake into cells of the SGZ (Kelsen et al., 2006; Kelsen et al., 2010) and thus, no adverse effect on NPC proliferation. In adrenalectomized rats the loss of dentate granule neurons was accompanied by stellate microglia and yet,

neurogenesis was enhanced (Battista et al., 2006). In this case the authors speculated that the activated but non-amoeboid microglia served a different function and expressed the anti-inflammatory cytokine, TGFβ1, rather than the pro-inflammatory cytokines normally produced by their fully activated amoeboid counterparts. It is likely that a distinction can be made as it relates to the level and inducer of the response and possibly to the composition of the factors released by microglia.

The potential for pro-inflammatory cytokines to directly impact NPCs is suggested by *in vivo* and *in vitro* studies demonstrating that hippocampal NPCs express receptors for TNF, IL-1, and IL-6 (Iosif et al., 2006; Koo and Duman, 2008; McPherson et al., 2011a). Upon a general review of the existing literature, activation of these receptors by pro-inflammatory cytokines is deemed to adversely impact neurogenesis by altering proliferation, survival or neuronal differentiation of NPCs (Aimone et al., 2010; Das and Basu, 2008; Mathieu et al., 2010). However data from this dissertation demonstrated the $BrdU^+$ cells (NPCs) in the SGZ selectively expressed the TNFp75R and were devoid of TNFp55R suggesting that the newly generated cells utilize TNFα within the high inflammatory environment as a growth-promoting factor (McPherson et al., 2011b). In support of this hypothesis is the observation that the migration of $BrdU^+$ cells into the GCL following injury appeared diminished in *TNFp75R* $^{-/-}$ mice following TMT injury (McPherson et al., 2011b) or with status epilecticus (Iosif et al., 2006).

Using an *in vivo* model of direct IL-1β delivery to the hippocampus, Koo and Duman (2008) demonstrated that activation of IL-1R1 inhibits the basal level of NPC proliferation and that these anti-proliferative effects could be blocked with the co-infusion of IL-1Ra. A role for IL-1R1 signaling in stress-induced reduction of NPC proliferation was similarly demonstrated with blockage by IL-1Ra (Koo and Duman, 2008). While these studies suggested activation of IL-1R1 diminishes hippocampal neurogenesis, Spulber et al. (2008) reported that blockage of IL-1R1 by IL-1Ra decreased NPC proliferation normally induced by excitotoxic injury. In the current study the expression of IL-1R1 on hippocampal NPCs, the induction of proliferation *in vitro* with recombinant IL-1α, and the ability of an IL-1α neutralizing antibody to block the increase in proliferation induced by TMT (Appendix A) demonstrated a specific effect for IL-1 signaling at this time point in the response. In additional studies conducted in our lab, preliminary findings suggest that NPC proliferation as indicated by BrdU labeling is diminished in mice deficient for IL-1R1. While interesting this observation requires additional evaluation for any full interpretation of the findings. For proliferation induced with hippocampal neuronal death, and seizure, IL-1R1 activation appears to play a contributory role. In contrast, the IL-1R1 associated reduction of NPC proliferation induced by a mild insult such as stress may represent changes that occur with a lower level of IL-1α or IL-1β rather than what would be seen with death. It is also possible that the differences observed between the stress and the injury conditions are related to the level of concurrent increase in IL-1Ra.

Recent research has focused on assessing the functional phenotypes of microglia or their inflammatory status, during injury or under neurodegenerative states based on the expression of pro-inflammatory (M1), anti-inflammatory (M2), and repair (M2) associated molecules as originally described for peripheral macrophages (Colton and Wilcock, 2010). When this approach was used to examine the brains from transgenic mouse models of Alzheimer's disease, a linear polarization of microglia from the M1 to M2 phenotype was not evident. Rather, the microglia displayed heterogeneous populations as defined by morphology and M1/M2 expression profile (Colton and Wilcock, 2010; Frieler et al., 2011). The authors concluded that the nature of the effect of microglia and neuroinflammation on neurons was dependent on the balance of pro- and anti-inflammatory cytokines.

While more of an acute model than the AD transgenic mice, a distinctive shift in the M1 to M2 markers did not occur during the period of repopulation following TMT. The prominent pattern observed was one of elevated NPC proliferation, migration of DCX^+ NPCs, and differentiation to $NeuN^+$ neurons. This coincided with a transition of the microglia from the fully activated amoeboid state to one represented by stellate, then ramified morphology. While the initial migration into the GCL occurred in the presence of amoeboid microglia, it is possible that differentiation and survival would benefit from microglia exhibiting a non-phagocytic phenotype. However it was found that as the new cells established a mature phenotype, genes associated with the M1 and M2 classifications of microglia were concurrently elevated (Fig. 3.13). Whether this

represented the heterogeneity observed in the morphology of the microglia within the region or the recruitment of other cells such as astrocytes into the neurogenic support group is not currently known. One would expect that indeed multiple cells are contributing to the repair response. While the current work was unable to address this specific question further development and availability of specific antibodies for immunohistochemistry will allow for identification of the cellular localization of the identified proteins.

Of interest is the transient pattern of the cytokine response and the secondary elevation in the DG that coincided with a stage of repair. It is likely that in this stage one may identify the role of classical inflammatory cytokines in remodeling and repairing the brain that would be applicable to various and more subtle types of injury. While the TMT model is a more acute type of injury/repair response, the pattern of changes with regards to M1/M2 signaling appears to follow a similar trend as the more chronic models of brain insult such as reports for the genetic AD mice (Wilcock et al., 2011). Thus, the well-defined temporal and spatial pattern of response may allow for the identification of distinct markers of the different microglia stages and the impact on the neuronal population. From such work, one may identify the trigger that will shift microglia from a neurodestructive to a neuroprotective phenotype. The fact that the model is so well defined would allow for testing of therapeutic approaches to modify the microglia response within various stages of the injury to identify critical factors to minimize brain damage and to promote brain repair. The heterogeneity of the microglia response may differ in the TMT injury as compared to other conditions

in which NPC proliferation is blunted. However such data on the actual cell morphology is rarely available from much of the published literature to support this hypothesis. It is possible that the differential stages of microglia may be representative of different levels of inflammatory factors as well as the potential for a different profile of factors released. Potentially providing not only the actions required upon cell injury but also actions to promote NPC proliferation and survival.

There is a contrast between the various studies examining the impact of pro-inflammatory cytokines and NPCs. How might one explain this discrepancy? There are a number of possibilities ranging from the model system, *in vitro* versus *in vivo,* source of brain macrophage (resident microglia or infiltrating peripheral macrophages), level of cytokine produced, and production of anti-inflammatory factors. A large proportion of the work on NPCs and inflammation has been conducted *in vitro*. This would effectively remove the cells from their *in vivo* “niche” and thus, change their basal level of cytokine receptor expression. Under such conditions, one would expect factors that serve to down-regulate cytokine signaling such as IL-1Ra, or soluble TNF receptor would not be present. Therefore while such studies demonstrate that the machinery is in place with regards to receptor expression, the regulatory component of the niche is absent.

An additional component of the TMT injury model that differs from many of the injury models in the literature is the massive clearance of dead dentate granule neurons within a very short time period. With the loss of DG neurons and successful clearance of the cellular debris, the environment may shift to one

much more conducive to the entry of new cells. Regardless of signaling events, just the depletion of a physical barrier represented by the granule neurons would offer less resistance to the newly generated cells. Not only do the microglia perform a direct support of injury-induced neurogenesis but they facilitate the migration and maturation of the cells into functioning neurons simply by providing the space and opening the routes for migration. Under these conditions it is possible that a signaling gradient can be established between microglia and NPCs.

In a model of experimental allergic encephalomyelitis (EAE), NPCs transplanted in the presence of $Iba1^{+}$ microglia in the acute phase of the injury showed evidence of migration; yet, when the cells were transplanted during the chronic phase of EAE when there are less $Iba1^{+}$ microglia a shorter migration distance was observed (Muja et al., 2011). This decrease in migratory distance coincided with the decrease in microglia along the NPC migratory path. It has been considered the release of chemokines and/or neurotrophic factors from microglia contributes to the migration (Neumann et al., 2009). This signaling hypothesis is somewhat supported by the work of Aarum et al. (2003) with the demonstration of precursor cell migration from the embryonic brain toward a gradient of microglial-conditioned media *in vitro*. Aarum et al. (2003) also reported that presence of microglia-conditioned media facilitated differentiation of precursor cells to neurons. It is possible that changes in the GCL environment, as a result of neuronal death and glial activation, not only clears the way for cell migration but also shifts to a more pro-migratory and pro-neuronal differentiation

environment providing appropriate signals to the NPC. We know that the chemokines MIP-1α and MIP-1β are some of the earliest and highest transcripts elevated in the hippocampus following TMT (Bruccoleri et al., 1998; Lefebvre d'Hellencourt and Harry, 2005) and are localized to microglia (Harry, personal communication). These chemokines remain elevated over the course of the first week of the injury. It is likely that microglia serve to stimulate and protect the new neurons, and they also serve in a role to promote and direct their migration.

It is the presumption that the activation of microglia and NPCs occurs as a result of the neuronal damage; however, it is possible that TMT can directly activate microglia leading to neuronal death. Earlier work demonstrated TMT stimulates the production of TNFα, and IL1 by microglia *in vitro* (Maier et al., 1997). Further work *in vitro* suggested that the production of TNFα was a causative factor for neuronal death (Harry et al., 2002). This was substantiated with the *in vivo* demonstration that the death of dentate granule neurons was a TNFR mediated event (Harry et al., 2008). Whether this was dependent upon a prominent presence of activated microglia has been previously discounted by the studies of Bruccoleri et al. (2000) using mice deficient in colony stimulating growth factor and thus deficient in microglia. This work demonstrated that while there was a substantial deficit in the actual number of microglia, their production if TNFα was 700% higher following TMT as compared to wildtype. In addition, TMT has been shown to directly induce proliferation of human neural stem cells *in vitro* (Dr. Tim Shafer, personal communication). These observations may allow us to use TMT to stimulate the cells of interest to address additional

questions regarding the interaction between these two cell types in the hippocampus.

For example, once a dose-response for stimulation of each cell type has been established in culture one could then translate that to the *in vivo* model. Using this approach, it is possible to begin to ask questions as they relate to the activation state of the microglia. It may be possible to maintain the microglia in a non-process bearing state for an extended period of time to determine the impact on NPC survival and migration. In addition, if the dose response data allows one to identify a sub-threshold dose of TMT for microglia activation that will stimulate NPC proliferation this may allow for testing the hypothesis of the requirement for microglia activation and/or the appearance of "space" to promote NPC migration. TMT may provide a tool with which to address a number of questions regarding cell interactions associated with hippocampal neurogenesis.

When comparing the overall body of literature examining the effects of inflammatory factors derived from brain macrophages on NPCs a common underlying theme emerges. These results suggest that the mode of activation, the intensity of the response, and source of the brain macrophage serves to determine whether a beneficial or detrimental effect on successful injury-induced neurogenesis will occur. Under normal conditions, the BBB prevents factors in the brain extracellular space from gaining access to the vascular lumen, and vice versa. With a physical injury such as trauma or ischemia, or during autoimmune events, the barrier is disrupted and blood-borne immune cells gain access to the brain parenchyma. Importantly, compared to resident microglia cells of the

peripheral immune system provide an enriched source of cytokine and inflammatory factors, therefore exhibiting exaggerated activation phenotypes as compared to those of microglia. In the current series of studies, it was confirmed that the brain macrophage response was limited to the resident microglia without the recruitment of peripheral macrophages. Given the higher level of inflammatory products produced by non-resident cells, their contribution in any injury likely drive the interpretation of a negative impact on neurogenesis.

As with any model, there are limitations that need to be considered. The strength of the TMT model lies in the rapid initiation of cell death, proliferation, migration and differentiation of new neurons. Yet these can also be confounders, in that any discussion of the molecular or cellular changes observed must be done with the knowledge that hippocampal neurogenesis is not the only repair mechanism employed. While a significant level of neuronal death occurs, there is a large population of neurons that survive this insult and the pro-inflammatory environment. Thus many of the signals observed within the DG will reflect local actions of neuronal death and neuronal survival, in addition to those of interest for successful neurogenesis. For example with the exception of IL-1α, there is little indication of induction of cytokines in the SGZ by hippocampal injury suggesting that cytokine contribution to NPC proliferation would be derived from neighboring areas, in this case the GCL. The overproduction of pro-inflammatory cytokines in the GCL associated with neuronal death could easily diffuse to the SGZ resulting in a stimulus for NPC proliferation. Once a more broad profile is generated other stimulatory signals may emerge that serve to drive the

production of new neurons for the replacement of dentate granule cells and the repair of the hippocampus. Teasing these components apart to identify critical aspects for regulating adult hippocampal neurogenesis following injury or in disease states becomes a bit more difficult.

The current opinion is that microglia are not pro- or anti-neurogenic *per se* but rather that the net outcome on NPCs depends upon a multitude of factors. While the primary interpretation of the data generated from this dissertation project has focused upon the temporal response of microglia and the induction of NPC proliferation and migration with injury and during repair, there are a number of other aspects of the system that need consideration not the least of which is the contribution from other cells within the environment. When interpreting the results of this project a number of take home points emerge. First, morphological phenotype may contribute to the identification and understanding of differential, shifting roles of microglia. Second, differential stages of microglial activation may contribute to the successful proliferation and migration of NPCs in the injured hippocampus. Third, the profile of molecular changes for inflammation suggests multiple cell types are involved. Further investigation of changes that occur within the primary and secondary neurogenic niches can contribute to unmasking critical triggers regulating cell responses and the development of targeted therapeutics to foster hippocampal self repair.

With regards to a translational aspect of the research, the decline in neurogenic potential observed as a function of aging and the potential for stimulation of this process for repair and recovery of function in

neurodegenerative disorders raises interesting questions with regards to the identification of regulatory factors for therapeutic potential. In comparing not only the proliferative potential but also the molecular environment of the SGZ as a function of age, a difference in inflammatory signaling was identified within the primary neurogenic niche during the initiation of the NPC proliferative response. The directly comparable effects of TMT on the dentate granule cells, regardless of age allowed for a relatively uniform model to examine critical features of the SGZ neurogenic niche that changed with age. In an unbiased molecular profile comparison between the SGZ as a function of age and TMT, the primary likely candidates of IL-1 and IL-6 were identified. This finding then focused subsequent studies on the differential effects of each cytokine on NPCs. However, given that a full array was conducted, there is a wealth of data that can be analyzed for the identification of other differentially regulated genes. Further comparisons are possible between the SGZ and the GCL in the adolescent and mature hippocampus. Using this approach, the gene profile and novel signaling pathways may be identified that are differentially expressed across the young and mature neurogenic niches. Building upon these findings, specific pathways identified at each age could be evaluated in cultured NPCs following a similar approach to that used for IL-6 and IL-1. The goal of this work would be to identify critical genes/signaling pathways that are activated in the adolescent for a robust level of repair but are absent in the more muted mature brain response. From this, one may be able to identify a few likely candidates that could be used to foster NPC proliferation and survival in the mature brain.

An additional approach could be taken to identify the molecular environment of the mature GCL that may serve to maintain regulatory control over the NPCs in the SGZ to prevent unnecessary proliferation. By identifying such factors, one may begin to identify ways to manipulate not only the SGZ niche but also the GCL niche to foster proliferation and neuronal differentiation. With further speculation, one could envision identifying genes that serve to make a non-neurogenic brain region resistant to NPC engraftment and thus, provide an approach to modify the region to foster the integration of transplantation of exogenous NPCs. Thus, data obtained from these series of experiments open up an array of directions for future examination that could lead to a better understanding not only of neuroinflammation but also how the regulatory aspect can be harnessed to facilitate brain repair in the human.

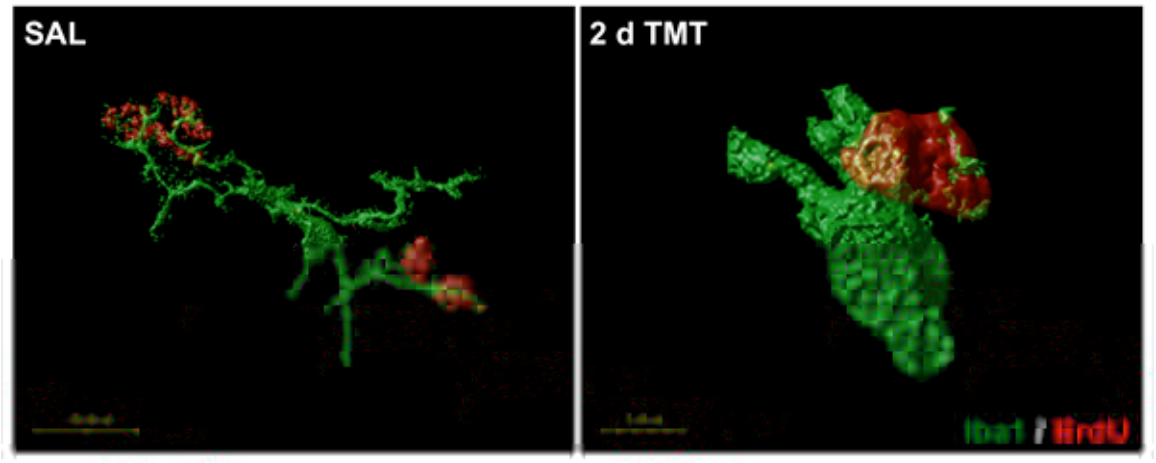

Figure 5.1. Representative images of BrdU / Iba1 in the SGZ.
Representative immunofluorescent images of 5'-bromo-2'-deoxyuridine (BrdU) (Red) and Iba1 (green) in the SGZ of saline control mice and (C, D) within the GCL 2 d post- TMT (2.3 mg/kg i.p.)

References

Aarum, J., Sandberg, K., Haeberlein, S.L., Persson, M.A., 2003. Migration and differentiation of neural precursor cells can be directed by microglia. Proc Natl Acad Sci U S A 100, 15983-15988.

Aimone, J.B., Deng, W., Gage, F.H., 2010. Adult neurogenesis: integrating theories and separating functions. Trends Cogn Sci 14, 325-337.

Battista, D., Ferrari, C.C., Gage, F.H., Pitossi, F.J., 2006. Neurogenic niche modulation by activated microglia: transforming growth factor beta increases neurogenesis in the adult dentate gyrus. Eur J Neurosci 23, 83-93.

Biebl, M., Cooper, C.M., Winkler, J., Kuhn, H.G., 2000. Analysis of neurogenesis and programmed cell death reveals a self-renewing capacity in the adult rat brain. Neurosci Lett 291, 17-20.

Bruccoleri, A., Brown, H., Harry, G.J., 1998. Cellular localization and temporal elevation of tumor necrosis factor-alpha, interleukin-1 alpha, and transforming growth factor-beta 1 mRNA in hippocampal injury response induced by trimethyltin. J Neurochem 71, 1577-1587.

Bruccoleri, A., Harry, G.J., 2000. Chemical-induced hippocampal neurodegeneration and elevations in TNFalpha, TNFbeta, IL-1alpha, IP-10, and MCP-1 mRNA in osteopetrotic (op/op) mice. J Neurosci Res 62, 146-155.

Butovsky, O., Ziv, Y., Schwartz, A., Landa, G., Talpalar, A.E., Pluchino, S., Martino, G., Schwartz, M., 2006. Microglia activated by IL-4 or IFN-gamma differentially induce neurogenesis and oligodendrogenesis from adult stem/progenitor cells. Mol Cell Neurosci 31, 149-160.

Cho, K.O., Kim, S.Y., 2010. Effects of brain insults and pharmacological manipulations on the adult hippocampal neurogenesis. Arch Pharm Res 33, 1475-1488.

Colton, C.A., Wilcock, D.M., 2010. Assessing activation states in microglia. CNS Neurol Disord Drug Targets 9, 174-191.

Das, S., Basu, A., 2008. Inflammation: a new candidate in modulating adult neurogenesis. J Neurosci Res 86, 1199-1208.

Ekdahl, C.T., Claasen, J.H., Bonde, S., Kokaia, Z., Lindvall, O., 2003. Inflammation is detrimental for neurogenesis in adult brain. Proc Natl Acad Sci U S A 100, 13632-13637.

Frieler, R.A., Meng, H., Duan, S.Z., Berger, S., Schutz, G., He, Y., Xi, G., Wang, M.M., Mortensen, R.M., 2011. Myeloid-specific deletion of the mineralocorticoid receptor reduces infarct volume and alters inflammation during cerebral ischemia. Stroke 42, 179-185.

Harry, G.J., Lefebvre d'Hellencourt, C., McPherson, C.A., Funk, J.A., Aoyama, M., Wine, R.N., 2008. Tumor necrosis factor p55 and p75 receptors are involved in chemical-induced apoptosis of dentate granule neurons. J Neurochem 106, 281-298.

Harry, G.J., Tyler, K., d'Hellencourt, C.L., Tilson, H.A., Maier, W.E., 2002. Morphological alterations and elevations in tumor necrosis factor-alpha, interleukin (IL)-1alpha, and IL-6 in mixed glia cultures following exposure to trimethyltin: modulation by proinflammatory cytokine recombinant proteins and neutralizing antibodies. Toxicol Appl Pharmacol 180, 205-218.

Iosif, R.E., Ekdahl, C.T., Ahlenius, H., Pronk, C.J., Bonde, S., Kokaia, Z., Jacobsen, S.E., Lindvall, O., 2006. Tumor necrosis factor receptor 1 is a negative regulator of progenitor proliferation in adult hippocampal neurogenesis. J Neurosci 26, 9703-9712.

Kee, N., Teixeira, C.M., Wang, A.H., Frankland, P.W., 2007. Preferential incorporation of adult-generated granule cells into spatial memory networks in the dentate gyrus. Nat Neurosci 10, 355-362.

Kelsen, J., Kjaer, K., Chen, G., Pedersen, M., Rohl, L., Frokiaer, J., Nielsen, S., Nyengaard, J.R., Ronn, L.C., 2006. Parecoxib is neuroprotective in spontaneously hypertensive rats after transient middle cerebral artery occlusion: a divided treatment response? J Neuroinflammation 3, 31.

Kelsen, J., Larsen, M.H., Sorensen, J.C., Moller, A., Frokiaer, J., Nielsen, S., Nyengaard, J.R., Mikkelsen, J.D., Ronn, L.C., 2010. Neuronal precursor cell proliferation in the hippocampus after transient cerebral ischemia: a comparative study of two rat strains using stereological tools. Exp Transl Stroke Med 2, 8.

Kempermann, G., Gast, D., Kronenberg, G., Yamaguchi, M., Gage, F.H., 2003. Early determination and long-term persistence of adult-generated new neurons in the hippocampus of mice. Development 130, 391-399.

Koo, J.W., Duman, R.S., 2008. IL-1beta is an essential mediator of the antineurogenic and anhedonic effects of stress. Proc Natl Acad Sci U S A 105, 751-756.

Kronenberg, G., Reuter, K., Steiner, B., Brandt, M.D., Jessberger, S., Yamaguchi, M., Kempermann, G., 2003. Subpopulations of proliferating cells of the adult hippocampus respond differently to physiologic neurogenic stimuli. J Comp Neurol 467, 455-463.

Lefebvre d'Hellencourt, C., Harry, G.J., 2005. Molecular profiles of mRNA levels in laser capture microdissected murine hippocampal regions differentially responsive to TMT-induced cell death. J Neurochem 93, 206-220.

Maier, W.E., Bartenbach, M.J., Brown, H.W., Tilson, H.A., Harry, G.J., 1997. Induction of tumor necrosis factor alpha in cultured glial cells by trimethyltin. Neurochem Int 30, 385-392.

Mathieu, P., Battista, D., Depino, A., Roca, V., Graciarena, M., Pitossi, F., 2010. The more you have, the less you get: the functional role of inflammation on neuronal differentiation of endogenous and transplanted neural stem cells in the adult brain. J Neurochem 112, 1368-1385.

Mattocks, M., Tropepe, V., 2010. Waste management and adult neurogenesis. Cell Stem Cell 7, 421-422.

McPherson, C.A., Aoyama, M., Harry, G.J., 2011a. Interleukin (IL)-1 and IL-6 regulation of neural progenitor cell proliferation with hippocampal injury: Differential regulatory pathways in the subgranular zone (SGZ) of the adolescent and mature mouse brain. Brain Behav Immun 25, 850-862.

McPherson, C.A., Kraft, A.D., Harry, G.J., 2011b. Injury-induced neurogenesis: consideration of resident microglia as supportive of neural progenitor cells. Neurotox Res 19, 341-352.

Ming, G.L., Song, H., 2005. Adult neurogenesis in the mammalian central nervous system. Annu Rev Neurosci 28, 223-250.

Monje, M.L., Toda, H., Palmer, T.D., 2003. Inflammatory blockade restores adult hippocampal neurogenesis. Science 302, 1760-1765.

Muja, N., Cohen, M.E., Zhang, J., Kim, H., Gilad, A.A., Walczak, P., Ben-Hur, T., Bulte, J.W., 2011. Neural precursors exhibit distinctly different patterns of cell migration upon transplantation during either the acute or chronic phase of EAE: a serial MR imaging study. Magn Reson Med 65, 1738-1749.

Neumann, H., Kotter, M.R., Franklin, R.J., 2009. Debris clearance by microglia: an essential link between degeneration and regeneration. Brain 132, 288-295.

Plumpe, T., Ehninger, D., Steiner, B., Klempin, F., Jessberger, S., Brandt, M., Romer, B., Rodriguez, G.R., Kronenberg, G., Kempermann, G., 2006. Variability of doublecortin-associated dendrite maturation in adult hippocampal neurogenesis is independent of the regulation of precursor cell proliferation. BMC Neurosci 7, 77.

Shapiro, L.A., Korn, M.J., Shan, Z., Ribak, C.E., 2005. GFAP-expressing radial glia-like cell bodies are involved in a one-to-one relationship with doublecortin-immunolabeled newborn neurons in the adult dentate gyrus. Brain Res 1040, 81-91.

Sierra, A., Encinas, J.M., Deudero, J.J., Chancey, J.H., Enikolopov, G., Overstreet-Wadiche, L.S., Tsirka, S.E., Maletic-Savatic, M., 2010. Microglia shape adult hippocampal neurogenesis through apoptosis-coupled phagocytosis. Cell Stem Cell 7, 483-495.

Spulber, S., Oprica, M., Bartfai, T., Winblad, B., Schultzberg, M., 2008. Blunted neurogenesis and gliosis due to transgenic overexpression of human soluble IL-1ra in the mouse. Eur J Neurosci 27, 549-558.

Steiner, B., Kronenberg, G., Jessberger, S., Brandt, M.D., Reuter, K., Kempermann, G., 2004. Differential regulation of gliogenesis in the context of adult hippocampal neurogenesis in mice. Glia 46, 41-52.

van Praag, H., Schinder, A.F., Christie, B.R., Toni, N., Palmer, T.D., Gage, F.H., 2002. Functional neurogenesis in the adult hippocampus. Nature 415, 1030-1034.

Young, D., Lawlor, P.A., Leone, P., Dragunow, M., During, M.J., 1999. Environmental enrichment inhibits spontaneous apoptosis, prevents seizures and is neuroprotective. Nat Med 5, 448-453.

Appendix A.

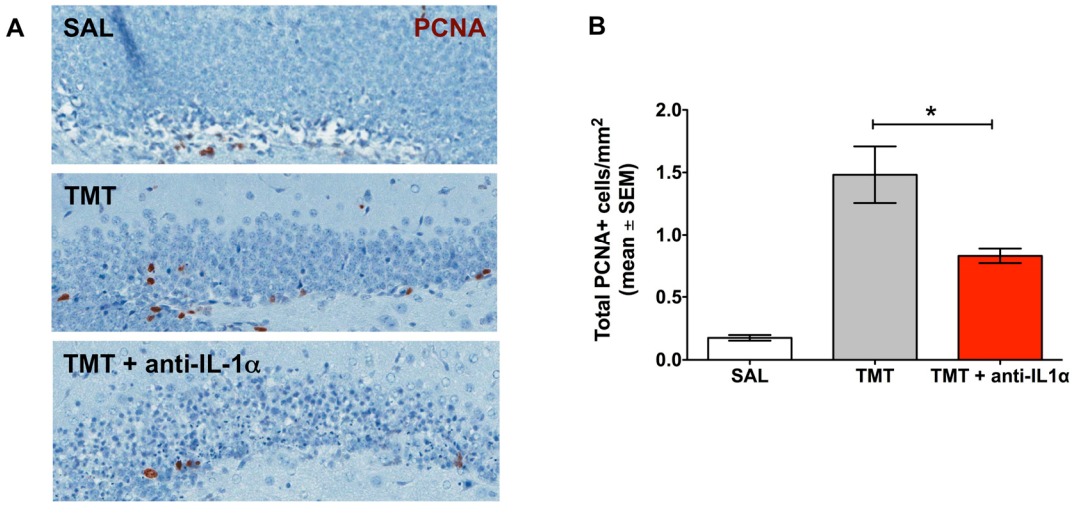

(A) Representative proliferating cellular nuclear antigen (PCNA) immunohistochemistry in the dentate gyrus of mice treated with SAL, TMT, or TMT + neutralizing antibody to IL-1α as described in the methods below. (B) Histogram represents mean number of PCNA positive cells counted from a single section in the dentate gyrus of SAL, TMT, and TMT + anti-IL-1α. Data represents mean ±SEM and was analyzed by one-way ANOVA followed by a Dunnett's multiple comparison test (*$p < 0.05$, n = 4-6). Treatment with neutralizing antibody blunted TMT-induced PCNA immunoreactivity.

Effects of IL-1α neutralizing antibody on SGZ proliferation in PND 21 mice.

An experiment was designed to examine the effects of a cytokine-neutralizing antibody on proliferative response in the SGZ following. In a previous study, we reported that peripheral cytokine TNFα signaling did not contribute to the TMT hippocampal pathology yet, a CNS delivery of TNFα antibody was sufficient to block neuronal death (Harry et al., 2003). Based upon these studies, a systemic injection of neutralizing antibody would not be expected to reach the brain tissue. Thus, we employed the approach used in this previous study (Harry et al., 2003) that allowed for a direct delivery of antibody to the ventricular system without causing a physical

injury to the brain tissue. In 21 day-old mice, an intracisternal (i.c.v.) injection into the fourth ventricle of the brain between the cerebellum and the cerebrum was possible. Each animal received an i.p. injection of either TMT (2.3 mg/kg) or saline (2 ml/kg) body weight. Three hours later mice received 2 ml artificial cerebral spinal fluid (ACSF) or a purified monoclonal neutralizing antibody (20 ng) to IL-1α (anti-mouse; R & D Systems). From pilot studies we confirmed that actions of the injected antibody were present for a minimum of 24 h and that tin levels can be detected in the brain within 3 h of injection peaking at 24 h, and that proliferation is initiated by 24 h. Based upon these data, hippocampal tissue was collected from all animals 36 hrs after the TMT injection. The dose selection for each antibody was determined based on our previous in vivo and in vitro studies (Harry et al., 2003; Harry et al., 2002) and the calculated Neutralization $Dose_{50}$ (ND_{50}) provided in the accompanying data sheet for each antibody (R & D Systems). Given that the injections were delivered directly into the ventricular system of the brain, initial dose estimates were obtained from in vitro studies demonstrating the level of each cytokine protein produced in mixed glia cultures with TMT exposure and the dose–response relationship to each antibody (Harry et al., 2002).

References

Harry, G., Bruccoleri, A., Lefebvre d'Hellencourt, C., 2003. Differential modulation of hippocampal chemical-induced injury response by ebselen, pentoxifylline, and TNFalpha-, IL-1alpha-, and IL-6-neutralizing antibodies. J Neurosci Res 73, 526-536.

Harry, G.J., Tyler, K., d'Hellencourt, C.L., Tilson, H.A., Maier, W.E., 2002. Morphological alterations and elevations in tumor necrosis factor-alpha, interleukin (IL)-1alpha, and IL-6 in mixed glia cultures following exposure to trimethyltin: modulation by proinflammatory cytokine recombinant proteins and neutralizing antibodies. Toxicol Appl Pharmacol 180, 205-218.